University of Strathclyde, Glasgow UK

Department of Chemical and Process Engineering

Control of nucleation

in continuous crystallisation processes

Ulrich Schacht

A thesis submitted to qualify for obtaining

the degree of Doctor of Philosophy

March 2014

Copyright Statement

The copyright of this thesis belongs to the author under the terms of the United Kingdom Copyrights Act as qualified by the University of Strathclyde Regulation 3.50. Due acknowledgement must always be made of the use of any material contained in, or derived from, this thesis.

Date:

Signature:

Dedication

This work is dedicated to Dr. Elisabeth A. Rohwer, who during my time in South Africa sparked my interest for research and played a key role in me being prepared to accept the PhD research opportunity / challenge when it came my way.

Acknowledgement

I would like to thank my supervisor Prof. Jan Sefcik and my second supervisor Prof. Alastair Florence for the opportunity as well as the support and guidance during the PhD project.

All members of the Department of Chemical and Process Engineering as well as the Centre for Innovative Manufacturing in Continuous Manufacturing and Crystallisation (CMAC) deserve gratitude and appreciation for the academic, administrative and technical support provided to make my PhD project a success.

I am very grateful for the ongoing support, sympathy and open ears of my parents and family throughout the duration of the PhD project, especially when times were a little more challenging.

Table of contents

Table of Figures

List of Tables

1 Summary

Crystallisation is an important separation and purification technology in the pharmaceutical and fine chemical industry. Crystallisation processes are designed to generate and control supersaturation, nucleate desired polymorphs as well as crystal shapes and growing product crystals to the required particle size distribution and purity. Traditionally crystallisation is carried out in batch mode, due to the necessary process flexibility, although continuous processing can offer advantages of reproducible product quality, more sustainability as well as lesser waste and lower carbon footprint. This work describes a route towards the development of continuous crystallisation processes for small organic molecules.

Supersaturation is the ultimate requirement for nucleation and in processes where mixing of two or more solutions is required to generate supersaturation, this step can affect nucleation.

This thesis shows that higher mixing intensities yield higher solid recoveries over time and a smaller particle size. However, this phenomenon only applies to low and medium mixing flow rates, whereas results for high mixing flow rates are at the same level as for the medium ones.

Furthermore, this effect was only observed in Valine – water:isopropanol (1:1) and at high supersaturations in Glycine – water:isopropanol (1:1) systems. In L-Glutamic acid – water:isopropanol (1:1) or L-Asparagine – water:isopropanol (1:1) systems this effect was not observed at all. Even the reactive precipitation of L-Glutamic acid (H-Glu) from Na-Glutamate and H_2SO_4 did not show any effects of mixing intensity on solid recovery over time.

The mixing insensitive reactive precipitation of H-Glu was used to study the effect of post-mixing flow treatment on solid recovery over time and final polymorphic population. Micromixed samples were exposed to different batch flow units with hydrodynamics of a quiescent crystalliser (QC), stirred tank crystalliser (STC), magnetically stirred crystalliser (MSC), peristaltic pump recirculation loop (PPL) and an oscillatory baffled crystalliser (OBC).

Harsh hydrodynamic conditions or mechanical impact like in the STC, MSC or OBC yield the metastable prismatic Alpha H-Glu polymorph and significantly increase solid recovery over time. Milder hydrodynamics like in a QC or PPL yield the stable platelet/needle like Beta H-Glu polymorph, where the PPL shows enhanced solid recovery over the QC. Despite XRPD analysis indicating pure Beta phase, the QC samples also contain about 0.1 % of the Alpha form, which growth kinetics suggest that they must have formed very shortly after mixing.

Connecting the continuous mixing setup with a Beta enhancing flow-through PPL unit and a sample collection vessel made a fully continuous Beta H-Glu crystalliser. However, this system never reached steady-state operation, fouling and blockage was a major challenge and an unexpected change in the polymorph population from the stable Beta to the metastable Alpha was observed. This system did not perform satisfactorily and therefore experiments were discontinued.

For the mixing insensitive antisolvent crystallisation of H-Glu, a novel rapid continuous antisolvent crystallisation setup was developed to produce crystal suspension of the Beta polymorph with a small size and narrow particle size distribution. The system jet-injects aqueous H-Glu solution into the bulk of isopropanol antisolvent and its performance was characterised with respect to different antisolvent mass fraction, bulk supersaturation, polymorphic population, steady-state operation, solid recovery over time, crystal size, particle size distribution and scale-up capabilities.
Results show that increasing the antisolvent mass fraction reduces the final crystal size and particle size distribution, crystal product is of pure Beta form with a high yield, the system rapidly achieves very high supersaturation and reaches steady-state operations after about 20-30 min. Higher total flow rates and scale-up of the system did not show any effect on particle and system properties. The produced crystal slurry exhibits ideal properties of a Beta H-Glu seeding suspension for further crystal growth.

Continuously seeded continuous crystal growth cooling crystallisation experiments were carried out in a tubular continuous oscillatory baffled crystalliser (COBC). H-Glu solution of two different concentrations was pumped through the system and Beta H-Glu seeding suspension of two different seed loadings were injected into the saturated solution.

Mass balance calculations, supersaturation data, seed loading & solution concentration, crystal morphology information, crystal growth rates and mean residence time in each temperature section along the rig were used to predict solution concentration, desupersaturation behaviour and the temperature profile of the process. Online Focused Beam Reflectance Measurement (FBRM) analysis and offline laser diffraction particle sizing measurements recorded crystal growth in the system. Offline solid recovery analysis over time at various points along the rig successfully confirmed the predicted solution concentrations and desupersaturation profile of the COBC. However, micrographs and Scanning Electron Microscopy (SEM) analysis indicated that final product crystals are agglomerated.

The effect of seed loading & solution concentration on the final agglomerated particle size distribution and solid recovery over time was investigated. Higher solution concentration led to larger product crystals, whereas different seed loadings did not show a clear trend.

Steady-state crystallisation was demonstrated based on particle size distribution as well as supersaturation data after each crystalliser residence time and was achieved within 20 min after the system was conditioned with crystal slurry. Fouling and secondary Alpha nucleation was not a problem as long as the supersaturation did not exceed a level of 3.7 in the bulk solution.

2 Introduction

Crystallisation is a separation as well as purification technology and one of the essential processing steps in the pharmaceutical and fine chemical industry. A large number of active pharmaceutical ingredients (API), intermediates and other fine chemicals are synthesised in solution and later on crystallised as usable, solid materials.

The process of crystallisation is one of the oldest unit operations in history and was traditionally employed for inorganic materials like obtaining table salt from sea water. More recently this technology was also used for high value organic materials. Organic molecules of interest are typically synthesised from simpler precursor compounds, in a multistep organic synthesis until the final molecule is obtained. Separation of the desired compound from the bulk solution, which contains by-products from the chemical reactions and impurities from input materials, can often be advantageously achieved by crystallisation.

The processing steps in crystallisation, leading to manufacturing a crystal suspension, for example creating supersaturation in solution, seeding, nucleation and crystal growth, are known as primary processing. These steps are essential for controlling purity, polymorphism of the final product, particle size distribution, crystal shape and process yield. Unit operations which further process the crystalline product material, for example filtration, washing, drying, milling or classifying are known as secondary processing.
Improved sensitivity of analytical methods also increases regulatory demands for higher product purity, reproducible bioavailability and general physical properties. The high demands towards the product material needs to be met by the primary processes, which require a more careful consideration of the influencing parameters and the level of process control during manufacturing.

Impurities are a major challenge in crystallisation. Their influence on the process is extremely system dependent, they are often unknown or at least poorly characterised and the exact impact needs to be studied experimentally due to lack of a common theory. Generally they influence the solubility of the desired compound in the mother liquor and affect nucleation and growth kinetics. Crystallisation is an impurity rejection

process however, incorporation into the crystal lattice and a reduction of crystal purity is possible when the impurity occupies spaces meant for solute molecules or adsorbs to the crystal surface. Input materials with varying impurity levels add a high degree of process complexity and can lead to significant batch-to-batch variations.

A big challenge in crystallisation is that many APIs and other fine chemicals exhibit polymorphism. One compound can crystallise in various crystal structures, which can all have very different physical properties from each other. It is very important to discover all possible polymorphs, especially the thermodynamically stable form, of a compound at an early stage of the development phase as discoveries later on can lead to substantial regulatory as well as patent issues. Once the desired polymorph is obtained, careful attention needs to be paid to possible undesired transformation processes of a less stable to a more stable form. Depending on the processing conditions, transformation can happen in the mother liquor, during filtration, drying or milling, creating great challenges for reproducible manufacturing of a compound.

One of the most important physical parameters in crystallisation is the particle size distribution (PSD), which gives valuable insights into nucleation and growth processes. A narrow distribution of small particles indicates that nucleation processes are dominating, whereas a narrow distribution of larger crystal sizes suggests a growth dominated process. A broad distribution from small to large is caused by continuous nucleation, while already present crystals keep growing.

Good control over the PSD is crucial for drug development as it directly affects the dissolution rate and bioavailability of the API to the patient. Poorly water soluble drugs need to consist of small particles with a large surface area and a narrow PSD to deliver an acceptable bioavailability. Highly water soluble drugs on the other hand need a different PSD, which can increase or decrease the complexity of operation during the formulation step. Secondary processing, turning API into usable products, largely determines what kind of final crystal size is required. API, which is supposed to be tableted, can be in a range of a few hundred microns, whereas API meant for inhalation should range from 1 to 10 microns in order to access the lungs when inhaled.

An important influencing parameter in crystallisation is the crystal shape or habit, which is referred to as morphology and describes the physical appearance of a crystal but does not give direct information about the polymorph. Depending on the processing conditions, one polymorph can have various morphologies. Generally there are three common types of crystal morphologies: Needles (one key growth dimension), platelets (two key growth dimensions) and cubes (three key growth dimensions), which have different effects on down-stream processing.

The flowability, for example, is strongly dependent on morphology. Long needles exhibit a poor powder flowablity, which is disadvantageous during downstream processing. Reducing the aspect ratio, moving towards a more cube like crystal, significantly improves the flowability. Secondary processes are rely on crystals with favourable morphology and a narrow PSD in order to make, for example, tablets, which do not break apart after being produced. Advantageous for tableting are spherically agglomerated cube-like crystals with a good compressibility.

The crystal morphology also has an influence on filtration, where crystals need to be separated from the mother liquor. The crystal slurry is poured onto a filter, the liquid passes through the filter media and oversized solid crystals are retained. Small particles with the tendency to form thick filter cakes will block the filter, whereas large crystals tend to filter better. Crystal size and shape can often be associated with the cake permeability and the filtration behaviour can usually be changed by changing the crystal properties.

Looking at crystallisation from process optimisation or process economics points of view leads to the consideration of the overall process yield. For efficient crystallisation operations it is important that as much as possible of the desired compound in solution is turned into recoverable crystals and that losses, resulting from the solubility of the compound in the mother liquor, are reduced to a minimum.

Cooling the crystal slurry to low final temperatures and/or adding an antisolvent are two possible techniques how the final solubility of the desired compound in the mother liquor can be reduced. However, increasing the process yield also affects the ratio between compound molecules and impurities in the mother liquor, which leads to an increased incorporation of impurities into the final crystal.

After crystals are separated from the mother liquor they need to be dried to evaporate all remaining liquid and to obtain useable crystals for secondary processes. In a first step excess bulk liquid is evaporated, followed by liquid adhering to the crystals before finally bound liquids (solvates and hydrates) are driven off. The wet powder is exposed to elevated temperatures, reduced pressures and sometimes agitation in order to accelerate the drying process. However, elevated temperatures and lowered pressures can lead to polymorphic transformation of the crystals, which is undesirable. The drying process itself can lead to agglomeration and bridging of particles, which can make down-stream processing more challenging. Agitation itself can lead to abrasion and breakage, which has a negative influence on the PSD. Additionally, mechanical stress on particles during drying is almost impossible to predict, scale-up and reproducible processing is extremely difficult and for that reason good understanding is necessary if and when stirring is at all required.

General physical properties of crystals produced in primary processing can be influenced by a tight control over the nucleation event. However, controlling nucleation (generation of a new solid particle), the polymorph, morphology and PSD is a difficult task and depends on various factors like supersaturation, temperature, stirring, a stochastic onset of nucleation and the resulting nucleation rate. Even crystal growth (systematic addition of solute material and impurities to an existing crystal) is not straightforward due to its dependence on supersaturation, influencing crystal purity and downstream handling properties. As nucleation and growth both compete for the available supersaturation and both processes can happen at the same time, it is obvious that this increases the complexity of the process.

Crystallisation starts with the generation of supersaturation of the solute in the bulk solution, which is essential to generate the driving force for nucleation and growth. Low supersaturation has a low driving force and crystallisation is slow. In many systems a higher supersaturation corresponds to quicker, sometimes even undesired, spontaneous crystallisation or oiling-out with poor control over the process.

The addition of small seed crystals, which grow to a desired final size, can solve many problems in crystallisation. The stochastic nucleation step with its uncertainty and variability is no longer required as seeds of the correct polymorph, morphology and

narrow PSD can be added to the slightly supersaturated bulk solution. The purpose is to avoid spontaneous nucleation and to maintain good process control.

However, the generation of seeds itself is not a straightforward process either. It can involve several challenging processing steps like handling/conveying of solids, milling and resuspension of crystals to make up a seeding slurry. On top of that, the optimal point of seeding (when the solution concentration for the first time crosses the solubility curve) as well as the number of seeds added to the process needs to be worked out. However, batch-to-batch variations and different impurity levels shift the solubility curve, resulting in the risk of fully dissolving the seeds or of adding them into an already highly supersaturated or nucleated solution.

Supersaturation in solution can be generated by cooling a hot-saturated solution to a lower temperature and if the solubility difference for the solute is large enough crystals will appear. Batch natural cooling, based on environmental conditions and the heat transfer characteristics of the crystallisation vessel, is straightforward but generates varying supersaturation profiles with poor reproducibility and process control. Under these conditions the optimal point for seeding might be missed, supersaturation in the bulk solution can reach values where uncontrolled, spontaneous nucleation might occur, crystals might occlude solvent or impurities and particles can agglomerate creating a broad PSD. Another area of concern are the vessel walls, which are always a little cooler and therefore supersaturation in the liquid-wall boundary layer is a little higher than in the bulk solution. This can lead to crystals sticking to the cooling surfaces, non-uniform crystal growth and a non-reproducible product, which should be avoided.

An alternative to natural cooling is so called batch controlled cooling of a jacketed crystallisation vessel with a tightly temperature controlled heat exchange fluid (mostly water or oil). This process does not depend on environmental conditions, it allows slower cooling rates and the temperature in the bulk can even be kept constant, if required, to achieve good control over supersaturation in the seeding or near growth area. A slow cooling profile can also minimise the temperature difference between the bulk solution and the vessel walls to avoid unwanted crystal growth on cooling surfaces. Controlled cooling hence provides more and better control over the crystallisation

process and helps achieving reproducible manufacturing and more uniform product crystals.

One system dependent challenge both techniques are facing is the large temperature zone the process travels through during operation. Even in seeded crystallisation, cooling through temperature zones with potentially different polymorph stabilities is a problem as the desired polymorph might dissolve, leading to uncontrolled nucleation of an undesired form. In some cases the final product turns out to be purely the undesired polymorph, other cases might yield a polymorph mixture.

A different approach to create supersaturation in a bulk solution is to concentrate the solute by evaporating off solvent from the solution. The volatile compounds will leave the solution creating an increased concentration of non-volatile compounds (this can also include impurities), which in turn experience supersaturation and start crystallising. Batch evaporative crystallisation has several challenges starting with a supersaturation gradient from the bottom to the surface, where volatile compounds leave the solution and nucleation is most likely to occur. But also the boiling liquid/vapour interfaces and heating surfaces of the crystallisation vessel generate a considerable source for nucleation and subsequent encrustation of crystals on submerged surfaces. Control of supersaturation is the key issue in evaporative crystallisation as poor control can lead to a completely non-reproducible crystal product output. Seeding such processes is extremely difficult as the concentrated impurities in the bulk solution have a severe impact on the solubility curve of the desired compound. This makes it very difficult to predict when the solubility line is crossed and to find the correct point of seeding. Evaporative crystallisation is used for a few, mostly water based, very large scale products like the production of table salt or sugar as well as some industrial chemicals but is very rarely used in the pharmaceutical or fine chemical industry. This could also be because evaporation of large volumes of organic solvents creates a big health and safety issue.

A popular alternative for the creation of supersaturation is the mixing of two fluids, one exhibiting a good solubility and the other one a very poor solubility for the solute. In batch antisolvent crystallisation good control over supersaturation can be achieved by controlling the antisolvent/solution addition rate to the bulk mixture. However, in order to

avoid undesired local high supersaturation at the addition point, it is necessary to ensure rapid, proper mixing of the two streams.

The proper determination of the seeding point is one of the key challenges in antisolvent crystallisation and the changing solubility as well as dilution effects make it a more complex operation than single-solvent systems. Another disadvantage is the reduced volumetric productivity due to the necessity of creating a solvent mixture and the associated efforts of separating and recovering solvents.

However, antisolvent crystallisation is widely used throughout industry as it has advantages over batch cooling and evaporative crystallisation in terms of supersaturation and process control.

A different principle of creating supersaturation for crystallisation is utilised in batch reactive crystallisation, where the solute supersaturation is generated by the formation of the desired solute molecule through a chemical reaction. The reaction can take place between two complex organic molecules or it can be a neutralisation step, using a simple acid or base, to form a salt or acid of the desired compound.

One of the key operating steps in reactive crystallisation is the mixing of the two streams to ensure proper micromixing before nucleation starts. However, chemical reactions can be very fast compared to mass transfer, nucleation and crystal growth rates, which, despite proper micromixing, can lead to local high supersaturation, uncontrolled nucleation and broad PSD. It is very difficult to slow down chemical reactions, which results in poor control over the local supersaturation. However, by adjusting the addition rate of reactants, some control can be obtained over the global supersaturation.

Seeding a reactive crystallisation process is not straightforward due to the challenge of very fast reactions and poor control over local supersaturation. Seeds can be used to control global supersaturation but the local supersaturation might still trigger excessive nucleation.

The large number of poorly understood influencing factors on crystallisation as well as the broad diversity of techniques and limited process control makes crystallisation a rather complex unit operation, which requires a high degree of operating flexibility. Traditionally in the pharmaceutical and fine chemical industry such flexibility is achieved

by batch processing, which is very versatile and can adapt processing conditions to the specific needs of an individual batch of product and its properties. One production line can accommodate a large number of different products with different physical properties, produced under completely different processing conditions, from small to large scale. However, batch processing is also inefficient as a lot of potential processing time is lost to filling input materials, heating/cooling and discharging the bulk solution as well as cleaning the equipment for the next batch. It is a labour intensive way of running equipment and the operating costs are considered to be fairly high.

Other industries with less complex unit operations (automotive industry), tighter control over their processes (oil and gas industry) or when huge bulk quantities are needed (bulk chemical industry) turned away from batch processing and focus on continuous manufacturing. The concept of production in flow without interruptions is based on reactors with constant inlet & outlet flow and usually run 24/7, only stopping production for infrequent maintenance work. Continuous processes are highly automated, less labour intensive and very economic for large scale production. They constantly deliver better product quality, are more sustainable and have a lower waste & carbon footprint. However, continuous manufacturing lines are usually purposely designed for a single product and require full process understanding to ensure proper operations. The high degree of required process understanding in continuous crystallisation makes batch processes the preferred mode of operation in the pharmaceutical and fine chemical industry.

Nevertheless, several attempts have been made recently by various research groups and commercial companies to also turn pharmaceutical and fine chemical crystallisation processes continuous. Considerable literature is available on performing continuous crystallisation of small organic molecules using static and in-line mixers, stirred tank cascades, tubular crystallisers, oscillatory flow units and combinations of the above.

Researchers at ETH Zurich, for example, worked with static mixers to investigate nucleation and crystal growth kinetics and in-line mixers to study micromixing in systems with fast reaction kinetics [8.8 – 8.10]. At the Graz University of Technology various continuous crystallisation setups consisting of static mixers and tubular crystal growth units were studied in order to assess effects of different tube length,

temperatures, seed loadings, sonocrystallisation and how these parameters can help controlling final crystal size distribution [10.3, 10.7, 10.8].

A different route towards continuous crystallisation, using a cascade of stirred tank crystallisers, was explored by the Novartis-MIT Center for Continuous Manufacturing. Various ways of combining the tanks led to several different setups allowing researchers to investigate either cooling crystallisation or antisolvent/cooling crystallisation with or without a recycle loop. The work was predominantly focused on arranging different setups and understanding the connection between residence time, yield and purity [10.2, 10.13, 10.14]

One of the first commercial companies investigating the novel Continuous Oscillatory Baffled Crystalliser (COBC) and batch Oscillatory Baffled Crystalliser (OBC) was AstraZeneca. In a detailed study performed in 2009 results from OBC & COBC experiments were compared by assessing processability, crystal morphology, final size distribution and batch filterability [10.1].

Despite great academic and industrial efforts at laboratory and commercial scale to date only a very limited number of small molecules and APIs have made it into continuous manufacturing successfully.

The present work ties into the aim to accelerate the adoption of continuous manufacturing of high-value chemical products, in order to achieve more precise control of particulate product attributes, such as solid form, particle size distribution and morphology.

Batch manufacturing provides a high degree of operational flexibility where the same process equipment can be used for multiple processes in a sequence of distinct batch operations. Continuous manufacturing typically provides less flexibility as specific process equipment is dedicated to each step of the manufacturing process, but it allows for steady state operation which can provide consistent product quality. Reliable steady state operation may require a high level of process understanding facilitated by implementation of appropriate process monitoring and control approaches.

Optimal conditions for nucleation are different from optimal conditions for crystal growth and each step comes with individual challenges, which need to be understood and dealt with separately during process optimisation. In this context, the spatial segregation of continuously nucleating seed suspension from subsequent continuous growth

processes will be focused on. Decoupling the two processes into separate unit operations allows better control, modelling and optimisation of each step, as seed crystals can be nucleated under very different conditions compared to those under which they are grown. Seeding suspension can be injected into a crystal growth solution, coming from work up, providing solute molecules for crystal growth.

Based on the concept of separating nucleation of seed crystals from subsequent crystal growth it is desirable to develop a Plug & Play crystalliser system with a set of various different platforms to nucleate and grow product crystals. Such a tool box would give a high degree of flexibility when it comes to choosing compound specific nucleation and growth units. [2.1-2.3, 7.12, 8.8, 8.9, 9.8, 9.15, 10.1, 10.3, 10.7]

3 Theoretical background

The underlying principle of many physical and chemical processes and their engineering applications is thermodynamics. It provides a connection between heat, energy and work in order to describe the state of a system through its macroscopic parameters like temperature, internal energy, enthalpy, entropy or pressure and their relations to each other.

Whether or not a physical or chemical process happens spontaneously can be assessed by studying its Gibbs free energy shown in Equation 3-1.

$$dG = dH - T\,dS$$
Equation 3-1

G: Gibbs free energy

H: Enthalpy

T: Temperature

S: Entropy

At fixed temperature systems try to minimise dG and the following rule applies:

dG> 0: Spontaneous change of the system is not possible

dG< 0: Spontaneous change of the system is possible

For most chemical reactions the assessment of dG is sufficient to tell whether or not a reaction will happen spontaneously. However, the molar Gibbs free energy or in other words the chemical potential of a system is of broader significance as it provides a more general definition. It is a parameter which describes the potential of a substance to bring physical (phase transition or phase stability) or chemical change (reactions) to a system.

Only if the chemical potential between substances and phases present in the system is equal there is true equilibrium. However, if the chemical potential of a system at point 1 is higher compared to point 2 there is the tendency of spontaneous transfer in order to decrease the difference in chemical potential.

But even if a system is in equilibrium and the desired process is to force a chemical reaction to reverse, e.g. compress a gas or to cool an object below ambient conditions, this is still possible but it will not happen spontaneously and requires work to be done on the system.

3.1 Phase diagram

The chemical potential of a system can be influenced and changed by external parameters like temperature or pressure. Once the parameters are set, the system will try to re-establish equilibrium and equal chemical potentials between all phases present in the system. This can lead to the appearance of a new, more stable phase or the disappearance of a less stable phase within the system. Phase changes occur due to the system decreasing its Gibbs free energy.

A phase diagram indicates how external parameters affect the thermodynamic stability of the phases a system can develop. Equilibrium lines separate areas in which certain phases are stable and indicate under what conditions they become unstable. Figure 3.1-1 illustrates that at low temperature and high pressure water in its solid form (ice) would be the most thermodynamically stable phase, whereas at high temperature and low pressure ice becomes unstable and water vapour is the most stable phase.
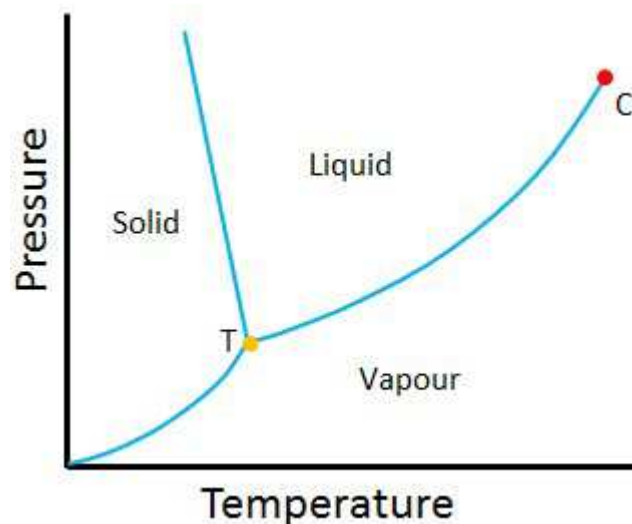
Figure 3.1-1: Phase diagram of water

T: Triple point   =>   Three phases in equilibrium

C: Critical point =>   Phase boundaries disappear

The Gibbs rule of phases, see Equation 3-2, describes how many degrees of freedom, that is parameters such as temperature, pressure or concentration, can be changed independently in a system with a given number components and phases in mutual equilibrium:

$$F = C - P + 2$$

F: Degrees of freedom of a system

C: Number of components (compounds of different chemical structure)

P: Number of thermodynamic phases (solid, liquid, gas)

A pure substance (e.g., water – one compound) present as one thermodynamic phase (e.g., liquid) has got two degrees of freedom and it is hence possible to vary two parameters independently while the water remains liquid.

In the case of water (one compound) present as two phases (liquid water + solid water (ice)) according to the phase rule there is only one degree of freedom and it is hence possible to independently change only one process parameters (either pressure or temperature) without the system being out of equilibrium. The process parameters now depend on each other while the system stays in equilibrium. If the temperature is to be increased slightly and the water-ice composition has to stay constant then the pressure on the system also has to be changed in order to prevent the ice from melting. [2.2]

3.2 Solubility

In a pure solvent, at given temperature and pressure, the chemical potential is equal throughout and no spontaneous changes in the system should be expected. With the addition of a solute into the solvent, the chemical potential between solvent, dissolved solute and undissolved solid is disturbed and the system tries to re-establish equilibrium, which leads to the dissolution of the solute in the solvent. If the amount of solute is small, it will be dissolved completely. However, if the amount of solute is high, the system will naturally approach an equilibrium between dissolved solute and remaining undissolved solid until the solution is saturated.

For many solvent/solute systems this equilibrium depends on a number of different parameters such as temperature, pressure, solute concentration, solvent composition or the pH and the system responds to changes of these parameters. Figure 3.2-1 shows an example phase diagram of a solvent/solute system as it could typically be used in the design of a cooling crystallisation process. At high temperature a lot of solute can be dissolved in the solution. As

Figure 3.2-1: Phase diagram of solvent/solute system (P: Different phases present in system). Orange dashed line describes ideal concentration trajectory along solubility curve (blue).

the solution is cooled down it reaches the blue equilibrium concentration line (solubility line) at point 1. Cooled past that point a single homogeneous solution becomes thermodynamically metastable or unstable and a system of dissolved solute + undissolved solid becomes thermodynamically stable. At this stage the solid coexists with a leaner solution of dissolved solute.

At continued slow cooling the solute concentration will follow the blue/orange dashed line and more solid will come out of solution until the final temperature is reached at point 2.

When the final temperature is reached, the system equalises the chemical potential between the solvent, dissolved solute and undissolved solid and establishes a dynamic equilibrium. If all operating parameters remain unchanged, there is no tendency for the system to undergo any further changes.

Accurate solubility data is essential for successful crystallisation process development. It needs to be obtained experimentally at an early stage and will be explained in more detail in the methods section (see 4.6). The maximum amount of solute which can be dissolved before crystallisation starts, as well as the amount of solute which remains in solution after the crystallisation is finished are important parameters and depend on the substance, solvent composition and operating parameters.

Solubilities can be expressed in many different units based on mass or moles of solute in mass, volume or moles of either solvent or total solution. If volume based units are used, special attention must be paid to densities, which is less of an issue when working with masses only.

3.3 Supersaturation

If a solvent/solute system is cooled past the solubility line at point 1, as shown in Figure 3.3-1, it enters the area where undissolved solid coexists with dissolved solute. However, if the generation of the undissolved solid is kinetically hindered, solute concentration remains constant and follows the orange dashed line despite the fact that solid should theoretically come out of solution. The solution is then considered supersaturated with respect to the solute and possesses the ability to crystallise.
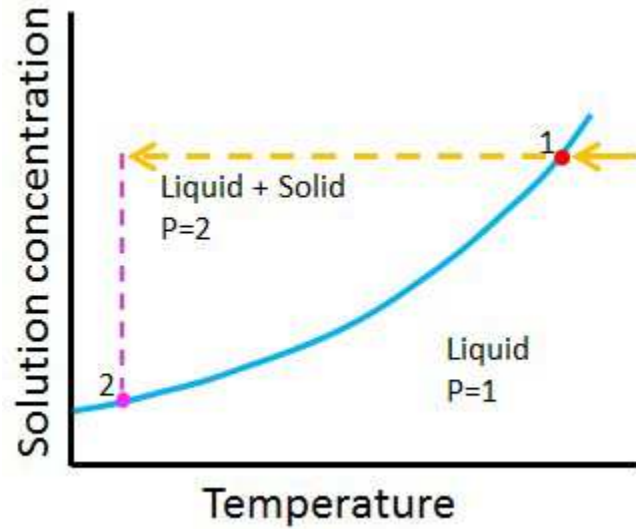
Figure 3.3-1: Phase diagram of supersaturated solvent/solute system. Pink line indicates degree of total supersaturation before nucleation.

Supersaturation is obtained whenever a solution contains more solute than thermodynamic equilibrium allows to be dissolved under the current operating conditions. Supersaturation is the driving force for both nucleation of new crystals and growth of existing crystals. In crystallisation, a high degree of supersaturation generally leads to the formation of large numbers of very small crystals, whereas lower supersation leads to a smaller number of larger crystals. The generation of homogeneous supersaturation throughout the entire sample is essential in order to achieve consistent and reproducible product crystals.

3.4 Metastable Zone & Metastable Zone Width

The formation of crystals in solution theoretically starts as soon as the solution concentration crosses the solubility curve. However, located behind the solubility curve is a metastable zone, as shown in Figure 3.4-1, in which already existing crystals can grow to larger sizes but the nucleation of new crystals from solution is very slow. Instantaneous nucleation of new crystals only happen once

Figure 3.4-1: Phase diagram of solvent/solute system with metastable zone. Orange dashed line describes possible realistic concentration trajectoy.

the reducing temperature drives the supersaturation into the unstable zone.

The amount of supersaturation required to penetrate the metastable zone depends on the individual compound, hydrodynamics and operating conditions. Vigorous stirring and slow cooling generally reduces the metastable zone, whereas slow stirring and crash cooling broadens the metastable zone.

Detailed knowledge as well as careful determination of the metastable zone under specific flow conditions and cooling rates is very important for successful process control. Depending on the process requirements it might be desirable to either have a very small or, for different objectives, a very broad metastable zone.

In seeded crystallisation processes the seeds should be added to the system when the solution concentration is located in the centre of the metastable zone to avoid dissolution or unwanted spontaneous nucleation. In systems where primarily crystal growth is desired a wide metastable zone is advantageous as it allows a higher degree of processing flexibility.

3.5 Induction time

During the cooling procedure of a sample and when the solution concentration crosses the solubility curve, the generation of supersaturation is started. However, initially the crystal formation is very slow due to a low crystallisation driving force and the existence of the metastable zone close to the solubility curve. As cooling proceeds and more supersaturation is generated, spontaneous crystallisation will happen when the solution concentration hits the unstable zone. The time from when the first supersaturaton was generated until the first crystals can visually be detected is known as induction time.

Several factors have an influence on the induction time of a system, for example, the temperature, solution supersaturation, the mode of agitation, solvent composition, seed crystals, undissolved solid particles and dissolved impurities. The experimental observations on the effects of relevant processing parameter and obtained data should be carried out with care due to the many influencing factors and potential huge variability.

Another challenge is that the induction time covers the event of nucleation as well as the event of crystal growth. If a system very quickly nucleates crystals below the detectable size but existing crystals grow very slowly then the induction time might appear to be very long. On the other hand, if a system slowly nucleates few, very fast growing crystals then the induction time might appear to be very short.

3.6 Nucleation

The starting point of crystallisation is the formation of a new solid phase from the bulk solution. Local concentration fluctuation causes the dissolved solute to continuously form and decompose molecular clusters and supersaturation is the absolute requirement for the rate of formation being greater than the rate of decomposition. These days two major nucleation theories are available which will briefly be discussed in the following sections.

3.6.1 One step nucleation theory

Molecules in solute are considered to be building blocks, which attach to each other on a one-by-one basis to form a nucleus. However, the attachment of building blocks is kinetically hindered and work is required to overcome the gain in surface energy obtained due to a larger surface area of the forming cluster. This process is illustrated in Figure 3.6-1

For very small clusters the work to overcome the surface energy is larger than the reduction in free energy due to the formation of a new thermodynamic phase but once a critical size is reached, further addition becomes favourable and will result in a stable new phase. Nucleation can hence be considered the successive addition of building blocks to a critical molecular cluster (nucleus) and the classical nucleation mechanism can be described by Equation 3-3.
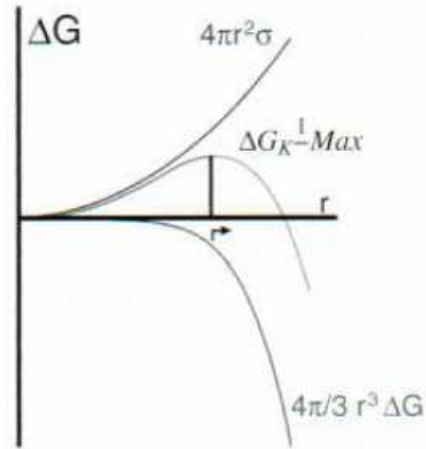
Figure 3.6-1: Nucleation and growth of a new thermodynamic phase from supersaturated phase. Building blocks aggregate until critical nuclei size is reached and growth of the new thermodynamic phase takes over. [2.1]

$$\Delta_k G_r = \frac{4\pi}{3} r^3 \Delta_V G - 4\pi r^2 \sigma$$

Equation 3-3

$\Delta_k G_r$	= Free energy of formation
$4\pi r^2 \sigma$	= Energy of surface formation
$\frac{4\pi}{3} r^3 \Delta_V G$	= Energy of condensation
r	= Radius of cluster
σ	= Surface tension
$\Delta_V G$	= Bulk free energy per unit volume of new phase

3.6.2 Two step nucleation theory

A different nucleation mechanism was described by Vekilov (2010) in which the molecules of solute in supersaturated phase do not directly form nuclei of the resulting new phase. Instead, concentration fluctuation makes solute molecules form denser areas, leaving the rest of the solution a little leaner in solute. Once these clusters or droplets of denser solute phase overcome the critical cluster size they become unstable and nucleate a new macroscopic phase. This mechanism is illustrated in Figure 3.6-2.

However, these complex procedures are difficult to detect with current analytical methods and there is no consensus as to how large a nuclei is, which makes nucleation a poorly understood and hard to control event. On top of that nucleation can occur according to three different mechanisms in the absence or presence of solid material, which provides a source for nucleation. [3.3]
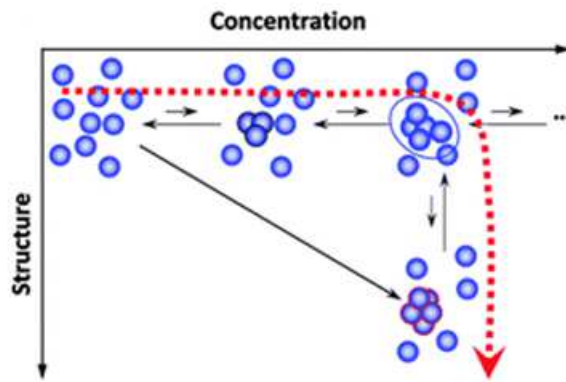
Figure 3.6-2: Mechanism of two step nucleation theory. Solute molecules form areas of denser solute phase, the critical cluster size is exceeded and nucleation starts [3.3]

A phenomenon sometimes seen during crystallisation is that the supersaturated solution undergoes liquid-liquid separation forming macroscopic droplets before any crystallisation occurs. The liquid droplets can coalesce into a separate organic rich (oily) layer and that is why it is referred to as oiling-out. This behaviour is very compound specific and hard to predict. Since liquid-liquid phase separation in these systems leads to metastable phases with respect to liquid-solid (crystal) equilibrium, it is kinetically controlled and eventually crystal nucleation occurs in one of the liquid phases. Oiling-out depends on various process parameters, for example, the way how supersaturation is generated, agitation intensity, nucleation kinetics and impurities. It can cause major issues during crystallisation, such as high impurity levels, undesirable particle size distribution, poor filterability or high cake moister content. Therefore oiling-out should be avoided if possible.

3.6.3 Primary homogeneous nucleation

Is the formation of a nuclei in the absence or without the help of the same or any other foreign material. According to the classical nucleation theory, there is a system specific critical stable cluster size and smaller clusters dissolve again whereas larger clusters keep growing.

3.6.4 Primary heterogeneous nucleation

Describes the formation of a nuclei in the presence or with the help of a foreign material. The foreign surface lowers the energy barrier and acts like a catalyst for nucleation, which makes heterogeneous nucleation proceed significantly quicker than homogeneous nucleation.

3.6.5 Secondary nucleation

Is the particle formation process in the presence of pre-existing crystals of the same compound. This type of nucleation requires less supersaturation compared to primary nucleation as the new crystals can form on already existing parent crystals or originate from breakage / attrition of parent crystals.

In this respect, contact nucleation from crystal-crystal, crystal-impeller or crystal-vessel wall collisions are most common as the crystals get damaged or molecular clusters are removed by fluid shear.

Nucleation is the key operation during the entire crystallisation process and is influenced by a number of processing parameters like, for example, the level of supersaturation, solvent composition, impurities, intensity of mixing or the vessel geometry. A loss of control over the nucleation process can severely affect the nuclei generated and can eventually lead to off-specification product crystals.

A predominantly nucleation-driven crystallisation process generates fine product crystals with a high surface area and low bulk density. However, there is a high risk of large batch-to-batch variations, occlusion of solvent and impurities into the nuclei and scale-up difficulties, unless the level of supersaturation is well controlled.

3.7 Polymorphism

Tight control over the nucleation process is of great importance as some substances have the ability to crystallise in more than one crystal structure. Depending on the processing conditions molecules forming a crystal can arrange in different unit cell packings, which results in different polymorphs. These different polymorphs can have very different physical parameters, which might deviate substantially from the desired parameters of the desired crystal structure. One polymorph can be a potent drug with very good solubility, dissolution rate and bioavailability, whereas another polymorph can be ineffective due to low solubility, dissolution rate and bioavailability. Polymorphism can also affect secondary processing when an unwanted polymorph with broad particle size distribution clogs filters or different morphologies reduce the powder flowability. Downstream separation of undesired polymorphs from the bulk material is often very difficult or impossible and therefore it is necessary to make sure that undesired polymorphs do not nucleate in the first place.

However, according to the Ostwald rule of stages, it is not always possible to avoid the nucleation of undesired polymorphs as it often happens that the metastable form closest to the initial state of free energy in the system nucleates first. According to the rule, the metastable form then transforms to the stable one. The Ostwald rule applies to some systems but not to all and every system needs critical assessment whether or not it follows the rule.

The feature of polymorphism affects every stage of the drug development process from discovery through to clinical trials. All possible polymorphs of a substance need to be known at a very early stage during the development phase in order to avoid potential future problems and conflicts.

Polymorphs are classified into two different kinds. In a monotropic system there is one thermodynamically stable crystal form over the entire temperature range up to the melting point. In an enantiotropic system, on the other hand, for defined temperature ranges different polymorphs show thermodynamic stability with distinct transition temperatures.

In the case of solid material, phase transition from one polymorph to the other is very slow due to immobility of molecules in the crystal lattice. However, in the case of

solution-mediated transformation, where crystals are suspended in liquid, the transition can be rapid as the liquid increases molecule mobility substantially.

Special care must be taken during unit operations like filtration, drying or milling of crystalline material as changed operating conditions (pressure, temperature or mechanic shear) can shift thermodynamic stabilities and cause polymorphic transformation.

Various analytical methods are available to identify new polymorphs or analyse the polymorphic population of a sample. Useful tools for showing differences in the solid state composition of single crystals or powder samples are X-ray diffraction (XRD), nuclear magnetic resonance (NMR) or Raman spectroscopy.

Additional methods utilising thermal analytical techniques, for example, differential thermal analysis (DTA), differential scanning calorimetry (DSC) or thermogravimetry (TG) can provide further useful insights.

3.8 Morphology

Unlike liquids or gases, crystals have a well-defined three-dimensional appearance and come in different shapes and aspect ratios. Diverse molecular packing in the crystal unit cell often but not always leads to a different visual appearance of the crystal however, a different shape gives no definite indication of its internal crystal properties or the polymorph. The different crystal shapes can generally be classed into three common morphologies.

- Needle-like: Only one key dimension length and growth into one direction
- Plate-like: Two key dimension lengths and growth into two directions
- Cube-like: Three key dimension lengths and growth into three directions

In the same way as different polymorphs can have completely different physical properties, crystals of different morphology can have different mechanical properties. The flowability behaviour of needles, for example, is poor compared to cubes and spherically agglomerated cubes are favourable for good compressibility properties. The morphology of particles affects downstream processing like filterability and drying behaviour as well as numerous operations during secondary processing.

Different solvent systems can yield different crystal morphologies and it is advisable investigating what solvent yields the desired shape. Optical and scanning electron microscopy are very useful tools in identifying crystal morphologies.

3.9 Growth

The first step of the crystallisation process is the nucleation of a new crystalline phase of desired polymorph and morphology. In the second step, assuming sufficient supersaturation is still available, the newly formed nuclei grow to a larger crystal size until all or most of the remaining supersaturation is consumed. In contrast to the nucleation event, crystal growth can easily be detected by measuring the particle size distribution of the sample, unless agglomeration or crystal breakage is present.

Crystal growth is an impurity rejection process and a low degree of supersaturation, even within the metastable zone where no primary nucleation would happen, is preferable. During growth the rate of integrating molecules into the crystal lattice is greater than the release of molecules from the crystal surface and the classical view is that this process happens at a constant velocity, independent of the crystal size.

Growth is envisioned to happen in a layer-by-layer fashion as molecules reach the crystal surface however, there are different mechanisms how a crystal can grow.

- Continuous growth:
  A sufficiently high number of kink & step sites ensure that all approaching growth units are integrated with minimal complication
- Two-dimensional nucleation:
  Smooth crystal surfaces need steps to be generated in order to accept approaching growth units. Nucleation on the crystal surface is the starting point for a layer to spread (birth & spread)
- Spiral growth:
  Stress within the crystal causes dislocation of the lattice and incoming growth units form new crystal layers spiralling around the dislocation

A predominantly growth-dominated crystallisation process yields large product crystals of high purity, which are easy to handle in downstream processes like filtration, washing or drying. However, larger crystals become more sensitive to attrition and breakage, which causes secondary nucleation and interference with the benefits of crystal growth processes.

3.10 Balance of nucleation and growth

Crystallisation is a process driven and dominated by supersaturation and results heavily depend on careful process control. High levels of supersaturation lead to excessive nucleation of fine particles, whereas low supersaturation leads to growth of the particles to larger crystals. The balance between nucleation and growth determines physical and mechanical properties of the product crystals and how well chemical impurities are rejected by the growing crystal. [2.1, 2.2, 3.1 - 3.3]

4 Methods

4.1 X-ray powder diffraction (XRPD)

The crystal unit cell is unique for each compound in terms of atomic arrangement, spacing between the atoms and their angles to each other. The atoms in the crystal arrange in a periodical, three dimensional fashion and thus define many of the physical properties of the compound. XRPD is a rapid and non-destructive spectroscopic method to characterise the unit cell parameters of crystalline material.

The visible record generated by XRPD analysis is called a diffraction pattern and consists of a set of intensity peaks dependent on the incident angle of the X-ray beam. Different unit cell parameters result in different polymorphs of a crystalline material which are determined and compared
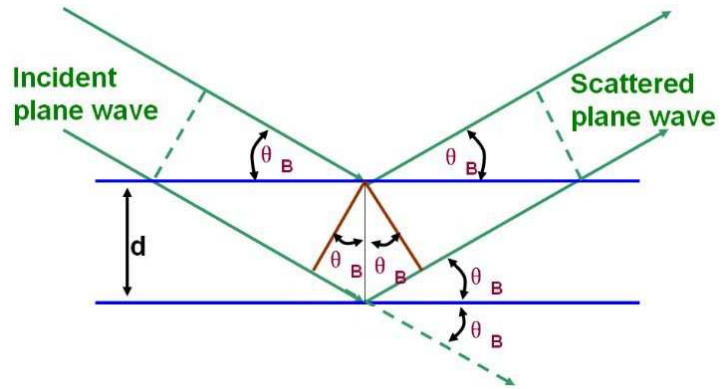
Figure 4.1-1: Principle of X-ray powder diffraction [4.1]

against a library for identification. W. Bragg in 1913 showed that diffracted X-ray beams are reflected from different planes in a crystal, similarly to a mirror. Figure 4.1-1 illustrates the reflection of incident beams when hitting the atoms of a unit cell. The angles of the reflected beams are detected and the Bragg $n\lambda=2d\sin\theta$ Equation **4-1** can be used to determine the space between the lattice planes.

$$n\lambda = 2d\sin\theta$$
Equation 4-1

n: Integer value relative to diffraction plane

λ: Wavelength of the radiation used

d: Perpendicular space between the lattice planes in the crystal

Θ: Angle of the incident and reflected X-ray beam

XRPD can be used for Bragg Scattering of crystalline solids. An amorphous sample gives broad background signals, which are not suitable for unit cell characterisation. The position and relative intensity of peaks generate a fingerprint, which can be used for identification of a compound. However, a mixture of multiple compounds also generates superimposed spectra of all individual compounds.

When a unit cell undergoes transformation from a thermodynamically metastable to a more stable form, XRPD can pick up the change in atomic arrangement in the unit cell. The change can be picked up by disappearing old peaks and appearing new peaks in a different 2Θ.

This makes XRPD the chief method for characterisation of crystal structures.

Single crystals exhibit very distinct sets of lattice spacing and diffraction patterns may only be observed for special angles of incident X-ray beams. Other angles will not contribute to the diffraction pattern. However, if the crystal is rotated in the beam, additional patterns can be observed.

The majority of crystals, on the other hand, are no single crystals and can be considered a mosaic of blocks of different unit cells. These blocks are all slightly misaligned in comparison to their neighbouring unit cells. That is why it is possible that over a small range of Θ some reflection can be observed in almost any orientation. [4.2]

In order to prepare a powder for XRPD analysis it first needs to be crushed with a mortar & pestle to obtain a representative sample. The XRPD sample holder is an aluminium tray covered with an X-ray inactive foil, generating a little pit, which holds a small amount of the sample.

The sample holder is placed inside the machine and when the analysis is started, the X-ray source moves across the pit covering angles between the source and detector of 4-35 degrees. The diffraction pattern is generated by the reflection of the X-ray beam at various crystal planes as the X-ray source moves across the sample.

4.2　Laser diffraction particle sizing

Nucleation is considered to be a stochastic process, depending on various parameters, with some crystals nucleating earlier and others at a later point in time. Different times of nucleation lead to different exposure times of the crystals to supersaturated solution and thus different particle sizes of the individual crystals are obtained. Laser diffraction particle sizing is a non-destructive, spectroscopic method to determine the diameter or a diameter distribution of particles under the assumption that all particles are of perfectly spherical shape. [4.3, 4.4]

Real crystals often deviate from perfect spherical shape and exhibit various different shapes like needles, platelets or prisms. The measurement generates a volume based particle size distribution comparing the actual scattering to that of perfect spheres. Laser diffraction particle sizing assesses the angular variation in light scattering behaviour of particles with variable shape, matches it to the size of a perfect sphere, which would scatter in the same way and reports the diameter as a volume equivalent sphere diameter. [4.3]

Figure 4.2-1 shows a schematic set up of a laser diffraction particle sizing instrument. During the measurement a sample passes through a flow cell in which it is exposed to the laser and scatters the laser light according to the size distribution present in the sample. Detectors located around the flow cell measure the scattering pattern covering a wide range of different angles to generate the particle size distribution graph. [4.5]
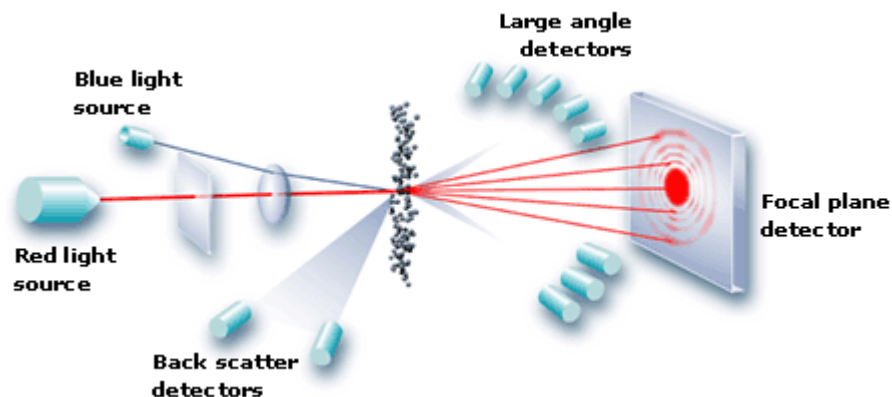
Figure 4.2-1: Setup: Particle sizing by light scattering [4.5]

In order to prepare a sample for particle size measurement it is essential to operate the equipment with the same fluid as is present in the sample to be measured. Ideally the fluid is an antisolvent for the compound to be measured or the fluid needs to be saturated with respect to the compound to avoid dissolution. Before each measurement, the background scattering needs to be accounted for by zeroing the instrument with working fluid alone.

When the machine is ready, the sample slurry can be added to the sample container until the working slurry reaches a sufficiently high concentration for the measurement. After the measurement, the particle size data is provided by an appropriate software package. [4.3 – 4.5]

4.3   Focused Beam Reflectance Measurement (FBRM)

A chord is a line segment, which connects two points on a curve and its length indicates the beginning and end point of an object intersecting the curve. Figure 4.3-1 shows a focused laser beam following a circular path while scanning over a set of crystals. The chord length can be used to determine the width of a particle in that area but does not give sufficient information about the dimensions or shape of the entire particle. It is hence not possible to use this technology for particle size measurements. FBRM is a rapid and non-destructive spectroscopic method to characterise chord lengths of a particle.

The irregular nature of crystals and the random orientation while intersecting the laser beam curve results in a number of different chord lengths being measured by FBRM. Figure 4.3-2 illustrates how the particle detection leads to an output signal similar to a digital signal, which can be converted into a chord length distribution (CLD). The output of an FBRM analysis is a graph showing the CLD in form of a bell shape.
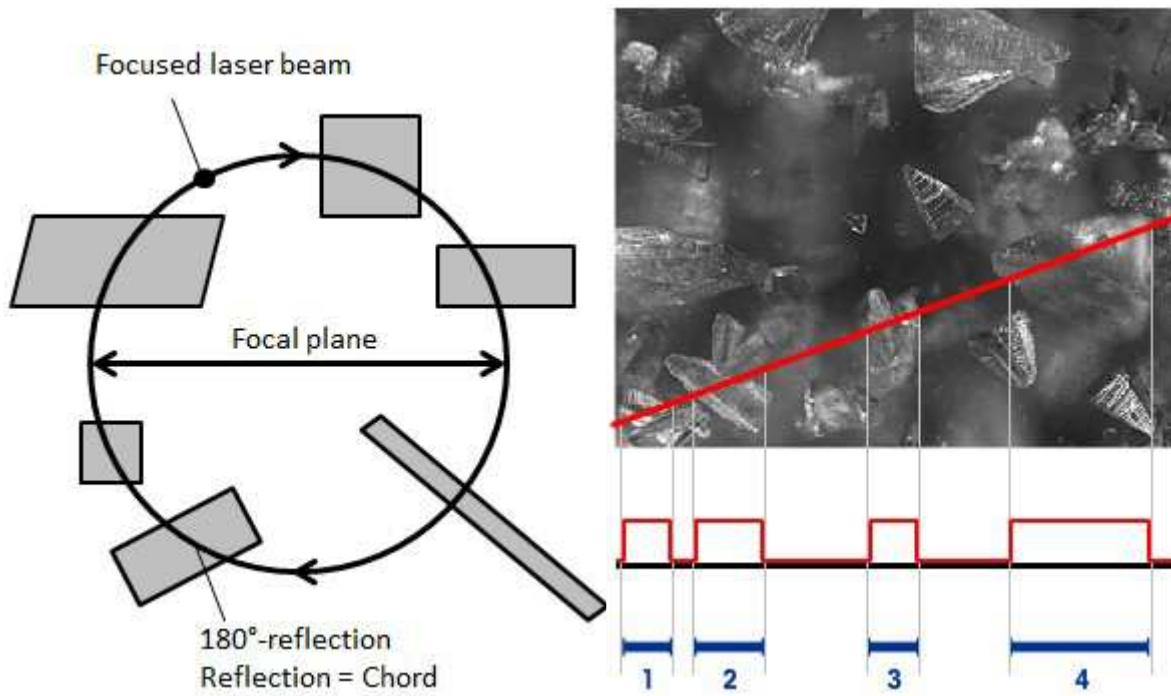
Figure 4.3-1: Rotating laser beam intersects particles, measuring distance across particles (chord length).

Figure 4.3-2: Crystals reflect laser light. Chord length is calculated from duration of reflection and scanning velocity [4.6]

A schematic diagram of an FBRM probe is shown in Figure 4.3-3, which is connected to a laser source generating a continuous beam of monochromatic light. The focal point of the laser lies at constant distance in front of the probe window and a rotating optics generates the circular path of the beam. In operation the probe is constantly scanning the crystals moving through the focal position.

Crystals are detected by their backscattering of laser light into the probe, where it is detected. The duration of backscattering, the distance the beam scanned over the crystal surface and the rotation velocity of the optics allows to calculate the chord length.
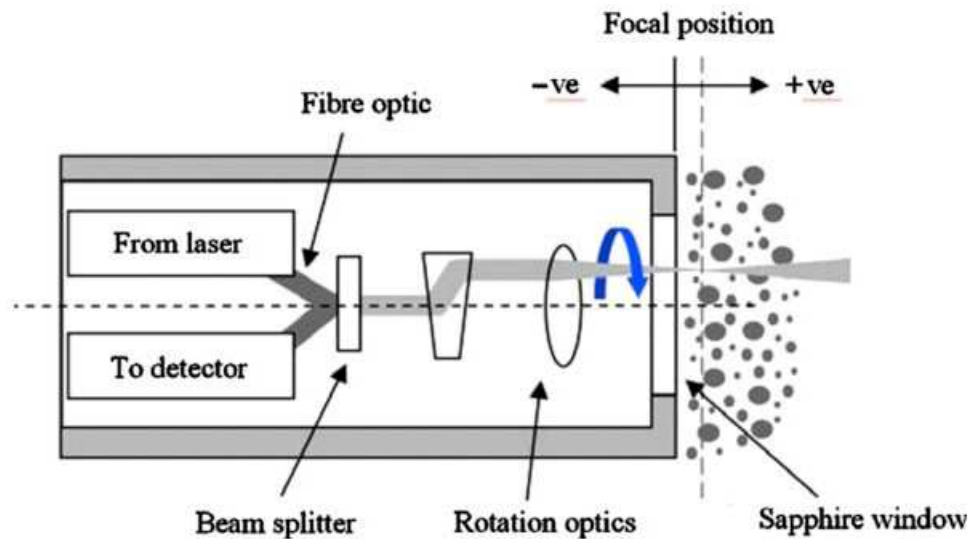
Figure 4.3-3: Schematic of a FBRM probe showing the probe interior [4.7]

Apart from chord length measurements, FBRM can also be used to obtain solubility, induction time as well as metastable zone width information. The count based technique is particularly sensitive to small particles and is suitable for detecting dissolution and nucleation events.

In seeded crystallisation processes FBRM can monitor the efficiency of the seeding event as well as the effectiveness of the seeds in terms of their growth behaviour. This information can subsequently be used to determine the growth kinetics of the seed material.

Continuous monitoring of a crystal suspension with FBRM can be used to detect polymorphic transformation, for example, from a cube to a needle like morphology. The different morphologies of the crystals lead to a change in CLD, which can be picked up during the process. However, FBRM can only track changes in crystal shape, it does not give crystal lattice information like obtained from XRPD analysis and can hence only track specific polymorph transformations.

The optical properties of a sample play a crucial role in the applicability of FBRM. Challenges for this technology occur when a sample contains transparent particles, which do not split chords or do not backscatter.

It must also be noted that the way the probe is positioned in the sample as well as stirring conditions and the hydrodynamics around the probe window can have a significant influence on the CLD.

FBRM is a very sensitive technique to detect changes in particle numbers and their dimensions but as of now no solution for the conversion from CLD to particle size distribution has been proposed. [4.6]

In order to conduct a FBRM measurement it is very important to clean the probe window from all adhering particles in order to avoid false measurements. The clean probe can then be inserted into the sample or a continuous set up at an angle of about 45°, which should secure proper particle flow around the probe window. As soon as the measurement is started, the instrument will generate a CLD of the sample.

4.4   Optical Microscopy

The human eye is designed to see objects of various sizes at various distances under changing levels of illumination. However, the resolution of the eye is limited and if an object is too small it might not be visible at eyesight anymore. Optical microscopy is a quick and non-destructive optical method to magnify small objects to make their structure visible for the human eye.

In crystallisation it is impractical and usually takes too long to grow crystals to such sizes that they can be studied without the help of magnification. Usual microscopes, as shown in Figure 4.4-1, are set up of sets of lenses and prisms, which achieve a magnification of the object studied. They operate at magnification factors between 4 – 1000x and can visualise objects in the large to mid nanometer length scale.

This range is a natural limitation of optical methods and can be explained by the Abbe diffraction limit. Ernst Abbe found in 1873 that

Figure 4.4-1: Optical microscope [4.8]

light can only visualise particles in the dimension of half the wavelength of the light. If the particles get smaller, light of shorter wavelength and different techniques are required.

Optical microscopy is mainly used for magnification purposes and to visualise what otherwise would have been left hidden to the observer. In this respect it is also feasible to attach a camera on top of a microscope and to take pictures of the magnified object. Due to a large variety of different crystal morphologies and sizes, it is essential to document the optical evidence of the crystal form present in the sample.

Various image analysis tools can be used to perform particle size measurements, which is very helpful for better process understanding when compared with other particle data from other techniques. [4.9]

For a microscopic measurement the sample is placed on a glass sample slide. Liquid containing samples can directly be covered with a cover slide, which should exclude possible air bubbles. Dry samples need the addition of a drop of liquid in which the sample is insoluble before the cover slide is added and air bubbles are excluded.

The sample slide is place on the microscope, light source and camera are switched on and an appropriate magnification is selected. The sample is brought in focus and a picture can be captured.

4.5   Scanning Electron Microscopy (SEM)

Surfaces and surface properties play a major role in many chemical and physical processes which, amongst others, also include crystallisation. Crystal surfaces which are exposed to supersaturated solution exhibit crystal growth and it even happens that a different polymorph nucleates on already existing crystal surfaces. [4.10] A proper visualisation of surfaces with a very high resolution is extremely important. SEM is a non-destructive method to characterise and image the topography and composition of a sample surface.

SEM analysis generates a picture, which shows a 2D image of the structure of the sample. The resolution is very high so that objects down to 1 µm in size can be visualised and a good understanding of surfaces and crystal form can be obtained.

The SEM operates with a focused beam of electrons, which have a large kinetic energy. The impact of electrons on the sample results in the dissipation of this kinetic energy. Some electrons diffract and are backscattered while others generate secondary electrons. The backscattered and secondary electrons are detected and are used to generate the SEM image.

Apart from generating high resolution images, SEM can also be used for elemental mapping as well as mapping of trace elements in the analysed surfaces. When the focused electron beam hits the sample, it also generates photons and X-rays which reveal the chemical composition of the surfaces.

However, in order to perform SEM analysis the sample should be solid and should fit into the microscope chamber, which is usually 5x10 cm large. Most SEM operate with a very high vacuum of 10^{-8} – 10^{-9} bar, which makes this technique unsuitable for samples containing volatile compounds (e.g. hydrocarbons or water) or for those which swell under vacuum.

For better resolution and the best performance of the instrument, it is often necessary to apply a gold coating in order to make the sample conductive. [4.11]

To prepare a sample for SEM analysis it is important to stick a little piece of conductive carbon tape on top of the sample holder. The sample is then placed on the carbon tape and can be coated with gold. After the coating the sample is ready for the SEM, it is placed in the microscope chamber and the analysis is started. The picture of the sample appears on a computer screen and it is possible to zoom in and out on the sample. Once an area of interest has been located, a picture of the sample can be taken.

4.6 Solubility

For chemical and physical process operations it is important that reactants or heat are homogeneously distributed throughout the whole reactor. Dissolving a solid significantly increases mass and heat transfer and makes the compound a lot more workable compared to its solid state. Various processes depend on substances being available in solution such as drug absorption and transportation within the human body. Solubility describes how much solid, liquid or gas (solute) can be dissolved
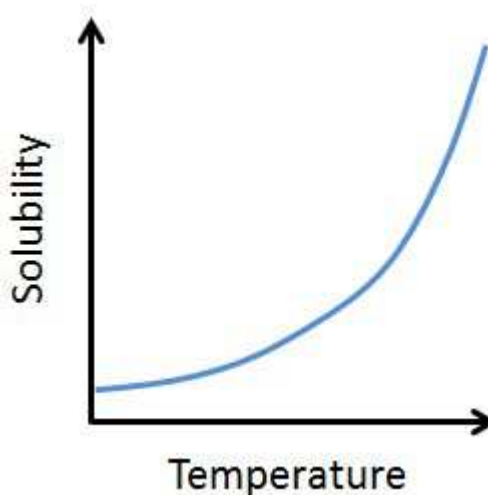
Figure 4.6-1: Example solubility curve

in another solid, liquid or gas (solvent) to form a homogeneous solution. The majority of solute : solvent systems exhibit solubility limits, which depend on physical and chemical properties such as temperature, pressure, solvent mixtures or pH-value. This means that for a specific set of parameters, a saturation concentration can be reached where further addition of solute no longer leads to an increase in solution concentration.

In order to dissolve even more solute, the operating parameters can be changed so that the saturation concentration is increased. Figure 4.6-1 shows an example where the solubility increases with increasing temperature. [2.2]

In order to obtain solubility data for a certain solute : solvent system under various specific operating conditions, it is necessary to conduct experimental solubility measurements. The techniques, which are common in our laboratory, will be explained in a little more detail.

4.6.1 Sample dissolution:

A known portion of solvent is prepared in a vial and a known portion of solute is added in excess with respect to the desired operating temperature. The mixture is heated and stirred for preferably 24h in order to allow the saturation concentration to be reached. After that the saturated suspension is filtered, the filter cake is dried until it attains constant mass and the mass of recovered solute is determined. The solubility can be determined by dividing the amount of dissolved solute over the known amount of total solution.

Additional information about the saturation concentration can be obtained from analysis of the filtrate using appropriate analytical methods.

4.6.2 Sample crystallisation:

A different route to determine solubility is to approach the equilibrium concentration by crystallising out excessive solute material. A solution of known solute and solvent quantities is saturated, for example, 20 °C above the operating temperature of interest,

the solution is filtered to remove all possible impurities or undissolved solute and then set to the lower target temperature.

After again 24h the slurry is filtered and mass balance or appropriate analytical methods can be used to determine the solubility at the temperature of interest.

4.6.3   High throughput devices (e.g. Crystal 16)

A known mass of solvent is prepared in a vial and a known mass of solute is added, exceeding the solubility concentration at ambient operating conditions. A vial with pure solvent is place inside the crystal 16 machine to zero the instrument. After that the solvent vial is replaced by the sample vial and the degree of sample transmission is determined.

Slow heating leads to an increase in saturation concentration and the solute continues to dissolve which in turn increases the sample transmission. The temperature gradient is recorded and the point of dissolution is reached when the sample transmission reaches 100%.

In this way the solubility of a specifically known sample concentration is directly connected to a dissolution temperature.

4.7   Gravimetric solid recovery

Supersaturation in a crystallisation process describes how much recoverable desired material is present in a sample. Due to economic considerations and a drive towards minimising wastage of desired product it is important to design processes which generate a high yield. Gravimetric solid recovery is a quick and reliable way to assess how much solid can be recovered from a product stream and how much remains dissolved in the solution.

Every crystalline substance has its compound specific nucleation and growth kinetics, which need to be considered when it comes to selecting crystalliser residence times in a crystallisation process. Too short residence times do not provide the crystals with enough time to deplete supersaturation and to grow to the desired size. However, too

long residence times can have a negative impact on product quality in terms of agglomeration or crystal breakage. It is therefore desirable to process crystals just as long as necessary to deplete supersaturation and to obtain the optimal crystal size.

In batch operation the residence time in the crystalliser is flexible and can be altered accordingly in case more or less time is required to deplete supersaturation. In this situation the solid recovery data indicates when the batch is desupersaturated and ready for further processing.
In continuous operation, on the other hand, the residence time is fixed and solid recovery measurements are used to assess the yield, map desupersaturation and steady-state operation of the process.

In order to perform solid recovery analysis a representative sample of known mass is collected from the crystal suspension. The sample is filtered using a vacuum, the filter cake is dried until it is mass consistent and the mass of recovered solute is determined.
For the assessment of how desupersaturated the sample is, it is necessary to obtain theoretical solid recovery data from mass balance calculations and compare it to the actual values. In the case where the theoretical and actual solid recoveries match, the sample can be considered desupersaturated. For those cases where the actual solid recovery is only a fraction of the theoretical, the sample can still be considered supersaturated with respect to the desired compound.

5 Equipment

5.1 Positive displacement pumps

Significant fluctuation in supersaturation during the crystallisation process changes the crystallisation behaviour and leads to undesired non-uniform product.

In continuous antisolvent crystallisation, a constant level of supersaturation can only be achieved when equal flow rates of solution are rapidly and continuously mixed with equal flow rates of antisolvent. Positive displacement pumps transport fluid from a confined space by reducing the volume of the confined space and theoretically deliver

the same flow rate independently of the discharge pressure. The most vivid example of a positive displacement pump is a piston pump, which consists of a mobile piston moving inside a cylinder as shown in Figure 5.1-1.
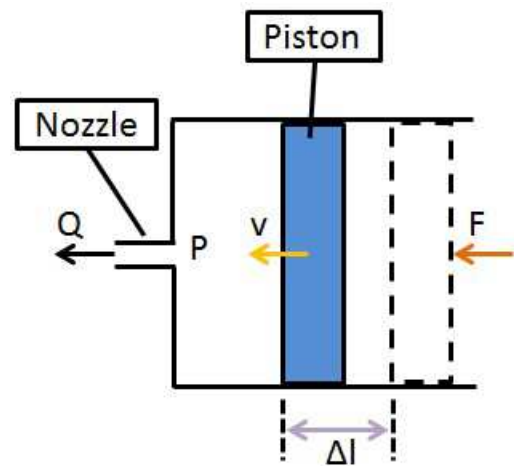
F: Force on piston

Δl: Length travelled by piston

v: Velocity of piston

P: Pressure of the fluid

Q: Flow rate

Figure 5.1-1: Schematic positive displacement pump. Piston moving from right to left.

To describe the mechanism of constant flow, it is necessary to make a few assumptions: that liquids are completely incompressible, all equipment fits perfectly, permitting no leaks and no friction between the piston and the cylinder wall.

Force is applied to the piston and pressurises the liquid which is forced through the nozzle. The continuously moving piston further reduces the volume available for the liquid and if the motion is uniform the same volume of liquid is displaced per each unit time. A piston pump can only deliver a fixed volume of liquid depending on the dimensions of the cylinder and is not suitable for continuous operation.

5.1.1 Peristaltic pumps

To achieve continuous fluid delivery the principle of reducing the volume of a confined space has to be approached differently. A peristaltic pump, as shown in Figure 5.1-2, consists of a fluid containing flexible tube in a circular pump casing.

The rotating rollers compress the tube, permitting no back flow from the pressure to the suction side and push the contained liquid forward. As the tube relaxes from the compression underpressure is generated on the suction side, which draws more liquid into the tube. In

Figure 5.1-2: Watson-Marlow 520S with Marprene tubing (Watson-Marlow polymer) fitted into pump head.

peristaltic pumps any contact between liquid and moving parts is avoided, which makes it suitable for handling slurries as well as aggressive media. [5.1, 5.2]

The diversity of available tubing material plays a key role in the applicability of this type of pumps. It is very important that the tubing is inert against the chemical substances to be conveyed. Knowledge about chemical resistance of tubing and/or compatibility experiments are essential.

Figure 5.1-2 shows a Watson-Marlow (WM) 520S peristaltic pump with Marprene (thermoplastic elastomer) tubing, which is resistant to a wide range of chemicals. This combination of pump and tubing is commonly used in our laboratories.

The achievable flow rate of a peristaltic pump depends on the tube inner diameter as well as the range of RPM the motor can deliver and is typically between 1 ml/min. and 3.5 l/min. The motor of this type of pump is controllable with an accuracy of 0.1 RPM, which enables very small and accurate changes in flow rate.

One of the major disadvantages of this type of pump in terms of crystallisation is its mechanism of operation. The compression of the tubing, which drives the fluid forward, can have a negative impact on the crystal slurry. The mechanical impact of the roller on the crystals can lead to crystal breakage as well as to unwanted secondary nucleation in case the medium is supersaturated.

Setting a WM 520S up for operation is a straightforward procedure. The yellow clamp space holders, as shown on the right in Figure 5.1-2, need to be set for the appropriate tube size after which the tubing can be inserted into the casing.

As the flow rate depends on motor RPM as well as internal tube diameter, it is important to have a good understanding of which tubing delivers what flow rate at a set RPM. To be able to understand this relationship it is necessary to calibrate the flow rate against motor RPM for the specific type of tubing used. Once this information is available, it allows measuring specific flow rates by setting certain motor RPM.

5.1.2   External Gear pumps

A different technique to achieve constant fluid delivery uses the same principle of reducing the volume of a confined space however, in a different way. A gear pump, as shown in Figure 5.1-3, consists of two identical gears, which are rotating against each other in a closely fitted casing.

The volume expansion on the suction side draws liquid into the spaces between the gear teeth. As the gears rotate the liquid is trapped in the pockets between the teeth and the casing, permitting no back flow,

Figure 5.1-3: External gear pump indicating direction of liquid flow [5.3]

and travels from the suction to the pressure side. Gear pumps are used for high pressure applications and the fluid is always in direct contact with the tightly fitting moving parts. [5.1, 5.2]

The construction material of the pump head plays a major role in the applicability of this type of pump. It is very important that all internal equipment is chemically inert with respect to the conveyed fluid. Pump heads can either be made from stainless steel or hastelloy depending on the required chemical resistance.

Figure 5.1-4 shows a Ismatec MCP-Z external gear pump with stainless steel pump heads. Such a pump head exhibits good chemical resistance against most substances worked with and is commonly used in our laboratory. The achievable flow rate of a gear

Figure 5.1-4: Ismatec MCP-Z external gear pump

pump depends on the dimensions of the pump head as well as the range of RPM the motor can deliver and is typically between 1 ml/min. and 7 l/min. A motor of this type can control the flow rate with an accuracy of 0.01 ml/min. which enables very small and accurate changes in flow rate.

One major disadvantage of gear pumps is the overall tightly fitting internal equipment of the pump head. The interior must never run dry as the conveyed fluid acts as a lubricant between the gears and the casing in order to minimise wear.

Another disadvantage is that the conveyed fluid must be totally free of particles, which again would cause abrasion and could lead to leakages, unwanted back flow and losses in pressure.

Setting up an Ismatec gear pump is a straightforward procedure. The working fluid is charged on the suction side and the RPM are adjusted to deliver the required flow rate. The flow rate can be double checked with a scale and adjusted, if necessary.

5.2 Mixers

In the chemical industry it is of great importance to have good control over physical and chemical processes in order to avoid unplanned operation. Predicting system behaviour makes the assumption of homogeneity, the uniformity over the entire spread of the system, essential. The primary aim of mixers is to generate homogeneity by blending at least two pure compounds to a single phase on a molecular level. [2.2]

Mixing is one of the basic unit operations in process engineering and is achieved by relative movement of the compounds to each other. It does not generate new substances, all raw materials in the mixture are the same as before, they do however become unrecognisable as the mixture has different physical properties compared to the raw materials. [5.4]

In terms of liquids there are many ways how molecule movement relative to each other can be achieved. The two approaches commonly used in our laboratory will be described in more detail.

One option is to stir a liquid with a moving stirrer, which provides kinetic energy and generates turbulent fluid movement. The second liquid is then added into the vessel and the turbulent nature of flow achieves mixing of the two fluids. The timescale until molecular mixing is achieved depends on processing parameters of the flow unit.

In a different approach, two separate liquid streams are provided with kinetic energy using pumps, which push both liquids into a so called static mixer. A static mixer does not contain any moving parts and mixing is achieved by highly turbulent fluid flow on impact of the two streams in the mixing chamber. Pump flow rates and static mixer dimensions determine the residence time of the fluid in the mixer. In order to ensure molecular mixing, the characteristic mixing time should always be shorter than the mixer residence time.

Static mixers show uniform, reproducible and scalable mixing behaviour and for these reasons are used extensively in our laboratories. Those mixers commonly used will be explained in more detail.

5.2.1 T-shaped static mixer

One of the more basic mixer designs can be seen in Figure 5.2-1. It consists of two opposing inlet streams and an outlet in perpendicular orientation compared to the inlets. A schematic drawing for better illustration is shown in Figure 5.2-2. Its shape looks like a "T" which gives it the name T-shaped static mixer.

Our model is 1/8 inch in dimension and made from stainless steel, which exhibits good chemical

Figure 5.2-1: T-Shaped static mixer
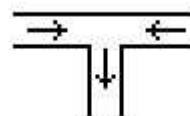
Figure 5.2-2: Schematic of T-mixer

resistance against a wide range of typically used solvents and acids. The nut & ferrule compression fitting screw connections make the mixer suitable for high flow rates and pressures of several hundred bar.

The total flow rate achieved depends on the pumps connected to the T-mixer and the pressure these are able to build up. In our case, two gear pumps delivered the required fluid in an operating window of 60 – 1200 g/min.

However, previous studies of this system showed that a minimum total flow rate of 100 g/min is required to achieve molecular mixing within the mixer residence time [5.5]. It must also be noted that a T-mixer has to be operated at close to equal flow rates from both streams to ensure proper mixing and mixture composition. Another disadvantage is that supersaturated solution is always in direct contact with the mixer walls and the opague nature of stainless steel makes it impossible to detect fouling in the mixer.

Setting up a T-mixer for operation involves connecting the two pipes from the pumps to the mixer and tightening the nuts to prevent leakages. The outlet can be connected to a straight tube for sampling or any other downstream equipment.

5.2.2 Confined impinging jet mixer (CIJ)

A more advanced mixer design can be seen in Figure 5.2-3, which again consists of two opposing inlet streams and an outlet in perpendicular orientation compared to the inlets. However, the schematic drawing in Figure 5.2-4 clearly shows the major difference of the CIJ compared to the T-mixer. In the CIJ the design of the mixing chamber allows the two inlet streams to impinge each other leading to highly turbulent hydrodynamics and very effective mixing.

Figure 5.2-3: Confined Impinging Jet mixer (CIJ)
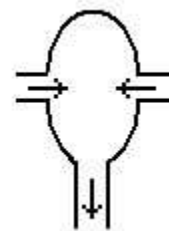
Figure 5.2-4: Schematic of CIJ

Our model is designed with screw connectors to fit on 1/8 inch pipes coming from the pumps. The inner diameter of the two inlets are 1 mm each, the mixing chamber holds a volume of 0.447 ml and the inner diameter of the outlet is 2 mm. The mixer is made from stainless steel, which exhibits good chemical resistance against a wide range of typically used solvents and acids.

The total flow rate achieved depends on the pumps connected to the CIJ and the pressure these are able to build up. In our case two gear pumps delivered the required fluid in an operating window of 60 – 1200 g/min.

A major disadvantage of our particular mixer is that it was designed and built in metric dimensions but now had to be fitted to pipes of 1/8 inch in diameter. Considering the high flow rates, small diameters and high pressures it is quite a challenge to seal all connections properly so that no leakage occurs.

Similarly to the T-mixer, the CIJ needs a minimum total flow rate of about 100 g/min, mixing flow rates need to be close to equal and supersaturated solution is in direct contact with the mixer walls [5.5]. The mixer is set up by connecting it to the pipes coming from the pumps and tightening the nuts.

5.2.3 Jet-Injection mixer (JIM)

The latest design of a continuous mixing unit is shown in

Figure 5.2-5 and combines a static jet mixer with a conventional stirred tank mixing unit. This jacketed Mixed Suspension Mixed Product Removal (MSMPR) crystalliser is fitted with a stainless steel nozzle for jet-injection of stream 1 into the bulk solution, a tube for a freely falling (or water-falling) liquid stream 2 and the outlet stream 3. A thermometer close to the centre of the vessel collects the temperature in the bulk material.
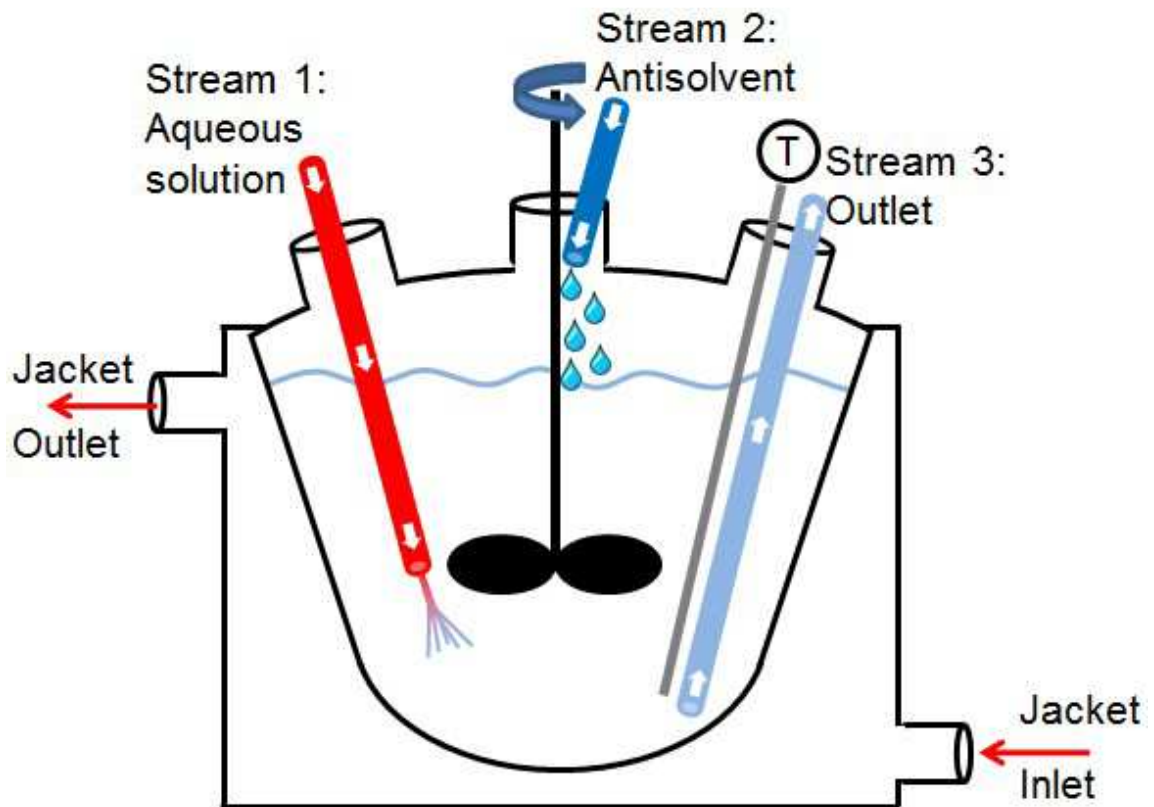
Figure 5.2-5: Schematic of a jacketed Jet-Injection Mixer (JIM). Stream 1 is jet-injected into the bulk solution. Stream 2 is free falling (water-falling) onto the surface of the liquid mixture. Stream 3 withdraws bulk liquid to maintain predetermined liquid level in the vessel.

The JIM design, in operation in Figure 5.2-6, blends two liquid streams according to two separate mixing actions, which both support each other. In this respect any flow rate ratio between stream one and two can be adopted. The submerged jet-injection of stream one into the bulk solution generates a turbulent flow regime and accounts for the first mixing action. The second mixing action is contributed by the stirred tank itself and complements the overall mixing.

Figure 5.2-6: JIM in operation, showing jet-injected Stream 1, water-falling Stream 2 and Outlet Stream 3.

A gear pump delivers stream 1 through a stainless steel pipe of 1/4 inch dimension, which is reduced to 1/16 inch dimension and a nozzle of 0.15 mm inner diameter. The nut & ferrule compression fitting screw connections allow operation at high flow rates and pressures. A picture of the jet-injection nozzle can be seen in Figure 5.2-7.

Stream 2 is delivered by a peristaltic pump through Marprene tubing of 1/4 inch dimension, which is reduced to 1/8 inch dimension to fit into the jacketed vessel.

The volume of the jacketed stirred tank can be freely selected as per the requirements of flow rate and residence time in the crystallisation unit. Due to the nature of a

Figure 5.2-7: JIM injection nozzle

flow unit, the desired total flow rate and mean residence time determine the volume of the crystalliser unit. The current design operates at mean crystalliser residence times of 30 sec. and covers vessels which can hold 40 – 400 g of slurry. This set up hence

allows total flow rates of about 80 - 800 g/min of product slurry and even bigger vessels can easily be fitted.

The outlet stream constantly withdraws product slurry from the crystalliser using a peristaltic pump and Marprene tubing of 1/4 inch dimension. The outlet flow rate is adjusted to match stream one and two in order to keep the liquid level in the crystalliser constant.

All materials (stainless steel, glass, Marprene, PTFE) used for this unit exhibit good chemical resistance against a wide range of typically used solvents and acids.

Challenges lie in the actual operation of this system and the requirement that a constant liquid level needs to be maintained in the vessel. As this is not always easy it might happen that due to surface renewal effects and possible evaporation a very thin rim of crystals appears near the liquid level.

Particularly careful attention needs to be paid to the crystallisation process itself and the supersaturation profile in the vessel. If the crystallisation process is not near to complete and the product slurry contains remaining supersaturation, it is very likely that a downstream blockage occurs and operations have to be stopped.

Setting up a JIM involves inserting the stainless steel pipe with nozzle, the Marprene tubing from the peristaltic pumps, the stirrer and the thermocouple into the vessel. In order to prevent breakage of equipment, it is very important to check, before the crystalliser is started, that no inserted equipment collides with each other. The mixer outlet tube can be used for sample collection or can be connected to any other downstream equipment.

5.3 Flow units

In crystallisation it is of great importance to expose supersaturated solution to the required hydrodynamic conditions for the right amount of time in order to obtain desired crystal product. Processes operated at too mild conditions can show poor mixing and might take too long to reach an acceptable yield. Too harsh conditions, on the other hand, can have a negative impact in terms of attrition and crystal breakage. A flow unit is an area where a solution can be treated exactly in the way required and they can be operated in either batch or continuous mode.

5.3.1 Batch mode

A vessel filled with supersaturated solution is exposed to the specific hydrodynamics generated by the flow unit. The exposure time can be chosen freely as per the requirements and at the end of the run the product crystals are ready for further processing or analysis.

5.3.2 Continuous mode

The ultimate requirement for continuous operation is the ability to carry out unit operations in a steady flow of solution over a long period of time. A continuous flow unit has an inlet through which the vessel is continuously supplied with fresh supersaturated solution and an outlet from where product slurry is continuously withdrawn. The exposure time depends on the flow rate as well as the vessel volume and needs to be sufficiently long in order to obtain the required product quality in the outlet stream. The crystal slurry withdrawn can be used for further processing or analysis. [2.1, 3.2]

Different flow units generate different hydrodynamic conditions and have a different impact on the supersaturated solution and product crystals. In our laboratory we designed and worked with various flow units and operated them in batch as well as continuous mode. The most commonly used units will be described in more detail.

5.3.3   Quiescent Crystalliser (QC)

The most basic design of a crystallisation unit consists of supersaturated solution in a beaker without any agitation or artificial fluid movement. A so called quiescent crystalliser, as shown in Figure 5.3-1, imposes the mildest hydrodynamic conditions on the sample and mass transfer processes can only happen through diffusion. In our laboratory there are

Figure 5.3-1: Quiescent crystalliser without stirring

various QC models available made from glass, stainless steel or PTFE, which show good chemical resistance against a wide range of typically used solvents and acids. The standard sized beaker holds a volume of about 250 ml.

A disadvantage of this flow unit is the poor suspension of particles, which leads to crystals settling on the bottom of the beaker. Growing crystals at the beaker bottom and slow, diffusion driven mass transfer leads to slow crystal growth and a supersaturation gradient from the bottom to the liquid surface.

A quiescent crystalliser is not suitable for continuous operation as the concept of no artificial fluid movement would be broken by the in- and outflowing streams. Another reason is that settling particles are not suitable for continuous operation.

Setting up a QC for batch experiments is straightforward. The homogeneously mixed sample is collected, the beaker is covered (in order to prevent evaporation) and placed on the bench top.

5.3.4   Magnetically Stirred Crystalliser (MSC)

One way to address the problem of settling crystals in the flow unit is the implementation of a stirrer. The MSC, as shown in Figure 5.3-2, design comes with a magnetic stirrer bar inside the beaker, which is placed on a magnetic stirring motor to rotate the bar inside the beaker. The rotating stirrer bar generates fluid movement which keeps the product crystals suspended. This type of flow

Figure 5.3-2: Magnetically Stirred Crystalliser

unit imposes very harsh operating conditions on the sample, which can generally be observed through very short induction times and high solid recoveries over time.

Due to the diversity in beaker material in our laboratory we can set up MSC units made of glass, stainless steel or PTFE, to study the effect of material of construction. A MSC can easily be turned into a continuous unit by constantly pumping in freshly mixed, supersaturated solution and at the same time withdrawing well mixed product suspension.

A disadvantage of this flow unit is the rotating stirrer bar which enhances secondary nucleation by grinding up product crystals as it bounces around the bottom of the beaker. In addition to that, the grinding process is not uniform which means that a MSC sample shows a higher degree of large, uncrushed as well as very small, multi-crushed crystals. This leads to an unfavourable broadening of the particle size distribution.

Another problem is that the crushing action in the MSC is neither scalable nor consistently reproducible. A non-scalable and unpredictable flow unit should not be the first choice for experimental or process design.

To set up an MSC for batch mode, a micromixed sample is collected in a beaker and the magnetic stirrer bar is added to it. The beaker is placed on a magnetic stirring motor, covered to avoid evaporation and agitation can be started.

5.3.5 Stirred Tank Crystalliser (STC)

Another way to keep a sample agitated and to avoid settling of crystals in the flow unit is the usage of an overhead stirrer, as shown in Figure 5.3-3. A wide range of stirrer designs are available but commonly a two bladed impeller, driven by an overhead motor, is used to suspend the crystals. This type of flow unit, depending on the stirrer RPM, imposes mild to medium operating conditions on the sample. As the stirrer is located in the centre of the vessel, no direct grinding action is happening however, attrition and crystal breakage by the rotating impeller can still occur. Due to various stirrer materials (stainless steel, PTFE, Marprene) and the wide range of beaker materials in

Figure 5.3-3: Stirred Tank Crystalliser with overhead stirring

Figure 5.3-4: Stainless steel, PTFE and self-built Marprene stirrer

our laboratory we can set up different STC units as outlined in Table 5.3-1.

A Marprene stirrer was manufactured from Watson-Marlow peristaltic pump tubing made from a polymeric material (Marprene). Tubing was cut in half and straightened out with two metal pins, making its shape look like a stirrer blade and it was attached it to a stirrer shaft.

Table 5.3-1: Combination of different stirrer and beaker materials available in the laboratory and used in these experiments

Beaker \ Stirrer	Stainless steel	PTFE	Marprene (Watson Marlow polymer)
Glass	√	√	√
Stainless steel	√	√	√
PTFE	√	√	√

For batch operation, the homogeneously mixed sample is collected in a beaker and the overhead stirrer is inserted into the sample. The beaker is covered to avoid evaporation and agitation can be started. Providing a continuously freshly mixed, supersaturated inlet stream and withdrawing bulk slurry, turns the STC into a continuous unit.

5.3.6 Peristaltic Pump recirculation Loop (PPL)

A rather uncommon way to suspend particles in a vessel is the concept of recirculating sample with a pump, as shown in Figure 5.3-5, and using the outlet stream to create a turbulent flow regime in the vessel. The suction and pressure side of the pump are both immersed into the sample and the recirculation is driven by a peristaltic pump. This type of flow unit, depending on the pump RPM, imposes mild to medium operating conditions on the sample as the roller of the pump squeezes the tube together and
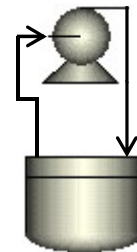
Figure 5.3-5: Peristaltic Pump recirculation Loop with suction and pressure tube in the same vessel.

pushes the liquid inside the tube forward. In a PPL there is no direct grinding action happening but it can be assumed that the squeezing by the roller causes attrition or crystals breakage in the pumped sample.

The peristaltic pump tubing was made from Watson Marlow's Marprene polymer and due to the diversity in beaker material options in our laboratory we can set up PPL units made of glass, stainless steel or PTFE. A PPL can also be turned into a continuous unit by continuously pumping in freshly mixed, supersaturated solution and at the same time withdrawing well mixed product suspension.

A major disadvantage of this flow unit is the fact that very high recirculation flow rates, in the order of litre/min, are required in order to properly suspend all particles in the vessel. If the flow rate is too low or particles get too big, settling in hydrodynamic quiet beaker areas can occur, which will lead to blockage of the whole system.

Setting up a PPL for batch experiments is a straightforward process. The well mixed sample is collected in a beaker and the suction and pressure tube of the peristaltic pump are inserted into the sample. The beaker is covered to avoid evaporation and recirculation can be started.

5.3.7   Oscillatory Baffled Crystalliser (OBC)

The conventional way of stirring a vessel utilises some or the other stirrer design and radial fluid movement is generated by rotating the stirrer around its axis at a certain rpm. A more novel approach towards stirring is shown in Figure 5.3-6 and consists of a baffle string, set up of several perforated plates in a row. The baffle string is vertically oscillated up and down in a stagnant fluid with a certain amplitude and frequency. Turbulent fluid movement is achieved as the baffle string generates vortexes and eddies
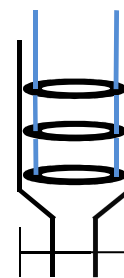
Figure 5.3-6: Oscillatory Baffled Crystalliser with three parallel baffles

in the vessel during operation. This type of flow unit is generally operated at a frequency of 1 - 3 Hz and amplitudes of 10 - 30 mm. In a tightly fitting system the baffles scrape against the vessel wall, which can lead to attrition or crystal breakage.

The baffles can be made from different materials such as stainless steel, PTFE or Peek and are connected by stainless steel rods to make up the baffle string. The crystalliser is a cylindrical vessel made from glass and comes in various capacities from 100 - 1000 ml.

Similarly to other flow units, connecting a continuous well-mixed inlet stream and withdrawing bulk product turns the OBC into a continuous unit.

A major disadvantage of the OBC can be generated by the unit itself and the fact that it consists of a moving baffle string. If the baffle string is too tightly fitting against the vessel walls, a scraping action occurs, which dramatically changes the behaviour of the unit. In this case very harsh operating conditions apply, similarly to the MSC, which can be observed in very short induction times, high solid recoveries over time and a large degree of damaged and broken crystals.

For OBC operations in batch mode, the micromixed sample is collected in the OBC and the baffle string is inserted into the vessel. The unit is covered to avoid splashing product slurry as well as evaporation and the oscillation can be started.

5.3.8   Continuous Oscillatory Baffled Crystalliser (COBC)

A different concept towards oscillatory flow was realised in a recently developed continuous crystallisation unit and is shown in Figure 5.3-7. This set up does not oscillate a baffle string through stagnant fluid but rather oscillates the fluid through a tube with fixed baffles. The required turbulent flow regime is achieved by vortexes and eddy, while a bellow, connected to a motor, oscillates the liquid back and forth.

This type of flow unit is usually operated at a frequency of 1 - 3 Hz and amplitudes of 10 - 30 mm. The crystal slurry is not exposed to any moving parts or scraping baffles and imposes mild operating conditions on the sample, causing little attrition or crystal breakage.
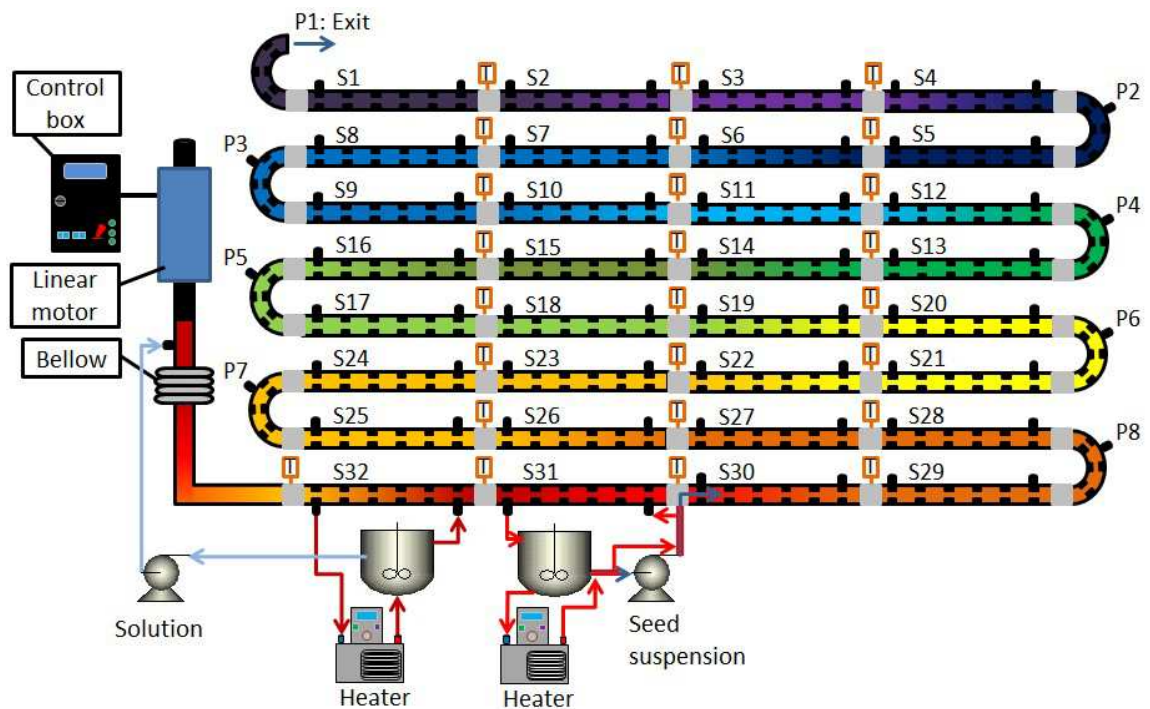
Figure 5.3-7: Continuous Oscillatory Baffled Crystalliser (COBC) consisting of control box, motor and bellow to generate oscillation. Growth solution and seeding suspension are provided in two jacketed and stirred holding tanks. Different colours along the rig represent different temperature zones from warm (red) to cold (violette).

The unit is a tubular reactor consisting of several individually baffled straights and is entirely made from glass. Only the seals (PTFE) and collars (Peek), which connect the straights and are used to implement thermocouples or other inserts, are made from different material. The total volume of the unit depends on the length of the rig as each straight has a volume of 120.4 ml and each bend a volume of 46.4 ml. The current set up consists of 32 straights and 8 bends covering a total volume of 4224 ml, which is the maximum length that can be set up in our laboratory.

General disadvantages, which originate from the nature of continuous processing, apply to this unit, for example, long preparation and start up times. Continuous manufacturing requires the supply of large quantities of bulk solutions, which need to be prepared and ready before a run can start. Sophisticated equipment like a COBC gives lots of

opportunities for failure or breakages and for that reason downtimes for repair can be quite excessive.

Another challenge during the start-up and operation of this unit is the presence of gas bubbles in the system during the filling procedure or the degassing of the solvents worked with during the run. The compressibility of gas bubbles can significantly dampen the oscillation amplitude leading to a loss of turbulent flow in the rig, which is the key property of the COBC.

Start-up of a COBC is not a straightforward process and a lot of practical experience with the unit is required for assembly and operation of the rig. Careful attention needs to be paid to the proper aligning of the motor with the bellow and the straights in order to prevent breakage.

Any changes in the length of the rig require a recalibration of the oscillation amplitude to ensure the desired operating parameters inside the unit are met. Relevant feed flow rates must be controlled very accurately as any deviation affects the residence time, solution composition, solid loading, supersaturation and final output. The desired cooling profile needs to be established by carefully adjusting various heater/chiller units until the desired temperature gradient is achieved over the entire rig. Once all the necessary set up work is finished, the oscillation as well as the feeding of work solution into the unit can be started. It must be noted that throughout the entire run time, flow rates and temperature gradients must be checked continuousl, in order to pick up any deviations from planned operation in the unit.

5.4 Ultrasonic bath

The first step in crystallisation is the event of nucelation followed by growth of the small nuclei to larger crystals. Heterogeneous nucleation has a lower energy barrier compared to homogeneous nucleation and is therefore more likely to occur due to thermodynamics [2.2]. Surfaces of all kinds, some better than others, as well as already present product crystals provide sources for heterogeneous nucleation. Crystal growth in unwanted locations like on thermocouples, on tubing or vessel walls is referred to as fouling and can, especially in continuous systems, result in blockage of the system. The

desire to develop continuous processes drives the necessity to prevent fouling and to extend the run time of processes without blockage. Ultrasonic baths are commonly used in laboratories to clean equipment and this feature could also help solving the problem of fouling by continuously cleaning surfaces in the crystalliser.

Humans can hear sounds in the frequency range from about 20 Hz - 20 kHz and sound frequencies beyond that are generally referred to as ultrasound, which can be used for cleaning applications. Ultrasonic baths are equipped with sound wave transducers, which radiate ultrasonic waves through the solution tank, generating an environment of high and low pressures. In a low pressure area millions of microbubbles form and grow, which is called cavitation as they form cavities. With the sudden change to high pressures these bubbles instantaneously collapse and, as they implode, huge amounts of energy are released. Imploding microbubbles act as scrubbers and clean every surface.

An ultrasonic bath can be operated in the direct or the indirect cleaning mode. The direct mode shows more effective cleaning as the item is directly inserted into the solution tank of the bath. In all experiments conducted in this work the indirect mode was chosen by submerging a jacketed crystalliser, containing the crystallisable solution into the ultrasonic bath.

The ultrasonic bath in our laboratory has a 0.5 l tank and is equipped with one industrial style 40 kHz (50 W) transducer. The tank is filled with water to the operation level (± 1 cm), the crystallisation vessel is placed inside the bath, not allowing it to sit on the bottom and the sonication can be switched on. [5.6]

6 Modes of crystallisation

In the pharmaceutical and fine chemical industry the majority of API and chemical compounds are synthesised in solution. However, in order to make useful products, these substances are mostly required in their solid form. There are various crystallisation techniques available, which turn the desired molecules into usable crystals and those relevant for this thesis will be explained in more detail.

6.1 Sample preparation

6.1.1 Cooling crystallisation

Known amounts of solute AB and solvent are mixed and dissolved in a stirred jacketed crystallisation vessel. Initially, the solute is in excess at room temperature but has to dissolve fully before the solvent starts boiling at high temperatures. Heating liquid is circulated through the jacket to heat up the slurry and increases the solubility until all solute dissolves. The solution is usually kept 10 -15 °C above its solubility temperature to ensure full dissolution of the solute.

6.1.2 Reactive crystallisation

Known quantities of reactant A (usually well soluble) as well as reactant B (also well soluble) are fully dissolved in known separate portions of solvents. Concentrations of reactant A and B are chosen so that the solution mixture at a predetermined mixing ratio generates supersaturation with respect to product AB (usually poorly soluble in solvent mixture). Both solutions are individually filtered in order to remove undissolved solute or solid impurities.

6.1.3 Antisolvent crystallisation

In a very good solvent, a solution of compound AB with known concentration is prepared, so that the solution concentration is close to the solubility concentration at ambient conditions. A filtration step ensures that undissolved solute or impurities are removed from the solution before further use.

6.2 Primary processing

6.2.1 Batch cooling crystallisation

The hot and undersaturated solution is cooled down by reducing the temperature of the heating fluid in the vessel jacket. Colder heat exchange surfaces bring a temperature change to the sample, the solution concentration reaches the solubility concentration and moves through the metastable zone.

When the unstable zone is hit, spontaneous and uncontrolled nucleation occurs which consumes supersaturation and moves the solution concentration back into the metastable zone. In this area further uncontrolled nucleation is stopped and crystal growth is the predominant mechanism.

6.2.2 Semi-batch reactive crystallisation

The entire solution of reactant A is provided in a stirred vessel and the solution containing reactant B is slowly added. A rapid chemical reaction forms product AB which is poorly soluble in the solvent mixture, and creates an AB supersaturation spike at the entry point of reactant B. However, due to an undersaturated bulk solution, the supersaturation at the addition point is quickly dispersed.

On further addition of reactant B and increased bulk supersaturation, the solution concentration penetrates the metastable zone, hits the unstable zone and causes uncontrolled nucleation at the entry point of reactant B. The event of nucleation consumes bulk supersaturation and moves the bulk solution concentration back into the metastable zone. However, at the addition point of reactant B, supersaturation is kept high and uncontrolled nucleation continues. The growth of older crystals in the presence of continuous nucleation leads to a broad particle size distributions in the final crystal product.

6.2.3 Semi-batch antisolvent crystallisation

A miscible antisolvent with poor solubility for compound AB is provided in a stirred vessel and the nearly saturated solution of compound AB is slowly added. At the solution addition point, the solubility of the solvent mixture is dramatically decreased and an extremely high level of supersaturation is achieved.

The solution concentration spikes far into the unstable zone, triggers excessive uncontrolled nucleation of fine crystals and due to the lack of available bulk supersaturation, crystallisation is almost complete. As more solution is added the solubility of the solvent mixture increases, the supersaturation spikes are reduced and more supersaturation is available for crystal growth.

6.2.4   Continuous cooling crystallisation

The hot and undersaturated solution is continuously pumped through, for example, a tubular counter current heat exchanger, which over time & distance reduces the solution temperature. Different locations in the rig correspond to different temperature zones and when a solution is cold enough for the solution concentration to hit the unstable zone, uncontrolled nucleation happens. Like in the batch experiments, nucleation consumes available bulk supersaturation and back in the metastable zone crystal growth is dominating.

6.2.5   Continuous reactive crystallisation

The two solutions of reactant A & B are continuously mixed in for example a static mixer, where micromixing of the two streams is achieved. A rapid chemical reaction forms product AB, which is poorly soluble in the solvent mixture, and causes the solution concentration to spike into the unstable zone. The occurring nucleation event moves the supersaturation back into the metastable zone, where crystal growth is predominant.

6.2.6   Continuous antisolvent crystallisation

The solution containing compound AB and the antisolvent with poor solubility for AB are continuously mixed in an in-flow mixing device like for example the jet-injection mixer in Figure 5.2-5. The solvent mixture exhibits a significantly lower solubility for AB compared to the initial solution and the solution concentration spikes far into the unstable zone. Nucleation reduces the degree of supersaturation and when the solution concentration moves back to the metastable zone, crystal growth is the dominating process.

6.3 Secondary processing

When the final crystallisation temperature is reached and all solutions and/or antisolvents are added and/or mixed, the crystals are allowed a holding period under constant conditions. During this time, the growing crystals consume available supersaturation until it is exhausted.

After that the slurry is withdrawn from the crystallisation vessel and crystals are separated from mother liquor applying a vacuum or pressure to speed up the filtration process. The remaining filter cake is washed with an easy to evaporate antisolvent to replace possibly remaining mother liquor from the crystal. In the last processing step, the filter cake is dried until it is mass consistent.

6.4 Specific challenges to cooling crystallisation

A not very well understood unit operation like crystallisation comes with significant general as well as process specific challenges and needs a lot of operational flexibility. Challenges specific to cooling crystallisation will be discussed below and general issues during crystallisation will be covered toward the end of this section.

The key parameter in cooling crystallisation is the cooling rate itself, as it is critical in many ways and influences the entire process. Slow cooling provides good control over the crystallisation process but can lead to excessively long process run times. Fast cooling, on the other hand, can generate very high supersaturation far in the unstable zone which leads to uncontrolled, spontaneous crystallisation of fines and possibly to unreproducible product crystals.

Once the temperature profile for the cooling liquid in the jacket has been selected, it depends on the heat exchange capabilities of the crystallisation vessel in what way the bulk slurry temperature follows the trajectory of the cooling liquid. Good heat exchange and large heat exchange surface area compared to bulk volume enables careful control over the cooling profile of the bulk slurry. Under these conditions a small temperature difference between bulk and jacket can be established. Poor heat exchange or little

heat exchange surface area compared to bulk volume leads to poor process control, large temperature differences between bulk and jacket and possibly significantly longer processing time to reach the final crystallisation temperature.

A large temperature difference between bulk and jacket causes cold heat exchange surfaces and supersaturation in the liquid-surface boundary layer to spike into the unstable zone before the bulk solution does. Subsequent fouling on heat exchange surfaces reduces heat transfer from bulk to jacket, control over the crystallisation process is lost and non-uniform product is obtained.

Another specific challenge in cooling crystallisation is the large range of temperatures the process moves through during operation. Polymorphs show different thermodynamic stabilities at different temperatures and it can happen that a polymorph stable at high temperature nucleates and later on at lower temperature a different polymorph nucleates. This scenario could result in a mixed product phase if no polymorphic transformation happens during the process.

6.5   Specific challenges to reactive crystallisation

Challenges specific to reactive crystallisation are discussed below, whereas general crystallsiation issues are discussed later.

The unit operation of mixing has a significant impact on the particle formation in reactive crystallisation. Mixing two liquids to the molecular level (micromixing) before a considerable degree of supersaturation is obtained is a major challenge. Micromixing is the key objective as it is critical to the chemical reaction, generation of homogeneous supersaturation, induction time and reproducible crystallisation. A processing step of this importance for crystallisation should be well controlled, reproducible and very quick, typically in the order of milliseconds. However, short mixing times require high mechanical or fluid shear rates, which can damage the newly formed crystals.

But high shear and crystal breakage is not only a challenge during mixing and nucleation but throughout the entire crystallisation process. In a scenario where two or more different polymorphs nucleate and grow competitively it can be down to shear

rates and crystal breakage behaviour which polymorph dominates the final crystal product. Awareness of this phenomenon can be used to selectively obtain one or the other polymorph.

Another important influencing factor for the final polymorph population is local and global supersaturation. Nucleation and growth kinetics of competing polymorphs can change based on the degree of supersaturation present. With changing supersaturation, the system might nucleate a different polymorph at the beginning compared to the end of the process, which would lead to a mixed population in the final crystal product.

Seeding a reactive crystallisation process is more difficult than in other modes of crystallisation. Very fast reactions, compared to mass transfer and growth rates, generate very high local supersaturation and excessive nucleation of fines before the available supersaturation could be consumed by seed crystal growth.

On top of that, the chemical reaction between reactant A & B produces side products which in turn affects the solubility of AB and the metastable zone in the solvent mixture. This scenario makes it increasingly difficult to determine the right point of seed addition.

6.6 Specific challenges in antisolvent crystallisation

The difference between antisolvent and other modes of crystallisation is that antisolvent crystallisation requires a miscible good and bad solvent with respect to the solute. Some compounds are moderately soluble in the majority of solvents typically used in a laboratory or industry and it can be difficult to find a suitable solvent system.

Mixing a solvent with a solution to initiate crystallisation increases the total working volume and reduces volumetric productivity. On top of that, it is required to separate the solvents again after the process is finished, which can be a different challenge on its own depending on the solvent system.

The unit operation of mixing has a significant impact on the particle formation in antisolvent crystallisation. To achieve micromixing of two streams, before a

considerable degree of supersaturation is obtained, is a major challenge but with a step so crucial for crystallisation it should be well controlled.

Similarly to reactive crystallisation local and global supersaturation have a significant effect on nucleation, and growth kinetics of competing polymorphs can change based on the degree of supersaturation present. With changing kinetics during the process, it is possible that different polymorphs nucleate at the beginning compared to the end, which can lead to a mixed population in the final crystal product.

6.7 General challenges in crystallisation

Many different methods are available to supersaturate a system and it is essential to identify the most suitable process depending on the desired compound. The complex interaction between supersaturation, rate and nature of nucleation and growth processes and the desire for reproducible product crystals require careful consideration in what way supersaturation can be generated.

Good control over a constant level of global supersaturation is required throughout the crystallisation process and makes this parameter key to any operation. However, due to the nature of crystallisation, varying levels of supersaturation or spikes of local high supersaturation might occur, which can adversely affect the process and the final product and require careful consideration.

Cooling crystallisation offers good control over supersaturation because the heat exchange surfaces can be cooled very slowly and consistently. Reactive and antisolvent crystallisation, on the other hand, deal with the challenge of local high supersaturation at the point of reactant or solution addition, if solutions are not instantly micromixed.

A phenomenon observed regardless of the method used to generate supersaturation is oiling out, which is a spontaneous split of the sample solution into two liquid phases instead of forming crystals. This process can occur when nucleation of a compound is slow or delayed due to high levels of impurities, supersaturation is high and rapidly generated in the absence of seeds or mixing is inadequate. Oiling out is difficult to

control and more likely to happen in nucleation dominated crystallisation processes than in crystal growth dominated processes.

If under the same operating conditions nucleation does occur there is the risk that the newly forming crystal includes solvent molecules or impurities into the crystal lattice. In this case, it is important that the small crystals are grown slowly, at low supersaturation, to larger product crystals so that growth can act as an impurity rejection process.

A common approach trying to control crystallisation is the addition of seed crystals, of desired polymorph and particle size distribution, to the process. Seeding helps controlling global supersaturation, prevents uncontrolled, spontaneous nucleation and moves crystallisation towards a growth dominated process.

However, it cannot be stressed enough that the success of seeding or seeded crystallisation heavily depends on the seeding strategy. A major challenge throughout all methods of crystallisation is the reproducible generation of seeds with constant quality and desired physical properties. Various techniques are available ranging from using crystals from a previous batch, producing one batch of seed crystals for multiple seeded crystallisation runs or jet-milling product down to the required particle size distribution.

Once desired seeds are obtained, the challenge of assessing the seed loading, number of seeds required and their way of introduction arises. Seed loadings can vary from using very few seeds to very large quantities and they are usually introduced as suspended slurry.

But the biggest challenge is the right timing for adding seeding suspension to the crystallisation process. Seeds added to an undersaturated system will readily dissolve, which defeats the purpose of seeding and no control over supersaturation is achieved. Seeds being added too late, into a system which already started to nucleate, is disadvantageous as seeds are supposed to prevent uncontrolled, spontaneous nucleation. Adding seeds to a system for which the supersaturation is located in the centre of the metastable zone is most effective in controlling crystallisation.

But even if a system is seeded and its supersaturation is well controlled, there is the challenge of colliding particles sticking together and continuing growth as an

agglomerate. Ongoing collisions between individual crystals can form large agglomerates, which can entrap solvent molecules or impurities and significantly reduce the effective surface area for crystal growth.

Another process happening despite low and well controlled supersaturation in the presence of existing crystals is secondary nucleation, which creates small new particles to consume the available supersaturation. Secondary nuclei can originate from collisions, attrition or breakage of existing crystals or when molecular clusters are being washed off the surface of parent crystals. In all cases however, secondary nucleation leads to a generation of fine crystals, a broad particle size distribution and difficulties in downstream processing.

In terms of batch operation, all specific and general crystallisation challenges are accompanied by batch-to-batch variations, making every single batch a unique additional challenge. Different levels of impurities change the solubility, supersaturation and metastable zone behaviour of each batch and hence require a large effort ensuring reproducible consistent product quality.

Continuous operations, on the other hand, can overcome some of the batch challenges at the requirement of much better process understanding and the cost of less flexibility.

Table 6.7-1 outlines some of the advantages and disadvantages of batch vs. continuous processing. [2.1, 2.2, 3.2]

Table 6.7-1: Selection of advantages of batch and continuous manufacturing

Pro Batch	Pro Continuous
Frequent cleaning of equipment without upsetting the process	Easier control over process critical parameters in steady-state operation
Frequent product changes	Plug flow behaviour / every molecule treated in the same way (in theory)
Slow processes with long residence times possible	Smaller equipment volume
When batch sizes do not justify start up and shut down waste of continuous process	Less waste, carbon footprint and inventory space
Lower capital cost	Less labour intensive – low operational cost
Mostly already present in industry	Very short downtime compared to production time
	One continuous mass stream (no storage of intermediate products)

7 Effect of Initial Mixing on Nucleation in Antisolvent Crystallisation of Valine

The work presented in this chapter was originally started by A. Brown, who carried out initial experiments and provided some preliminary data as reported in his PhD thesis (see [5.5]). This initial work was expanded by the author of this thesis who completed further experiments and analysed the data for the presentation in the current form.

An ideal crystallisation process requires homogeneous bulk supersaturation to ensure uniform and reproducible conditions for nucleation and growth. In cooling crystallisation different temperature gradients have an impact on the crystallisation process and can lead to different crystal products. In antisolvent or reactive crystallisation, on the other hand, bulk supersaturation is generated by either mixing a solution with an antisolvent or by mixing two solutions of reactants.

It can be assumed that mixing can have a potential effect on nucleation and hence on the final crystal properties, since concentration heterogeneities can lead to non-uniform supersaturation, before complete mixing is achieved.
The work in this chapter was started by A. Brown, who carried out initial experiments and provided preliminary data (also see [5.5]). This starting point was picked up by the author who completed and complemented experiments and brought the data into the current shape.

7.1 Introduction

Crystallisation is an important separation and purification technique utilised across a wide range of process industries including manufacturing of fine chemicals and pharmaceuticals. [2.2, 7.1] Since particle size distribution is crucial for product design [7.2, 7.3] as well as downstream processing [7.4-7.7], it is important to be able to manipulate processing conditions in such a way that desired particle size distributions are obtained in a crystallisation process [7.8-7.11]. Antisolvent crystallisation is one of

the common methods for inducing supersaturation. It involves mixing of a solution with a miscible antisolvent which reduces the solute solubility to create a supersaturated solution [7.12], where nucleation and subsequent crystal growth can proceed [7.13].

Rapid mixing of antisolvent with solution of a solute in a good solvent is required in order to quickly achieve homogeneity of the resulting mixture to avoid concentration heterogeneities, which could adversely affect consistency of the resulting particulate product. This can be achieved by utilising a static mixer, such as a T or Y shaped mixer or a confined impinging jet (CIJ) mixer. [7.18-7.20] A CIJ mixer consists of two opposing high velocity streams, which impinge against one another, creating a region with a high energy dissipation in a confined chamber through which all the fluid has to pass. Mixing times in a CIJ mixer have been estimated to be of the order of 10-100 milliseconds [7.11, 7.19], with residence time in the mixer of less than 1 sec. One limitation of the CIJ mixer is a constraint to have approximately equal flow rates due to a requirement of roughly equal momenta [7.21, 7.22].

It is often assumed that resulting supersaturated solutions are molecularly homogenous before particle formation commences, although this assumption is not valid when the characteristic time of mixing of solvent and antisolvent streams is comparable or longer than the characteristic time of particle formation at supersaturation equal to that in the fully mixed solution. [7.14] When microscale particle formation events involved in the crystallisation process, such as nucleation or precursor phase formation, have characteristic times similar to or less than that of mixing, particle formation kinetics become sensitive to the initial mixing conditions. [7.15]

Mixing can be considered over a range of length scales. Macromixing occurs on the scale of a vessel while micromixing occurs at the scale of molecular diffusion. In between these two extremes is mesomixing, which typically refers to the length scale of the feed stream. In turbulent flows, mesomixing acts through turbulent diffusion and inertial convection.
For example, in precipitation processes nucleation is often very rapid with timescales comparable to those of micromixing and therefore the initial mixing step is expected to have effect on nucleation kinetics [7.26]. While primary nucleation has been traditionally

thought of as a molecular scale process, it would be expected to be influenced only by molecular level mixing (i.e. micromixing) and large scale mixing (i.e. macromixing) having only an indirect influence [7.5, 7.15, 7.17]. However, if there are intermediate metastable phases at colloidal lengthscales, such as in a two-step nucleation mechanism [3.3], these intermediates may be influenced by mesoscopic scale mixing processes.

In this work we investigated antisolvent crystallisation of valine using a CIJ static mixer for the initial mixing step. We studied effects of supersaturation and flow rate through the static mixer on subsequent valine crystallisation kinetics under quiescent (unstirred) conditions. Even when resulting valine solutions (at lower supersaturations) were clear without presence of any detectable solids until some minutes after the initial rapid mixing, subsequent solid formation kinetics were strongly dependent on the flow rate through the mixer, i.e., initial mixing intensity. By investigating quiescent solutions, we aimed to eliminate effects such as secondary nucleation and breakage, in order not to interfere with effects of the initial mixing step on nucleation of valine in antisolvent crystallisation. [5.5]

7.2   Methods

7.2.1   Materials

DL-valine (99 %, Sigma-Aldrich) and isopropanol (99.5 %, Fisher Scientific) were used. Deionised water used in all experiments was obtained from a Thermo Scientific (USA) water purification system. All experiments were performed isothermally at 21⁰C. Crystallisation of valine was achieved through the shift in solubility due to the rapid mixing of its aqueous solution (solubility$_{(aq.)}$ ~70 g/L) with the isopropanol antisolvent (solubility$_{(mixture)}$ ~14 g/L). Valine ($C_5H_{11}NO_2$) is an essential amino acid which crystallises relatively easily with a single known solid state form and is used as a food supplement and a precursor for pharmaceuticals syntheses.

7.2.2 Solubility measurements

A pre-determined amount of valine (exceeding the expected solubility) was weighed into a jar and equal volumes of water and isopropanol (5 ml each) were added. The jar was closed, placed in a water bath set to a desired temperature and magnetically stirred for 24h. Afterwards it was filtered over a 0.45 µm Millipore filter and the mass of undissolved valine was determined by weighing how much valine was retained on the filter. The equilibrium solubility at a given temperature was determined from material balance of valine. All experiments were performed in triplicate over a temperature range of 10-30ºC.

7.3 Experimental setup

Pulse-free flow was obtained using micropump heads (GB series, suction shoe design gear pump) magnetically coupled with a pump driver (Ismatec MCP-Z Standard). Figure 7.3-1 shows a schematic diagram of the setup used in which all fittings, piping and the CIJ mixer were constructed of stainless steel. Pressure transducers were placed before and after the mixer to measure the pressure drop across the mixer. Pressure drop values can be translated to a total energy dissipation rate, if flow rates, physical properties and the mixer dimensions are known.
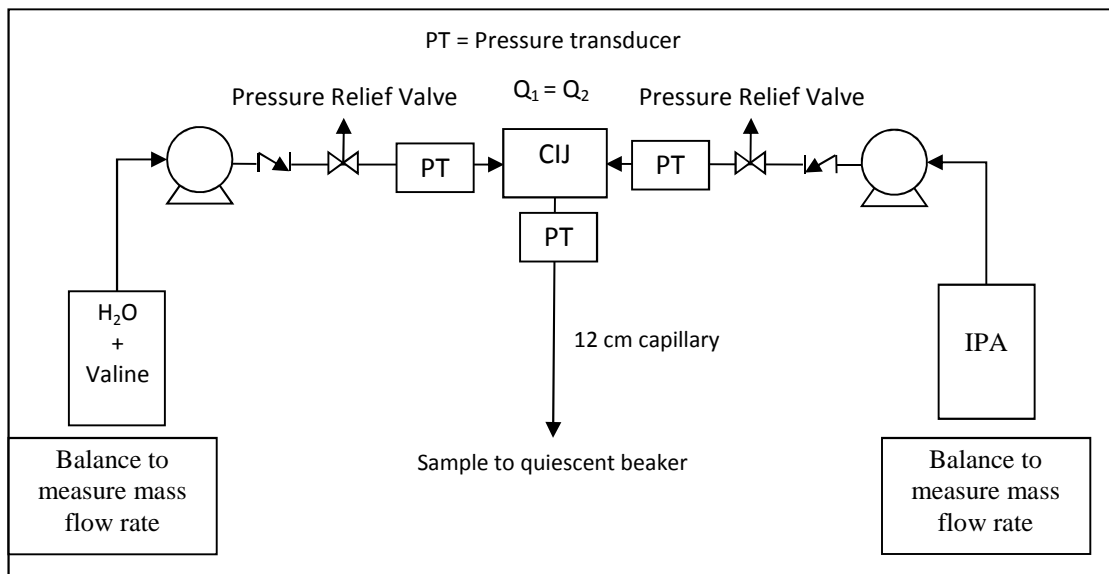
Figure 7.3-1: Antisolvent crystallisation set up consisting of feed vessels, pumps, valves and static CIJ mixer [5.5]
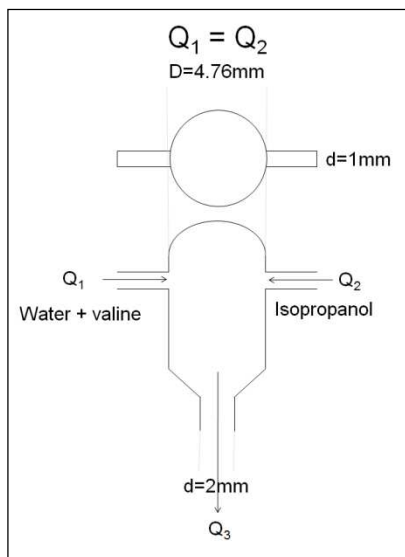
Figure 7.3-2: CIJ diagram [5.5]

7.4 Crystallisation experiments

Mixing of valine aqueous solution with isopropanol (1:1 v/v) was carried out using a static mixer setup described above, see Figure 7.3-2, with CIJ inlet flow rates ranging from 50 ml/min to 700 ml/min (from each side), resulting in a wide range of energy dissipation rates and corresponding mixing half-times. Valine aqueous solutions were prepared by dissolving valine powder in water and the solutions were filtered through 0.45 μm Millipore filter to ensure that any undissolved solids and impurities were removed. Initial valine concentrations in resulting water-isopropanol solutions ranged from 18 to 31 mg/g$_{solution}$. Gear pumps were calibrated with water and isopropanol, respectively, to provide required volumetric flow rates, with deviations smaller than 1%. Before and after each run the system was flushed with warm water, in order to clean possible residues. Mixing was operated continuously for a period of time, with the first three residence times discarded to ensure steady-state, after which about 150 ml of mixed solution were collected in each of several vessels, serving as parallel experiments for different crystallisation times. After the predetermined crystallisation period the whole content of a particular vessel was filtered, the filter cake was placed in an oven to dry for 2-3 h at 40-50 °C and the crystal dry mass was determined gravimetrically. Utilising the solubility data determined in the previous experiments, the solid recovery as a percentage of theoretical equilibrium recovery was determined. Crystal slurries were subject to particle sizing with laser diffraction using Mastersizer 2000. Samples for laser diffraction were diluted by a factor of six using mother liquor to quench further growth. The amount of mother liquor was chosen to strike a balance to ensure that the growth is adequately suppressed but that the obscuration was reasonable to allow reliable measurements. Optical transmittance measurements of crystallising quiescent solutions were also performed, since it was visually observed that at higher supersaturations and higher initial mixing intensities, significant turbidity developed during crystallisation. Immediately after the initial mixing (which took less than 1 s) solutions were transferred into a 1 cm optical path quartz cuvette, which was placed in the UV/Vis spectrometer (Cary 5000) and was scanned in the wavelength range of 800 – 200 nm. After identifying a suitable wavelength, single wavelength measurements were carried out at 248 nm. [5.5]

7.5 Static mixer characterisation

The CIJ mixer used for crystallisation experiments was characterised using a parallel competitive reaction scheme with well-known kinetics. The scheme chosen was a strong acid/base neutralisation competing for acid with the acid catalysed hydrolysis of dimethoxypropane (DMP) developed by Baldyga and Bourne [7.17] with the chemical reactions illustrated in Equation 7-1.

Rapid neutralisation of a strong base and strong acid:

$$HCl + NaOH \xrightarrow{\quad k_1 \quad} H_2O + NaCl$$

Equation 7-1

Acid catalysed hydrolysis of dimethoxypropane, as shown in Equation 7-2.

$$CH_3C(OCH_3)_2CH_3 + H^+ (+ H_2O) \xrightarrow{\quad k_2 \quad} CH_3COCH_3 + 2CH_3OH + H^+$$ Equation 7-2

The second, slower reaction, can be simplified to a second order reaction due to the ubiquity of water in the system, with a rate constant [7.5] given as a function of temperature and salt concentration in Equation 7-3.

$$k_2 = 7.32x10^7 \exp(-5556/T)10^{\left(0.05434 + 7.07x10^{-5}C_s\right)}$$

Equation 7-3

where C_s is the concentration of sodium chloride, which was added to both reactant streams, to ensure a moderate salt concentration always exists as the hydrolysis reaction has been found to accelerate with increasing salt concentration. The rate of hydrolysis reaction is much greater than the second reaction and can be considered instantaneous with respect to the mixing. The characteristic reaction time τ_r (Equation 7-4) can be expressed as the pseudo first order time constant of the slow reaction:

$$\tau_r = \frac{1}{k_2 C_{DMP}}$$

Equation 7-4

where C_{DMP} is the concentration of DMP.

The extent of mixing can be quantified by the fractional conversion of the DMP according to Equation 7-5.

$$X = 1 - \frac{C_{DMP}}{C_{DMP0}}$$

Equation 7-5

where C_{DMP0} is the initial concentration of DMP. A high fractional conversion in the resulting mixed solution indicates poor mixing and a low fractional conversion indicates good mixing. The method is limited by analytical sensitivity at good mixing conditions and reaction kinetics at the poor mixing. However, this can be tuned by varying the concentration of the reactant species.

DMP (98%, Sigma Aldrich) and NaOH (1 molar standard Solution, Sigma Aldrich) in stream 1 were mixed with stream 2 containing HCl (1 molar standard solution, Sigma Aldrich). A molar ratio of 1.05:1:1 for NaOH:HCl:DMP was used to ensure that all H^+ ions were consumed in the reaction (if H^+ was in excess the slow reaction would be free to progress until completion).

Concentrations of 210 mmol/L, 200 mmol/L and 200 mmol/L (NaOH, HCl and DMP, respectively) were used, 90 mmol/L of NaCl was dissolved in both reactant streams and the experiments were carried out at a temperature of 25°C. Under these conditions the characteristic reaction time of the slow reaction is 16.7ms.

During solution preparation the DMP was not contacted with any material of pH less than 8 to prevent any hydrolysis prior to mixing. All solutions were prepared by weight and were dissolved in a solution containing ethanol and water. The product distribution was then analysed by gas chromatography.

In the original reaction scheme, both reactant streams were blended with a solution containing 75% water and 25% ethanol solution by weight. This means that there was little difference in the physical properties between streams, which is not representative of many real mixing processes. Additional experiments were carried out with a modification added to create a difference in physical properties (viscosity) of the two streams but keeping reactant concentrations the same. The solvent composition of the acid stream was pure water and the DMP and base stream a blend of 50% ethanol and 50% water by weight. This closely corresponds to the maximum viscosity of an ethanol/water mixture and ensures the concentrations of all components upon mixing are identical, while the viscosity ratio of the two streams is close to 2:1.

The samples were analysed by gas chromatography using a Shimadzu 2014 gas chromatograph with manual injection. A 10m guard column was used to protect the analytical column (30m RTX1301) from non-volatiles. An injection volume of 2µL was used with a split ratio of 100:1 and a column temperature of 60°C. Ethanol was used as an internal standard. Fractional conversion was quantified on the basis of the amount of methanol produced with the amount produced from acetone used as an additional check for internal consistency.

The fractional conversion was converted to a theoretical mixing time by the comparable volume engulfment model which was developed by Baldgya and Bourne [7.15] and has also been utilised by Gillian and Kirwan [7.24]. Our approach [5.5] was based on that developed by Gillian and Kirwan [7.24]. Two mixing times are obtained, a mixing half-life corresponding to 50% completion which is useful for estimating the characteristic time of the mixing and the 90% mixing time which corresponds to 90% completion of the mixing, as quantified by the reduction of the acid to 10% of its initial value. The neutralisation reaction is instantaneous with respect to mixing, therefore this reaction can be used to quantify mixing completion. [5.5]

7.6 Results

7.6.1 Experimental Characterisation of Mixing Times

The experimental characterisation of the CIJ mixer using the parallel competitive reaction scheme provided data in terms of fractional conversion of DMP, which were then used to determine corresponding mixing times. Mixing characteristic times varied from 100 ms at the lowest flow rates to less than 10 ms at the highest flow rates used here. It is also important to compare the mixing time with the mixer residence time, in order to establish whether completion of mixing at the molecular level was achieved before the outlet stream leaves the mixer and is collected in the quiescent vessel. In Figure 7.6-1 and Figure 7.6-2 we show the comparison of residence and mixing timescales corresponding to 50% and 90% completion of the mixing for a viscosity ratio of 1:1 (Figure 7.6-1) and a viscosity ratio of 2:1 (Figure 7.6-2). The physical properties of the case with the viscosity ratio of 2:1 are close to those of the water and isopropanol system used here for antisolvent crystallisation of valine. From Figure 7.6-2 we can see that mixing may not be complete within the mixer residence time when the system is operating at the lowest inlet flow rate of 50 ml/min. However, the mixing time quickly decreases with increasing inlet flow rate and complete mixing is achieved for all higher flow rates.
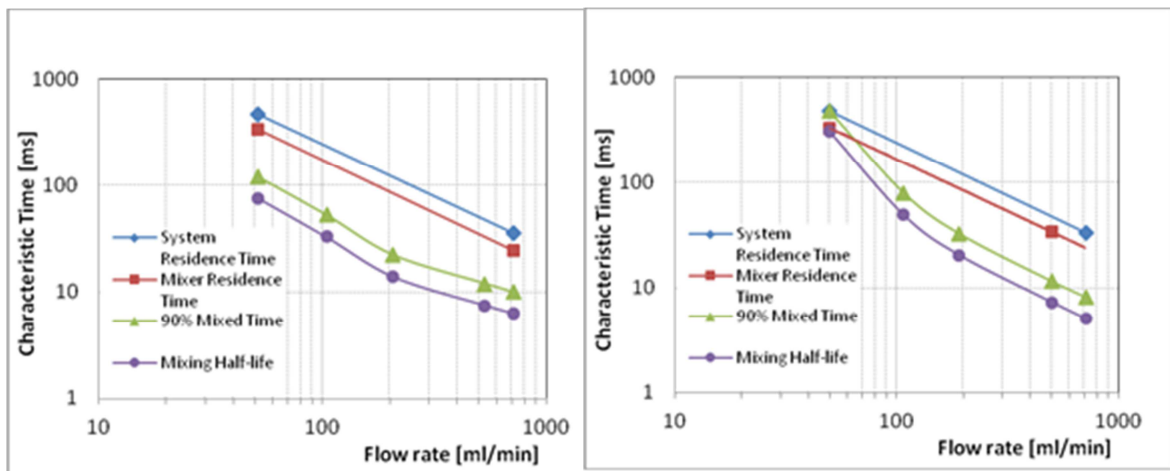
Comparison of mixing and residence times of CIJ mixer at various inlet flow rates: Figure 7.6-1 (left): Viscosity ratio of inlet streams equal to 1:1, Figure 7.6-2 (right): Viscosity ratio of inlet streams equal to 2:1

A significant micromixing contribution is indicated by viscosity dependence of mixing times at lower inlet flow rates (Figure 7.6-1 and Figure 7.6-2), since mesomixing occurs in the inertial range and is independent of viscosity. In the micromixing limit there is a higher power law exponent of dependence of mixing time on the turbulent energy dissipation rate than in the mesomixing limit, and so in a log-log plot of mixing time vs. inlet flow rate we expect to see a steeper gradient for micromixing limited behaviour than for mesomixing imited behaviour. As the inlet flow rate increases (i.e., the energy dissipation rate increases), the micromixing time decreases faster than the mesomixing time, and therefore micromixing effects become less important as the mixing regime transitions to the mesomixing limited one, and indeed such behaviour can be seen in Figure 7.6-1 and Figure 7.6-2. There is a change in mixing regime from a region where viscosity has a significant effect on the mixing time (inlet flow rates ≤ 200 ml/min) to one where it has little or no influence (inlet flow rates ≥ 400 ml/min), i.e., from a region with a micromixing dependency at low flow rates to a mesomixing limited behaviour at higher flow rates. [5.5]

7.6.2 Solubility measurements

The solubility of DL-valine in a water-isopropanol mixture (1:1 v/v) was determined in a temperature range of 10-30°C. Each measurement was repeated at least three times. The experimental results are shown in Figure 7.6-3. The fit equation shown can be used to calculate the solubility within the relevant temperature range.
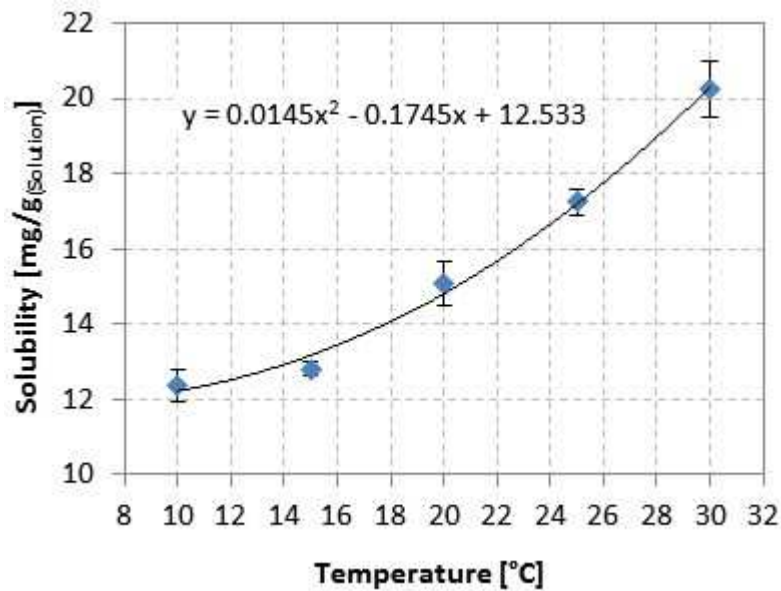
Figure 7.6-3: Solubility of DL-Valine in a water:isopropanol mixture (1:1 v/v)

$$y = 0.0145x^2 - 0.1745x + 12.533$$

7.6.3 Valine crystallisation

In order to assess the effect of the initial mixing of valine, aqueous solution with isopropanol (under well controlled mixing conditions in the CIJ mixer at various inlet flow rates) on nucleation of valine crystals, we used UV-VIS transmission measurements. The attenuation coefficient in quiescent supersaturated solutions was measured as a function of time after complete mixing was achieved. We note that all mixing and further measurements were done at a constant temperature. Figure 7.6-4 shows an example of transmittance measurements of the saturated solution of valine in water-isopropanol mixture (1:1 v/v) as well as of a supersaturated solution started at 3, 10 and 20 minutes after the initial mixing. From the saturated solution curve we can see that there is a negligible absorption from valine solutions in the visible and near UV region, while there is strong solvent contribution due to absorption at wavelengths below 240 nm. However, significant turbidity develops due to scattering from crystals forming in the supersaturated solution, contributing to the overall attenuation coefficient across the spectrum of visible and near UV wavelengths.
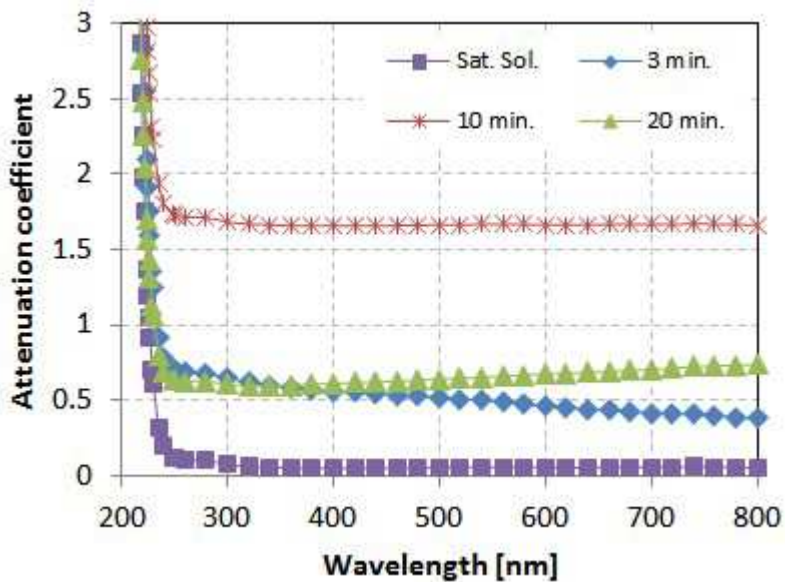
Figure 7.6-4: UV/Vis measurements of saturated and supersaturated valine solutions. Attenuation coefficients for supersaturated solutions (valine concentration 26.9 mg/g solution) correspond to scattering from crystal slurries formed in these solutions upon their initial mixing. Crystal size distributions change over time due to crystal growth and subsequent sedimentation of larger crystals, and therefore since scattering from suspended crystals depends on particles size and shape as well as wavelength, reported attenuation coefficients show varying dependence on wavelength as time progresses.

The first measurement starting at 3 minutes corresponds to an early phase of crystal formation, where turbidity increases over time while crystals are growing but still small enough so they have not started to sediment significantly. Hence the attenuation coefficient at a given wavelength is increasing over time initially. After 10 minutes crystals grow larger and sedimentation becomes appreciable and therefore the attenuation coefficient starts decreasing. As we can see from Figure 7.6-4, wavelengths between 240 and 800 nm as suitable for monitoring of turbidity evolution during crystallisation in this system, so further experiments for turbidity monitoring were performed at 248 nm.

In order to better understand the effect of the initial mixing on nucleation, measurements were performed over a range of valine concentrations and inlet flow rates. In Figure 7.6-5 we show a typical example of such measurements, which were qualitatively similar at all valine concentrations investigated, between 18 and 31 mg/g solutions, corresponding to supersaturations between 1.2 and 2.1 at 21°C.
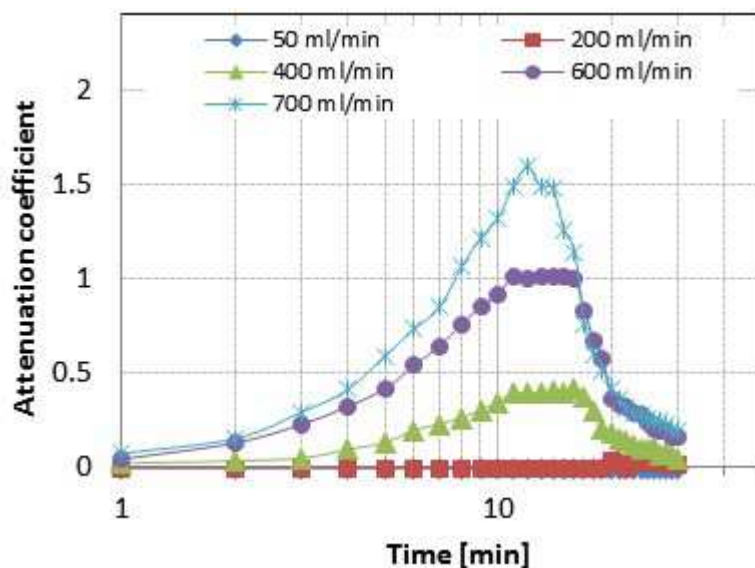
Figure 7.6-5: Time evolution of attenuation coefficient at 248 nm for different initial mixing flow rates

For lower inlet flow rates (50 and 200 ml/min) there was a very low attenuation coefficient measured throughout crystallisation, since only relatively few crystals formed which grew and sedimented without any significant contribution to the attenuation coefficient. However, at higher initial mixing flow rates (400 ml/min and higher) there was a strong increase in the attenuation coefficient, due to clearly visible turbidity caused by a large number of small crystals appearing in the solution. The same behaviour was seen at all valine concentrations, although evolution of turbidity in samples with higher initial mixing flow rates was faster at higher valine concentrations (i.e., higher supersaturations) as expected. [5.5]

In order to assess the extent of crystallisation through the mass of crystal solids obtained, the samples of quiescently growing crystal suspensions were filtered after a certain period of time. Depending on the inlet flow rate, two distinct regimes were observed for the crystallisation behaviour after the initial mixing for solutions at valine concentration of 26.9 mg/g solution. The sample mixed at the inlet flow rate of 50 ml/min looked visibly clear at 1 minute after mixing, however, the filtration was very slow (filtration time over 50 min) and the filtrate was visibly turbid. This indicates that the filtration process itself triggered nucleation resulting in clogging the filter, slowing down the filtration process and causing the filtrate to turn turbid. On the other hand, the sample mixed at inlet flow rate of 700 ml/min was clearly turbid immediately after mixing, but the filtration was rapid (filtration time less than 5 min) and the filtrate was clear. A summary of the filtration behaviour at all initial mixing flow rates can be found in Table 7.6-1. The filtrate was either turbid or clear. The filtration was rapid (below 5 min), slow (5-50 min) or very slow (over 50 min).

Table 7.6-1. Filtrate appearance and speed of filtration as a function of mixer inlet flow rate and crystallisation times. Solutions of valine in water-isopropanol (1:1 v/v) at 26.9 g/g solution. [5.5]

Mixer inlet flow rate [ml/min]	Crystallisation time [min]			
	1	5	10	30
50	Turbid Very slow	Turbid Very slow	Turbid Slow	Turbid Slow
200	Turbid Very slow	Turbid Slow	Clear Normal	Clear Normal
300	Turbid Very slow	Clear Normal	Clear Normal	Clear Normal
400	Turbid Slow	Clear Normal	Clear Normal	Clear Normal
600	Clear Normal	Clear Normal	Clear Normal	Clear Normal
700	Clear Normal	Clear Normal	Clear Normal	Clear Normal

As we have seen from transmission measurements, at inlet flow rates up to 200 ml/min, supersaturated solutions leaving the static mixer were clear and remained without appreciable turbidity throughout subsequent crystallisation, while those prepared at inlet flow rates of 400 ml/min and higher were turbid upon exiting the static mixer (at supersaturations 1.6 and higher) or turned so within few minutes (at supersaturation 1.2). Figure 7.6-6 and Figure 7.6-7 show the time evolution of solid recovery (defined as a percentage of the mass of crystalline solids obtained when solubility equilibrium is reached under given conditions) for various inlet flow rates for supersaturations 1.6 and 1.8. In line with observations from transmission measurements, there is a clear transition between inlet flow rates of 200 and 400 ml/min, with much faster solid formation at higher inlet flow rates. At the highest valine concentration (26.9 mg/g

solution, supersaturation 1.8) it can be seen that similar solid recovery rates were obtained over time for inlet flow rates of 400, 600 and 700 ml/min (Figure 7.6-7). This indicates that above a certain value of flow rate a plateau is reached and more intense initial mixing does not lead to faster nucleation anymore.
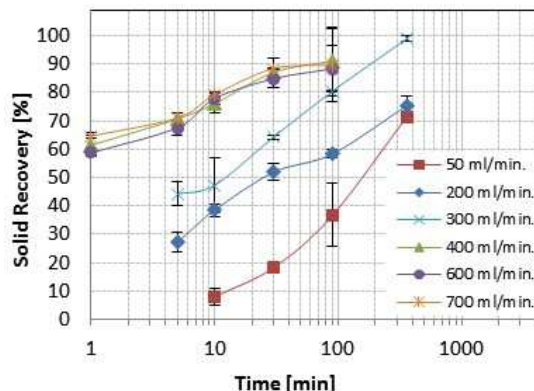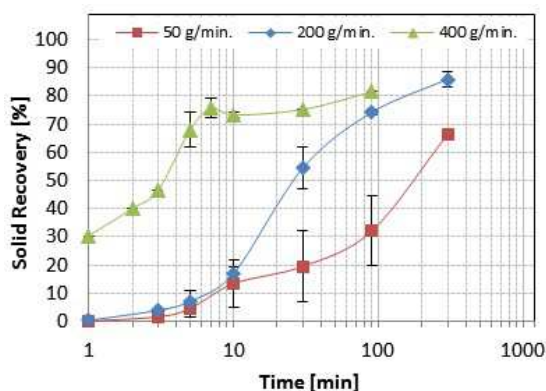
Solid recovery (as a percentage of equilibrium solubility) vs. time for supersaturated valine solution at different inlet flow rates as indicated: Figure 7.6-6 (left): 24 mg valine/g solution (supersaturation 1.6); Figure 7.6-7 (right): 26.9 mg valine/g solution (supersaturation 1.8)

Similar results were also obtained for valine solutions at concentration of 18 mg/g solution (supersaturation 1.2) with results shown in Figure 7.6-8. It can be seen that at the inlet flow rate of 50 ml/min no appreciable amount of solids can be recovered before crystallisation time of 90 min. Even after 1000 min the solid recovery only reached about 55 % of the equilibrium value. Under these conditions, supersaturated solutions left the mixing unit as a clear
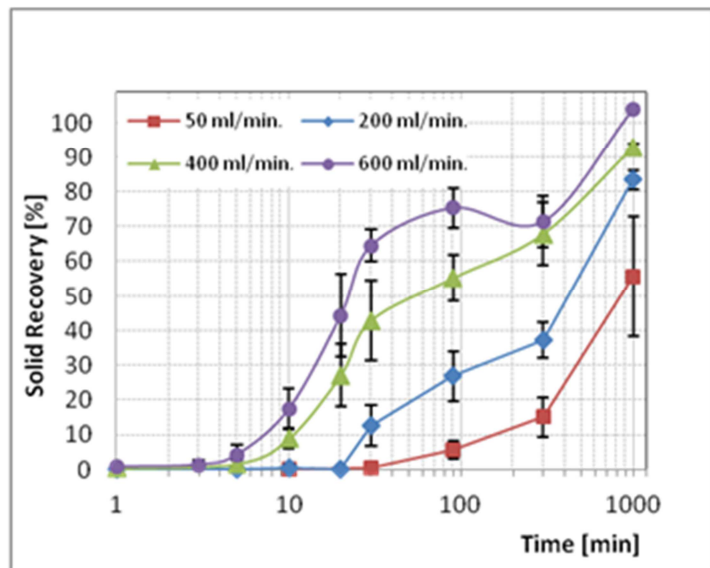
Figure 7.6-8: Solid recovery (as a percentage of equilibrium solubility) vs. time for supersaturated valine solution (18 mg/g solution) at different inlet flow rates as indicated

solution and never turned appreciably turbid. This was due to a small number of relatively large crystals that were formed, which readily sedimented in quiescent conditions and did not generate any turbidity. Again, there appears to be a transition between the initial flow rates of 200 and 400 ml/min as exemplified by behaviour of samples prepared at these respective initial mixing flow rates. While both samples left the static mixer as clear solutions, the 200 ml/min sample has not turned turbid similarly to the one prepared at 50 ml/min. Crystals in this sample mostly grew at the bottom of the quiescent vessel and the first solid could be recovered after 30 min. On the other hand, the 400 ml/min sample turned turbid within minutes after leaving the mixer, crystals grew rapidly in the bulk solution material and solids could be recovered after less than 10 min. Similarly, the 600 ml/min sample left the mixing unit as a clear solution and again turned turbid rather quickly, with 50% solid recovery reached in less than 30 minutes. It can be seen from Figure 7.6-8 that solid formation is more than one order of magnitude faster than that observed for samples with the initial mixing flow rate of 50 ml/min.

In Figure 7.6-9 we show a diagram illustrating the solid recovery, as a percentage of the equilibrium solid recovery, after 90 minutes as a function of valine concentration and initial mixing flow rate. The red dashed line indicates valine solubility.

It is apparent that there are two regions in this parameter space; a region of fast nucleation at higher concentrations and higher
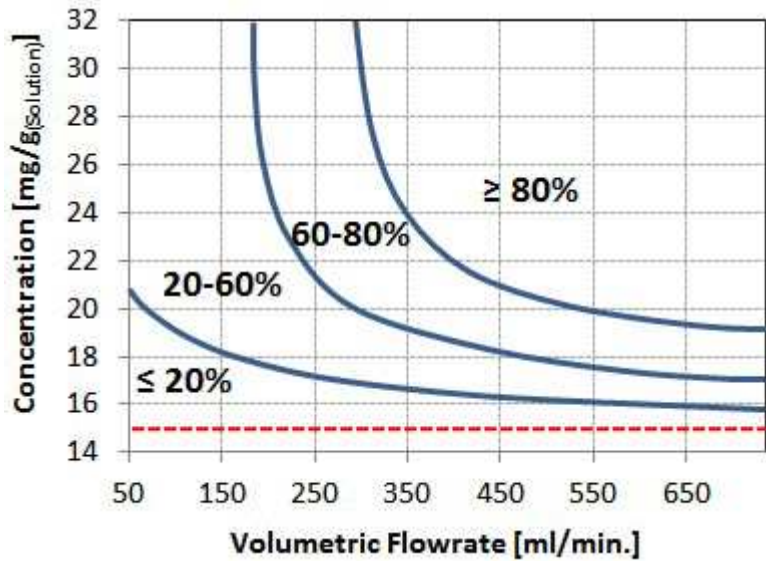
Figure 7.6-9: Diagram of solid recovery at 90 minutes after the initial mixing in the parameter space of initial mixing flow rate and valine concentration. Solubility concentration is indicated by dashed line.

initial mixing flow rates, and a region of slow crystallisation when either concentration or initial mixing rate are lower.

This plot illustrates the transition between initial mixing flow rates of 200 and 400 ml/min from slow to fast nucleation. Faster nucleation is promoted in this system either by higher supersaturation (as expected) or by more intense initial mixing, even at quite low supersaturation.

In Figure 7.6-10 we show results of particle size measurements for solids formed from supersaturated solutions prepared with different inlet flow rates but with the same valine concentration. The samples were taken at long times after the initial mixing, so that nearly 100% solid recovery (as compared to solubility equilibrium) was reached. It can be seen that higher initial mixing flow rates resulted in
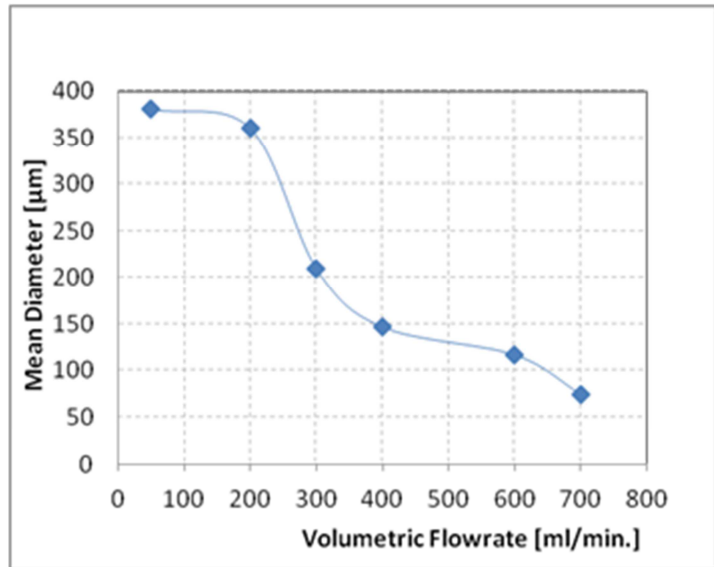
Figure 7.6-10: Dependence of mean particle diameter ($d_{4,3}$) measured by laser diffraction at 100% solid recovery for valine concentration of 26.9mg/g solution.

smaller mean particle size, which means that more crystals were formed. Again, there was a dramatic change in particle size between initial mixing flow rates 200ml/min and 400 ml/min, corresponding to a transition between low and high turbidity (Figure 7.6-5) as well as corresponding solid recovery (Figure 7.6-7) at shorter crystallisation times. Since the mean crystal diameter decreased approximately by a factor of 5, the number of crystals formed can be estimated to increase by about two orders of magnitude (since the same solid recovery was achieved) between the lowest and the highest initial mixing flow rate.

In nlet flow rates: (A: Figure 7.6-11, C: Figure 7.6-13, B: Figure 7.6-12 and D: Figure 7.6-14 we show images of crystals from solutions at valine concentration of 18 mg/g solution prepared at various inlet flow rates and isolated after 1000 min from the initial mixing. It can be seen that with increasing inlet flow rate a larger number of smaller crystals formed, consistent with observation at higher solution concentration (Figure 7.6-10). Again this shows that at a given solution concentration the intensity of initial mixing influences nucleation kinetics, so that at higher inlet flow rates. i.e., at higher energy dissipation rates and shorter mixing times, larger numbers of crystal nuclei are formed.
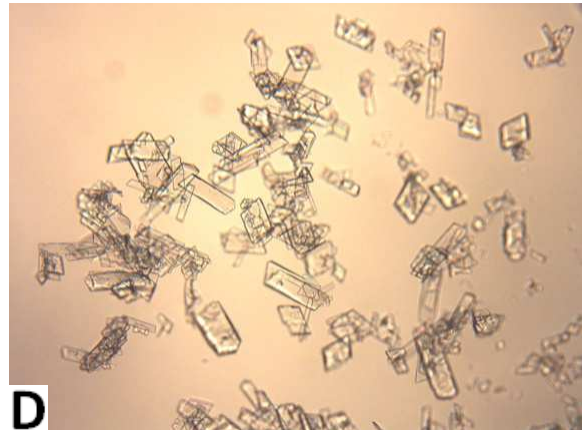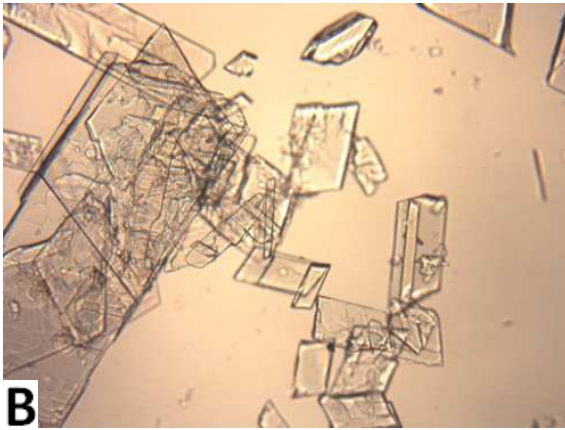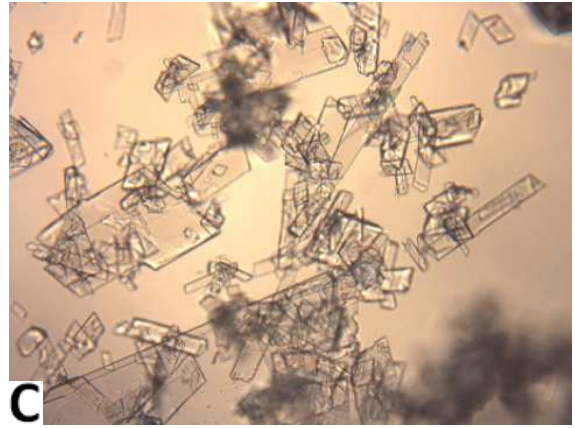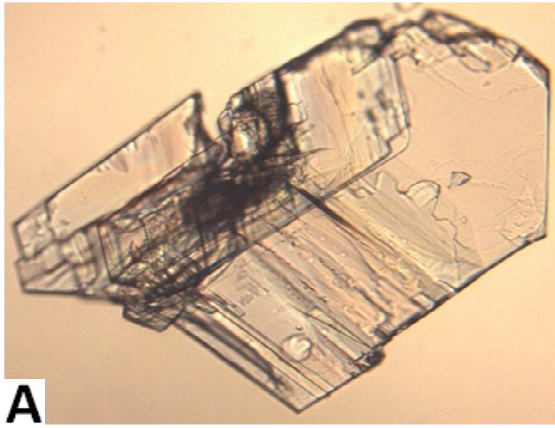
Microscopic images of valine crystals from solutions at concentration of 18 mg/g solution prepared at different mixer inlet flow rates: (A: Figure 7.6-11: 50 ml/min), (B: Figure 7.6-12: 200 ml/min), (C: Figure 7.6-13: 400 ml/min), (D: Figure 7.6-14: 600 ml/min. Magnification set to 20 times.

7.7   Discussion

We have characterised mixing times of the static mixer used here and found that at inlet mixing flow rates of at least 100 ml/min all solutions should be expected to be fully mixed at the molecular level. If the initial mixing had no effect on crystal nucleation, there would be no obvious difference between the crystallisation behaviour of samples prepared at different initial mixing flow rates at a given composition. Nuclei would have formed under identical conditions (quiescent solution) and solution supersaturation would be the only parameter distinguishing these solutions.

It is however evident from results reported above that this was not the case and hence it can be concluded that the initial mixing step clearly has an influence on nucleation of valine crystals in water-isopropanol solutions, even under conditions of slow crystallisation at relatively low supersaturation in completely mixed solutions. Considering mixing timescales involved (mixing half-times on the order of tens to hundreds of milliseconds) and static mixer residence times (less than one second), this process must involve crystal nuclei (or their precursors) forming on timescales of tens of milliseconds.

A possible explanation for the results observed is the two step nucleation theory proposed by Vekilov (2010). [3.3] In the first step the supersaturated solution forms dense liquid crystal precursor phases, followed by the transformation of those precursors into nuclei and crystals. The mixing intensity might have an influence on the number of precursors generated, which could possibly form on a timescale equal to or shorter than the characteristic time of mixing.

Sample streams experiencing low mixing intensities may only contain a few precursors, whereas high mixing intensities generates a high number of precursors. As nucleation is a stochastic event these precursors turn into nuclei/crystal according to their own kinetics, which could explain the different crystal sizes observed.

7.8   Conclusions

The purpose of this chapter was to investigate the effects of the initial mixing intensity on nucleation in antisolvent crystallisation of valine. Optically clear samples at low mixing flow rates and turbid samples at high mixing flow rates indicates that the event of nucleation depends on the initial mixing intensity.

Nuclei precursor phases formed at the point of mixing can make the system sensitive to different mixing intensities. Although nuclei precursor phases have not been investigated in this work, a recently published work [7.28] presents direct experimental evidence of mesoscale clusters in these solutions. However, we note that effect of the initial mixing step on these clusters has not been investigated in detail.

Future work should investigate crystallisation mechanisms right after the mixed solution left the mixer. If it would be possible to instantaneously stop phase transformation in the outlet stream it should be feasible to investigate whether crystals are already present or whether they only form at a later stage from precursor phases.

8 Crystallisation of L-Glutamic acid (H-Glu) polymorphs at constant temperature and under various flow conditions

In the previous chapter the effect of mixing intensity on nucleation of valine in an isopropanol-water system was investigated and it was found that the mixing intensity affects solid recovery over time and the final crystal size. The same experiments were carried out for H-Glu but for this compound no effect between mixing intensity, solid recovery over time and final crystal size was observed.

The same experimental setup as before was used to carry out reactive crystallisation experiments where Na-L-Glutamate was mixed with sulphuric acid to form H-Glu and sodium sulphate. Even in these experiments the mixing intensity had no effect on solid recovery over time or final crystal size.

Based on these experiments it was decided to study the reactive crystallisation of H-Glu from Na-L-Glutamate and sulphuric acid with respect to the effect of post-mixing flow treatment on solid recovery over time and the final polymorph population. Initially, these experiments were carried out in batch mode and were turned continuous later on.

8.1 Batch operation

8.1.1 Introduction

The ability to selectively crystallise desired polymorphs is of significant importance to the pharmaceutical, agrochemical and fine chemical industry. Polymorphism occurs when the molecules of a chemical substance can arrange in more than one way in the unit cell to form a crystal. [2.2]

Polymorphs can differ substantially from one another in respect to their physical properties such as solubility, melting point, mechanical strength or crystal morphology. Some are easier to process (e.g. filterability) than others and for that reason a thorough control over the crystal form is required.

The final polymorphic composition depends on thermodynamics, kinetics [2.2] as well as supersaturation. [8.1]

H-Glu is a well studied amino acid and can crystallise in two polymorphic forms. The prismatic, metastable Alpha form [8.2] and the needle [8.3] or platelet-like stable Beta form. The Alpha form is however preferred in industry due to easier processing.

The two H-Glu polymorphs have a different solubility and this leads to solution-mediated transformation, where Alpha (higher solubility) transforms to Beta (lower solubility). If the solution concentration has reached the solubility concentration of Alpha, it will start dissolving, while Beta can nucleate on Alpha crystals [4.10] and continues to grow. This process is however very slow at temperatures below 40 °C [8.5] and can be neglected at room temperature.

H-Glu serves as an experimental compound since a few decades. Already in the 1960s Y. Sakata [8.5] described a method to precipitate H-Glu through reactive crystallisation by mixing equal amounts of mono-sodium L-Glutamate monohydrate (Na-Glu) with hydrochloric acid (HCl). The exact procedure was not further specified but the experiments sometimes yielded Alpha and sometimes Beta.

Garti et. al. [8.6] (1997), Cashell et. al. [4.10] (2003) & [8.7] (2004), Schöll et. al. [8.8] (2006) & [8.9] (2007) and Cornel et. al. [8.10] (2009) adapted a procedure in which Na-Glu was placed in a stirred vessel and an equal portion of HCl was added until the isoelectric point of pH = 3.2 was reached.

The experiments covered studies in which Alpha was initially generated by magnetic stirring, followed by a crash cooled recrystallisation step to study solution-mediated transformation at 45 °C, which was complete after 3h [8.6].

SEM was employed to obtain pictures of secondary Beta nucleation on Alpha surfaces and it was concluded that this might be a widespread phenomenon in solution-mediated transformation processes [4.10].

During further experiments secondary nucleation of Beta on Alpha was confirmed, followed by further studies about the transformation behaviour [8.7].

Samples in a STC were analysed using Particle Vision and Measurement (PVM), Attenuated Total Reflection Fourier Transformation Infrared (ATR-FTIR) and FBRM to demonstrate that these technologies can monitor particle formation (FBRM), show the prismatic Alpha shape (PVM), measure concentration and supersaturation (ATR-FTIR) [8.8].

Analytical experiments (XRPD, Raman-spectroscopy and SEM) were used to determine the polymorphic purity of the product crystals, which were then used for growth rate determinations of different seed fractions [8.9].

Alpha crystals produced at 5 °C served as seeds to study Beta growth kinetics at 45 °C. The solution concentration remained at the Alpha solubility limit until all Alpha was dissolved and then approached the Beta solubility concentration. It was found that the Alpha seeds were contaminated with Beta polymorph and that large Alpha crystals contained more contamination. In this context, the lower detection limit for Beta in Alpha crystals by Raman spectroscopy was determined to be 5 % [8.10].

All experiments in which a MSC or a STC were used and temperatures were below 40 °C, yielded exclusively the Alpha polymorph.

A different approach to generate supersaturation, in contrast to the batch based addition of HCl to a provided Na-Glu solution, was described by Roeland [8.11] (2005). In this case two solutions at room temperature, Na-Glu and diluted sulphuric acid (H_2SO_4), were continuously mixed in a Y-shaped mixer with an in-built static mixer in the outlet tube.

The continuous mixing step was considered pre-mixing and sample post-mixing was either achieved in a MSC, STC or the sample was left in a QC. Analysis of the final polymorphic composition showed that the QC yielded the Beta form, whereas the MSC and STC yielded the Alpha form. This result is consistent with the previously obtained, batch based results.

It was concluded that both polymorphs nucleate simultaneously at a low rate, but Beta more quickly than Alpha. In the QC, Beta would deplete supersaturation due to the larger number of crystals.

Alpha, on the other hand, is the faster growing polymorph. In a post-mixed sample Alpha would quickly grow to a critical size and would be exposed to attrition earlier than the Beta crystals. This scenario creates many secondary nuclei, which even more rapidly deplete supersaturation due to substantially faster growth kinetics. The supersaturation in the sample would quickly be depleted, which leaves no chance for Beta to nucleate or grow.

In similar experiments Roelands et. al. [8.12] (2007) proposed that in a QC liquid-liquid phase separation (oiling out) leads to droplets, which subsequently nucleate Beta. In the STC or MSC this oiling out is disrupted due to agitation and homogenisation. In this case heterogeneous mechanisms result in the nucleation of Alpha prisms.

In this work we used a similar set up like Roelands but exposed the pre-mixed sample to a wider range of post-mixing flow conditions. The aim was to assess what kind of flow or treatment changes the polymorphic composition from Beta to Alpha. Another objective was to find out whether the slow nucleation and hence low yields of Beta could be sped up.

8.1.2 Methods

8.1.2.1 Materials

Na-Glu of $\geq 99\,\%$ purity as well as H_2SO_4 of $\geq 96\,\%$ were purchased from Sigma-Aldrich, Germany. Deionised water used in all experiments was obtained from a Thermo Scientific (USA) water purification system.

Experiments were performed in an air conditioned laboratory at $20 \pm 1\,°C$ at which H-Glu has a solubility in water of Alpha: 9.4 g/kg$_{(Solution)}$ and Beta: 7.1 g/kg$_{(Solution)}$.

The precipitation of H-Glu was achieved through a pH-shift to the isoelectric point of pH = 3.2. H-Glu is an amino acid commonly used in industry, which is considered to crystallise easily and serves as a food additive or precursor for pharmaceuticals.

8.1.2.2 Solubility

One of the key parameters in crystallisation is the solubility data. It was used to calculate supersaturations of the respective polymorphs and formed the basis for the solid recovery calculations. The solubility in Figure 8.1-1 was obtained by averaging already published data and extrapolating it in the range of 5 – 80 °C [8.13, 8.14].
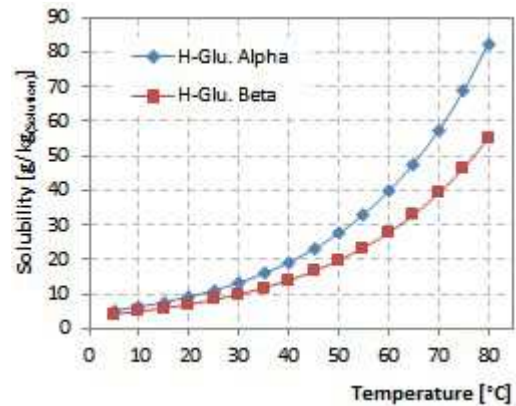
Figure 8.1-1: Solubility curve of Alpha (blue) and Beta (red) H-Glu in water

8.1.2.3 Mixing

One of the crucial parts in these experiments was the pre-mixing step, which had to ensure that sufficient micromixing was achieved before the sample left the pre-mixing unit. For this reason Roelands had to work with a static mixer in his mixer outlet tube [8.12]. In our system several static mixers (X, T, Vortex and Confined Impinging Jet) were characterised with respect to their micro-mixing performance using a Bourne IV
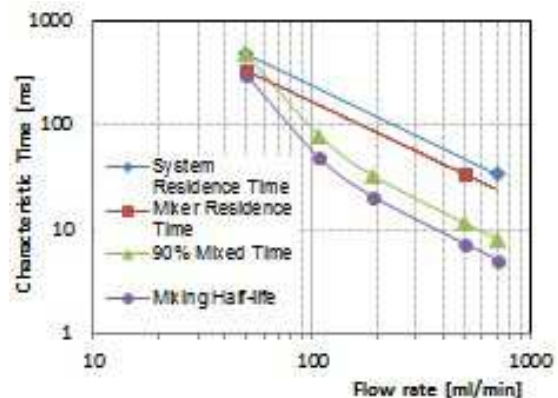
Figure 7.6-2: Mixing times and mixer residence times CIJ. Viscosity ratio of inlet streams equal to 2:1 [5.5]

competitive reaction. The results in Figure 7.6-2 show that at flow rates of 50 ml/min and above, the mixing time was shorter than the mixers residence time. It can hence be concluded that sufficient micromixing is achieved in our pre-mixing set up.

8.1.3 Experimental set-up

8.1.3.1 Pre-mixing

Two Ismatec gear pumps (MCP-Z) with magnetically coupled pump heads were used to deliver equal streams of Na-Glu and H_2SO_4 solution. The set-up with a 1/8" T-shaped static mixer and a 14 cm outlet capillary is illustrated in Figure 8.1-2. All tubing as well as the mixer were made from stainless steel. Initial experiments were carried out at flow rates of 30, 300 or 600 g/min but in reactive crystallisation different pre-mixing flow rates turned out to have no effect on the crystallisation behaviour. This finding is opposite to antisolvent crystallisation of H-Glu and Valine where the pre-mixing flow rates did have an effect on the crystallisation behaviour.

All experiments below were performed with a pre-mixing flow rate of 300 g/min. from each pump.
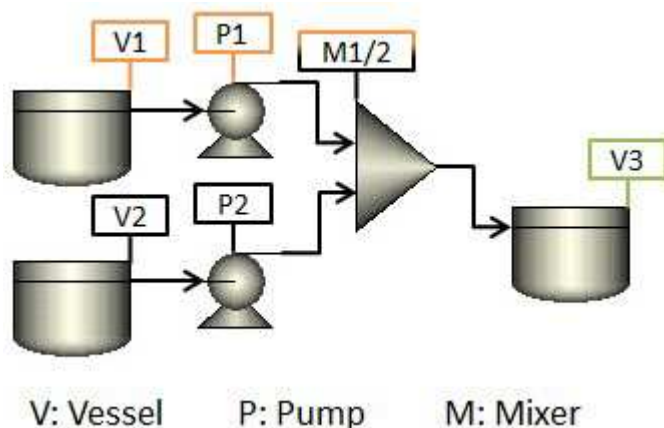
Figure 8.1-2: Continuous mixing setup consisting of two separate feed vessels for solution & antisolvent, two pumps, one static mixer and a sample collection vessel.

8.1.3.2 Post-mixing

Samples of approximately 100 – 150 g supersaturated solution were collected from the pre-mixing set up and exposed to post-mixing flow treatment. Typical post-mixing flow units were a QC displayed in Figure 8.1-3, STC with a stainless steel impeller (d = 33 · 10-3m, 700 rpm) in Figure 8.1-4, PPL with Marprene tubing 902.0064.016#16

(110 rpm, 850 g/min) where the suction and pressure side of the tubing were submerged in the same vessel in Figure 8.1-5, MSC with PTFE coated stirrer bar (d = 24 · 10-3m, 900 rpm) in Figure 8.1-6 and an Oscillatory Baffled Crystalliser (OBC) in Figure 8.1-7 with PEEK baffles on a stainless steel baffle string (V = 100 ml, three baffles, f = 3 Hz, A = 20 mm, baffle spacing = 50 mm, gap(baffle-reactor wall) = 2.5 mm, baffle thickness = 2.5 mm). This wide selection of flow units were used to study how their unique hydrodynamic properties would affect the yield and polymorphic composition of the final product.

Figure 8.1-3: Quiescent crystalliser (QC) without any agitation

Figure 8.1-4: Stirred Tank Crystalliser (STC) with overhead stirring
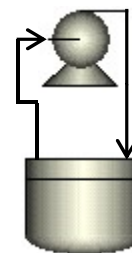
Figure 8.1-5: Peristaltic Pump recirculation Loop (PPL)

Figure 8.1-6: Magnetically Stirred Crystalliser (MSC) with magnetic stirrer bar
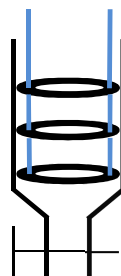
Figure 8.1-7: Oscillatory Baffled Crystalliser (OBC) with three baffles

8.1.4   Procedure

Na-Glu solution c = 95.6 g/kg$_{(Solution)}$, which corresponds to c(H-Glu) = 75.2 g/kg$_{(Solution)}$ and a H_2SO_4 solution c = 25.1 g/kg$_{(Solution)}$ were prepared and separately filtered over a Fisherbrand (FB59015, Range: QL100) filter, applying a vacuum. This ensured that there was no dust or other particles left in the feed solution.

The two gear pumps were calibrated with water to a flow rate of 300 g/min. each, before the first experiment and when the flow rates were changed. The accepted deviation between both streams was ≤ 1 %.

After the calibration the pumps were charged with the Na-Glu and H_2SO_4 solutions and the two streams were mixed at a ratio of 1:1, which created a supersaturation of SS = 4, calculated according to Equation 8-1

$$\left(SS = \frac{c_{(Solution)}}{c_{(Solubility \; \alpha/\beta \; (20°C))}} \right)$$

Equation 8-1

About 15 residence times of the run went into waste before samples were taken. After each run, a quick mass balance was carried out to double check that the flow rates delivered did not deviate more than 1 %.

The cleaning procedure for the set up consisted of 100 residence times of hot water, followed by 100 residence times of water at ambient temperature. As the solubility of H-Glu in hot water is reasonably high, the system can be considered clean and the unwanted seeding of the next run can be ruled out.

The samples were exposed to the different post-mixing flow units described above for different periods of time, in order to crystallise. After the post-mixing was stopped the pH value was measured and all samples were found to be between pH = 3.15-3.25.

The crystals were filtered out of solution using a Millipore Vacuum Filtration set up over a 0.45 μm HV Millipore Duraport Membrane Filter and were dried at 50-60 °C to mass consistency, typically 2h. The dry mass of crystals was determined by weighing in order to calculate the crystal solid recovery.

The theoretical crystal solid recovery was calculated on the basis of the mass balance and mass of the sample. The amount of H-Glu which stayed dissolved in the mother liquor was disregarded and only the amount of supersaturated H-Glu was considered as 100%. The practical crystal solid recovery (PSR) was calculated according to Equation 8-2.

$$\left(PSR\ [\%] = \frac{mass\ crystals\ recovered\ [g]}{theoretical\ recovery\ [g]} \right)$$

Equation 8-2

Micrographs of the product crystals gave an indication about the polymorphic composition, which was confirmed by XRD analysis.

8.1.5 Results and discussion

8.1.5.1 Primary post-mixing flow treatment

Figure 8.1-8 shows a summary of results obtained from our experiments in which the solid recovery of the different post-mixing flow units is plotted over time. All samples were prepared at a mixing flow rate of 300 g/min, each unit exhibits a unique kind of flow dynamics and promotes different crystal forms in the final product.
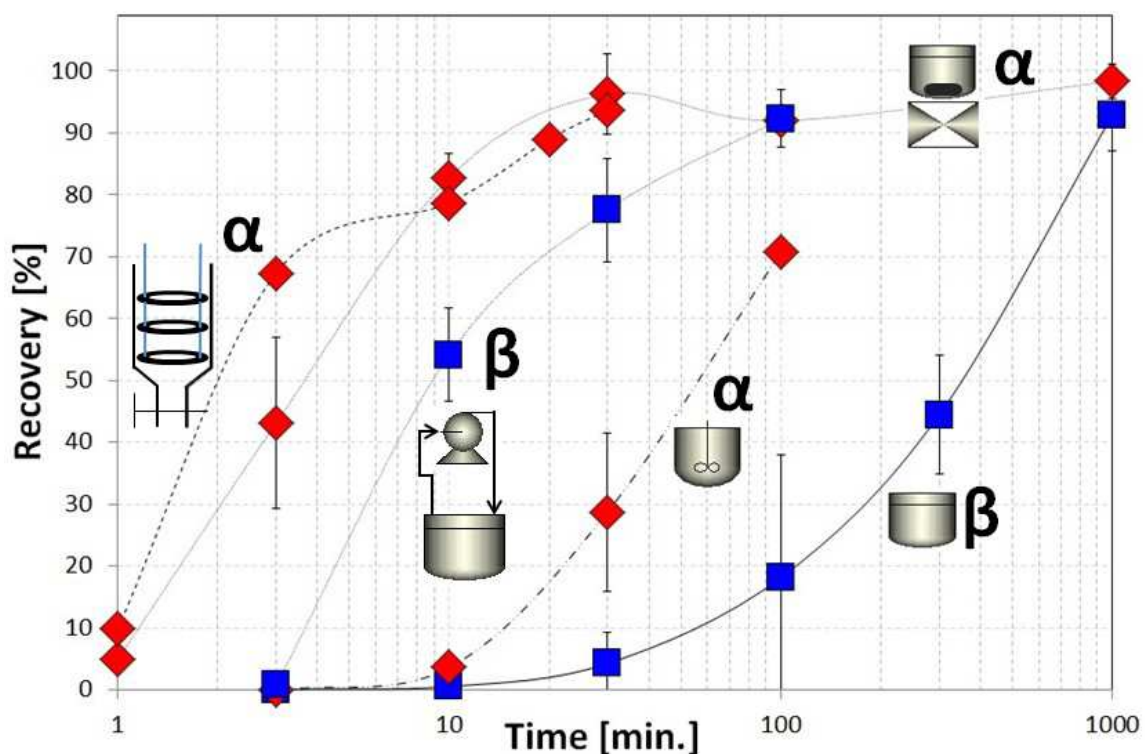
Figure 8.1-8: Crystal solid recovery over time as a function of equilibrium solubility. Images show the respective post mixing flow unit and markers indicate the polymorphic form obtained. Square: Beta, diamond: Alpha. (STC = 700 rpm (harsh))

8.1.5.2 Quiescent crystalliser

The induction time for a quiescent crystalliser (no post-mixing) was about 10 min, which is very long compared to other flow units. After that period crystals were observed at the bottom (glass-liquid interface) and at the surface (air-liquid interface). Over time the amount of crystals increased but the sample did not exhibit turbidity. The vast majority of the crystals grew at the bottom and formed a hard crust there.

XRPD measurements (Figure 8.1-9) confirmed that all quiescent samples yielded the Beta form, independent of the crystallisation time and no Alpha could be detected. These findings are consistent with Roeland 2007 [8.12].

Reference spectra of both alpha and beta L-Glutamic Acid were collected in-house. These reference XRPD patterns are used for overlay comparisons with samples generated throughout experimental work.
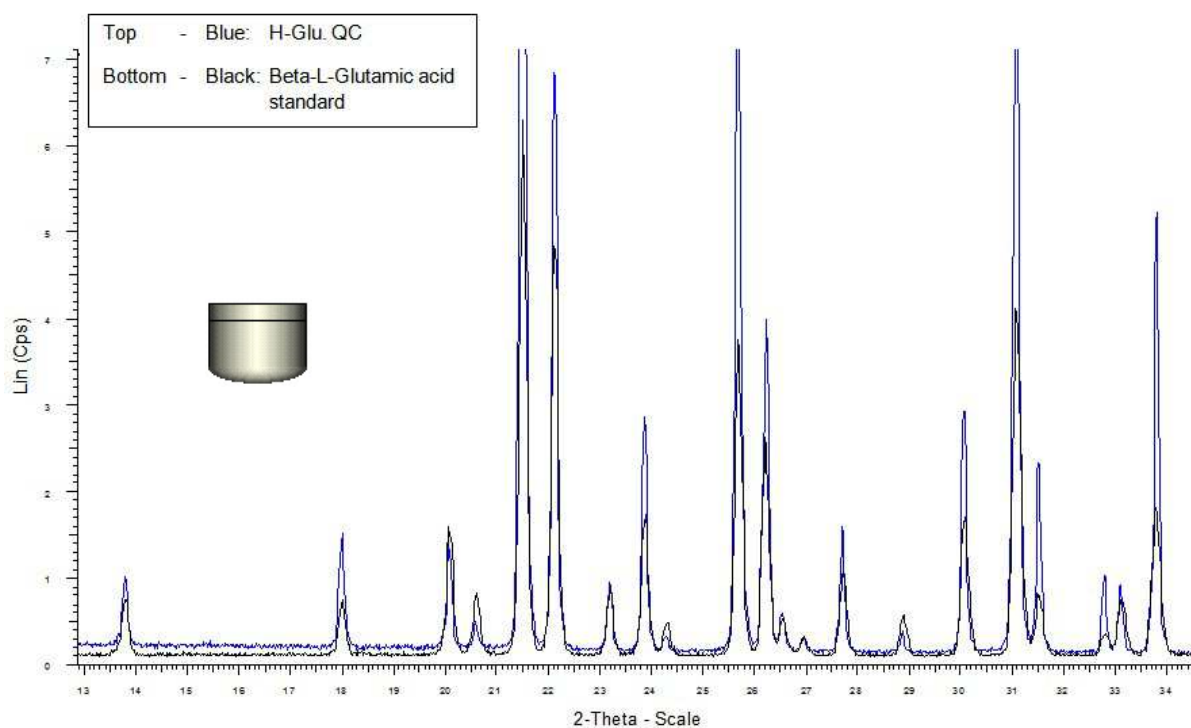
Figure 8.1-9: H-Glu XRPD pattern - Beta form from QC

Ostwald's rule of stages suggests that a thermodynamic system in change will move through all its metastable phases, before it reaches stable conditions [8.15]. This means that in our system the metastable Alpha polymorph should have nucleated first and should then have transformed to the stable Beta form. A search, under a microscope, only yielded three Alpha crystals in a total sample mass of 1.5 g of Beta crystals. These were however so big that they must have formed very shortly after mixing.

In a first possible scenario, Alpha nucleates and transforms to Beta, which is however unlikely due to the reported slow transformation kinetics at 20 °C [10.23]. The transformation process is only sufficiently fast above 40 °C.

It could also be imagined that the pre-mixed sample solution forms Alpha and Beta nuclei precursor, which nucleate according to their own kinetics. Beta would hence nucleate orders of magnitude faster than Alpha, would deplete the supersaturation and eventually there is not enough driving force left for Alpha to nucleate anymore.

8.1.5.3 Stirred tank crystalliser

Two different conditions were tested in terms of post-mixing flow treatment in the STC. Under soft conditions (70 rpm) the STC behaves similar to the QC. Crystals were first observed in the bulk due to the mixing action and the crystals recovered were of the Beta form. These conditions have not been investigated by Roeland 2007 [8.12] and challenges the hypothesis that oiling out is interrupted by stirring, which should have led to Alpha crystals.

However, under harsh conditions (700 rpm) the STC yielded exclusively the Alpha form, which was confirmed by XRPD (Figure 8.1-10) and agrees with Roeland 2007 [8.12]. It must be noted however, that the nucleation of Alpha under these conditions went with a substantial amount of Alpha fouling on the stainless steel stirrer.
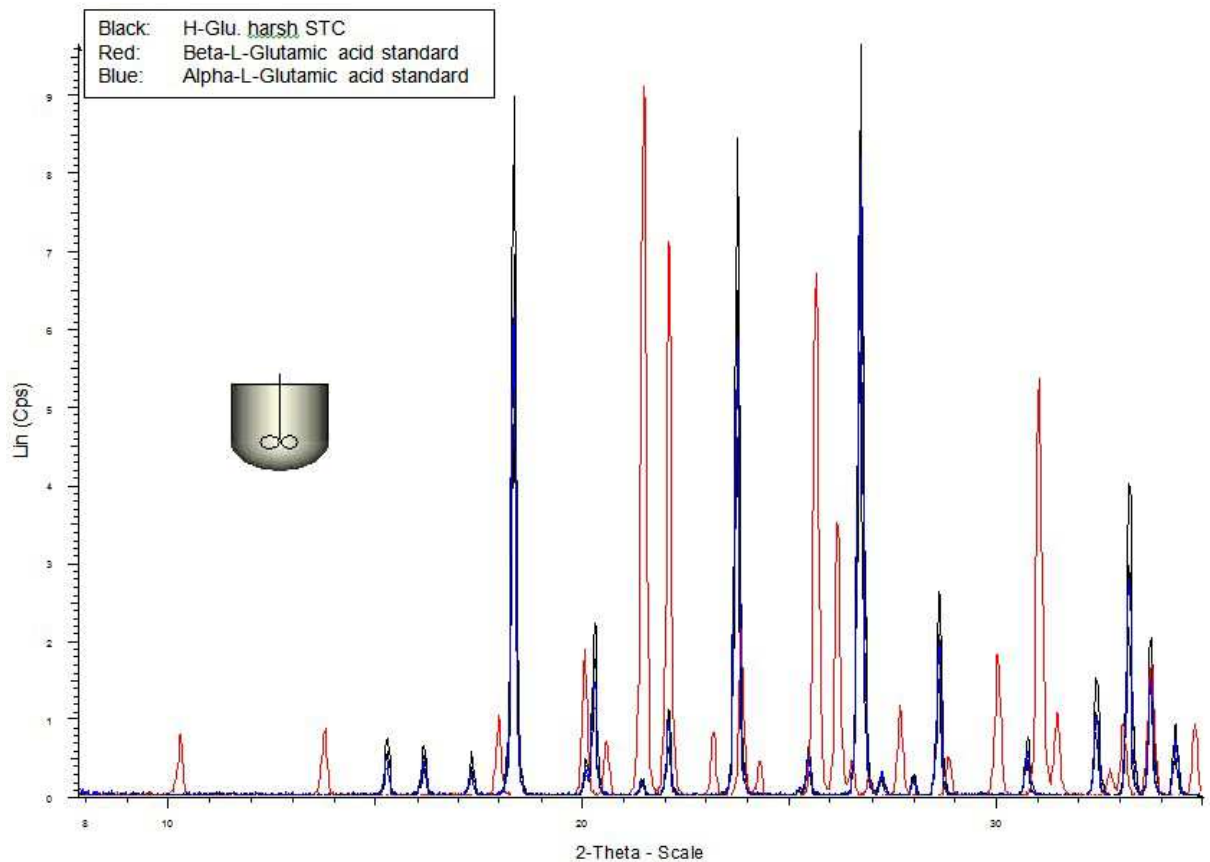
Figure 8.1-10: H-Glu XRPD pattern - Alpha form from harsh STC

Under soft conditions, the same nucleation mechanism might be applied as in the QC. Alpha & Beta nucleate according to their own kinetics, nucleation of Beta is quicker, depletes supersaturation and wins over Alpha. However, Alpha crystals which nucleated at a very early stage might be present in very small numbers (< 5%), due to slow nucleation. An interesting fact is that no fouling was observed on the impellor under soft conditions and the sample also did not turn turbid.

Under harsh conditions (which are plotted in Figure 8.1-8), on the other hand, the impact of the impellor and maybe surface effects have a significant influence on the nucleation behaviour and the sample turns turbid after about 6 min. of stirring. Beta will theoretically still be the polymorph with the quicker nucleation kinetics but the impact of the impellor with Alpha precursor enhances Alpha nucleation substantially. The

103

occurrence of significant fouling on the impellor could be taken as evidence that on impact with Alpha precursor nucleation is triggered and the newly formed nuclei stick to the surface of the impellor.

Present Alpha crystals give rise to secondary nucleation and as Alpha grows a lot quicker than Beta, it will rapidly deplete supersaturation and significantly slows down Beta's nucleation and growth. In agreement with Roelands 2007 [8.12] the crystal form under these conditions is Alpha. However, it cannot be ruled out that trace amounts of Beta (< 5%) are present in the sample due to earlier nucleation.

8.1.5.4 Peristaltic pump loop

Samples exposed to PPL post-mixing flow yielded different polymorphs, depending on roller RPM, which was confirmed by XRPD (Figure 8.1-11).

The experiments in Figure 8.1-8 indicate that this flow unit significantly increased the solid recovery compared to the QC. The sample turned visually turbid about 4 min. after the PPL post-mixing was started but fouling could not be observed.
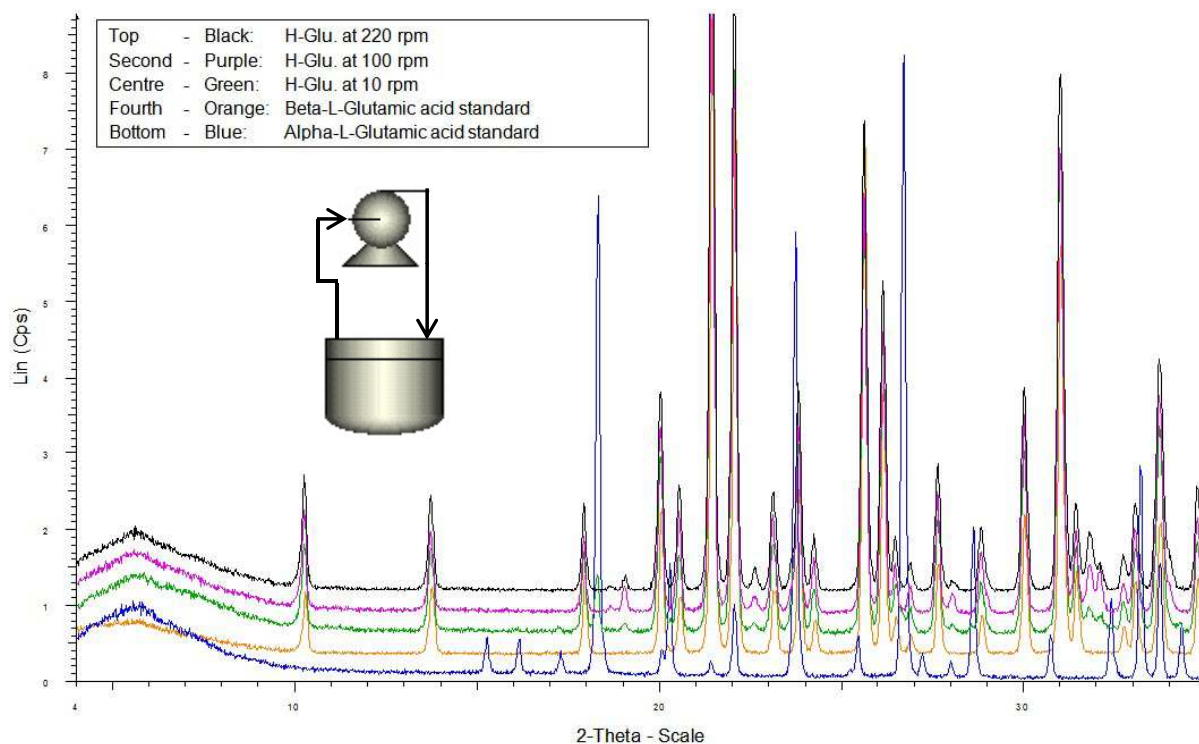
Figure 8.1-11: H-Glu XRPD pattern – Beta form from PPL

The impellor of a STC generates direct energy input into the sample by impact of the impellor with the solution, which yields Alpha. The rollers of the peristaltic pump, on the other hand, do not generate a hard impact with the sample. Liquid in the tube is pushed forward by a squeezing action of the soft Marprene tubing. The characteristic PPL treatment as well as the RPM might have a very different effect on the two polymorphs compared to the STC.

After the sample leaves the pre-mixing unit, the two polymorphs nucleate according to their own kinetics (Beta quicker than Alpha). If the sample is exposed to low PPL RPM the frequency of the grinding action by the rollers is low as well. This would lead to a low crystal crushing rate, supersaturation is depleted slowly, which gives Alpha a chance to nucleate over a longer period of time. This could be the reason why small amounts of Alpha can be detected in the sample.

At high PPL RPM the crushing rate is faster, supersaturation is depleted quicker and due to the slow nucleation kinetics of Alpha, it cannot be detected.

Another possible scenario could be that the prismatic Alpha is more rigid and less easily crushed than the needle like Beta. A low Beta crushing rate might give uncrushed Alpha more time to grow to a larger, a crushable sizes. Once Alpha reaches the crushable size it is subject to the same mechanism as the Beta needles.

High PPL RPM cause sufficiently quick depletion of supersaturation, so that Alpha does not get a chance to grow to a crushable size.

It could also be possible that the rollers crack Alpha crystals into two but shear Beta to a substantially larger number of small crystals. This would substantially enhance secondary Beta nucleation, which would happen at the expense of Alpha.

8.1.5.5   Magnetically stirred crystalliser

Two different conditions were tested in terms of post-mixing flow treatment in the MSC. However, unlike in the STC experiments, soft (75 rpm) and harsh (900 rpm) conditions exclusively yielded the Alpha form, which was confirmed by XRPD (Figure 8.1-12) and agrees with Roeland 2007 [8.12]. The experiments under harsh conditions are plotted in

Figure 8.1-8. Crystals were first observed in the bulk, both samples turned visually turbid very quickly (≤1 min.) and hardly any fouling could be observed. However, it must be noted that a very small number of thin fouling lines were present in the area where the stirrer bar rotated / bounced around.
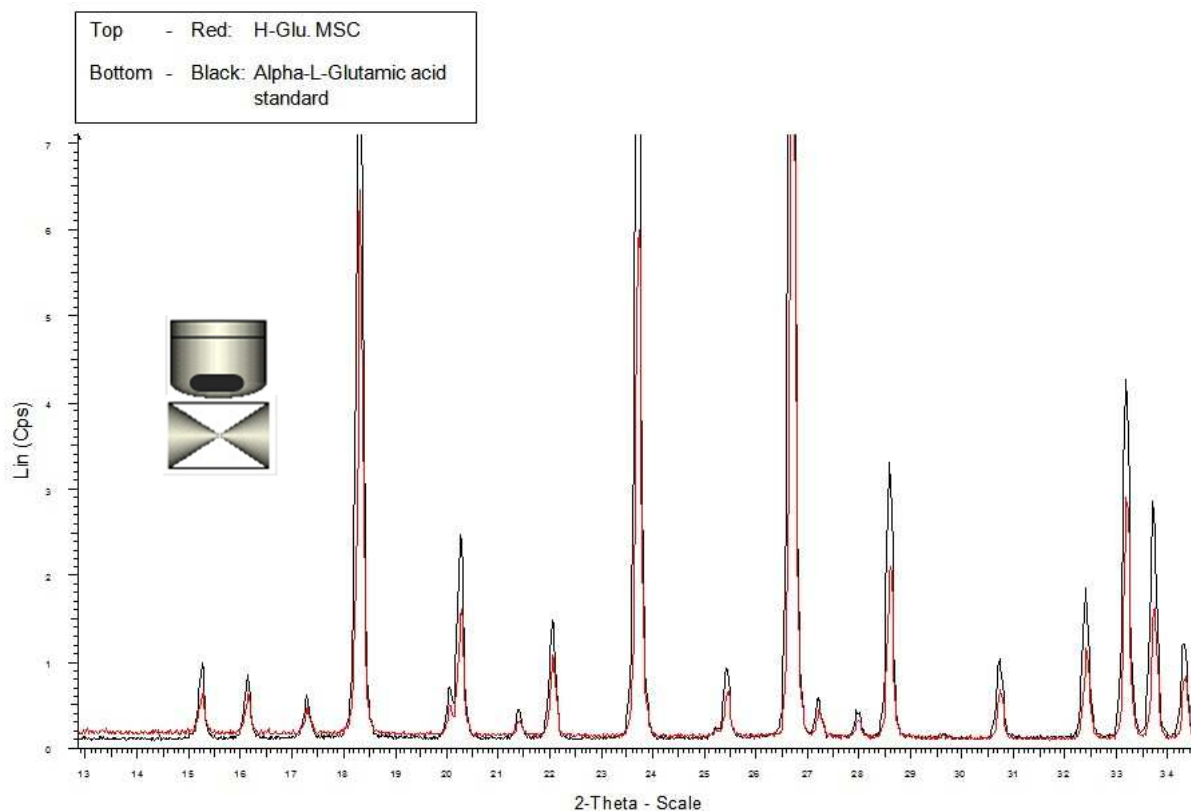
Figure 8.1-12: H-Glu XRPD pattern – Alpha form from MSC

It can be assumed that the MSC and the STC are very similar in their nucleation behaviour. The only difference is that the MSC stirrer bar bounces around the bottom of the beaker, which the stainless steel impellor does not.

In a MSC the required impact or shear for excessive Alpha nucleation is generated by the bouncing stirrer bar on the glass bottom. Newly nucleated crystals grow in the scratches of the glass bottom, the stirrer bar shears their tips off and tosses large numbers of Alpha nuclei into the bulk solution.

As Alpha is the quicker growing polymorph, it rapidly depletes supersaturation and does not leave a chance for Beta to nucleate or grow.

8.1.5.6 Oscillatory baffled crystalliser

Pre-mixed samples exposed to OBC post-mixing flow treatment rapidly turned visually turbid (≤1 min.) and exclusively yielded the Alpha polymorph, which was confirmed by XRPD (Figure 8.1-13). The results shown in Figure 8.1-8 indicate that the solid recovery over time is very similar to the one of the MSC.
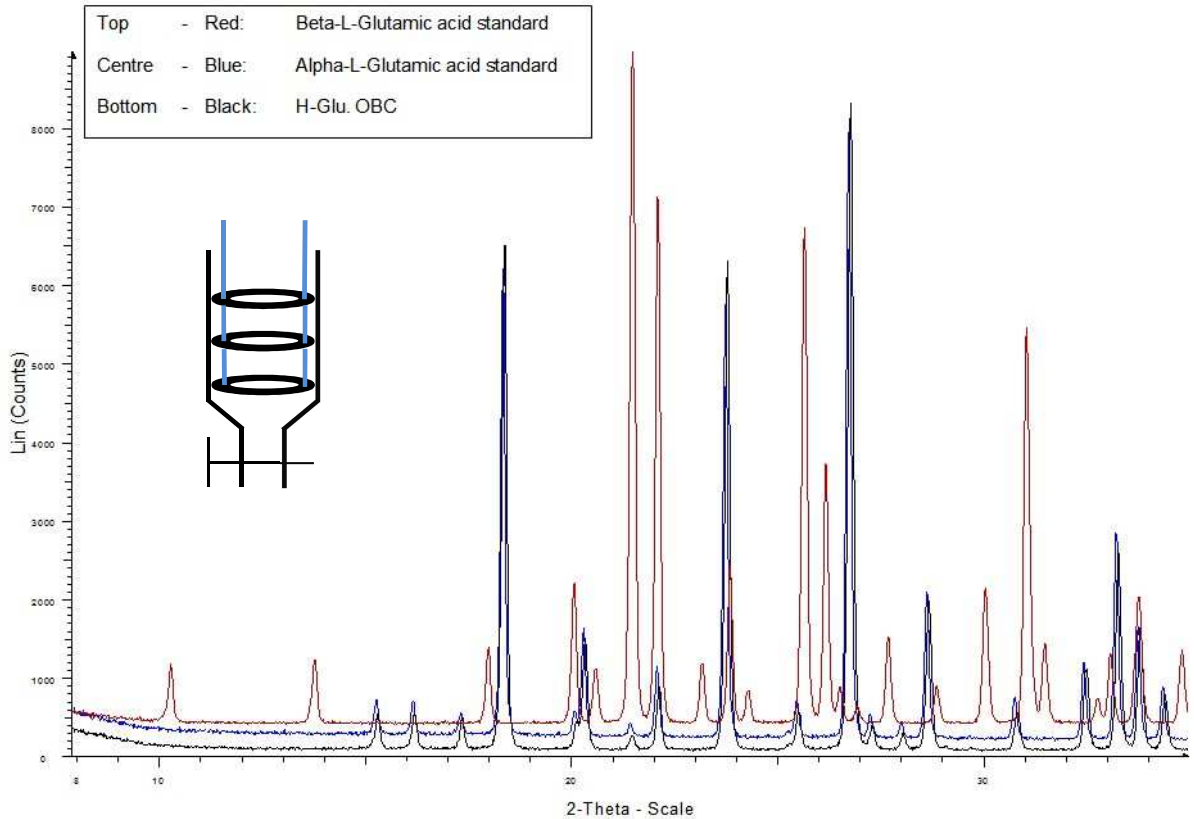
Figure 8.1-13: H-Glu XRPD pattern – Alpha form from OBC

The similarity between MSC and OBC could be because of the very small gap between baffles and reactor wall. The subsequent scraping action of the PEEK baffle on the glass wall could have a similar effect as the scraping / bouncing MSC stirrer bar. Well developed fouling lines were not observed but that could be due to the fact that they were hard to see through the jacketed OBC reactor.

Similarly to the MSC, Alpha and Beta crystals can be assumed to be present from early on and the scraping action on the walls enhances rapid Alpha nucleation. Alpha crystals stick to the reactor walls and their tips are sheared off by the up and down movement of the baffle string. In this way enough secondary Alpha nuclei are provided to quickly deplete supersaturation and to hinder Beta nucleation and growth.

It can however not be ruled out that trace amounts of Beta <5% are present in the sample.

8.1.5.7 Primary and Secondary post-mixing flow treatment

In the previous experiments it was shown that STC, MSC and OBC flow units yielded Alpha as their final crystal form and they will be referred to as Alpha promoters. QC and PPL flow units on the other hand yielded Beta as their final form and are hence Beta promoters. In the following experiments it was studied whether these units can actually promote the nucleation of Alpha/Beta or if some other parameters (i.e. solution mediated transformation) determine the final crystal form.

Samples were initially exposed to an Alpha promoter followed by exposure to a Beta promoter and vice versa. Primary exposure lasted a few seconds up to a few minutes, depending on the flow unit, until first crystals could visually be observed. The secondary exposure was significantly longer and exceeded the primary exposure by a factor of up to 60 times. Table 8.1-1 shows the final polymorphic form detected in the samples.

Table 8.1-1: Primary and Secondary flow treatment in flow units promoting different polymorphic forms (x = experiment not performed)

Primary / Secondary	MSC (α)	STC (α)	QC (β)	PPL (β)
MSC (α)	α	x	α	β / α
STC (α)	x	α	α	β / α
QC (β)	α	α	β	x
PPL (β)	α	β / α	x	β

8.1.5.7.1 Primary QC & Secondary MSC or STC

Samples exposed to primary QC flow treatment predominantly yielded the Alpha form. The first Beta crystals were observed after about 10 min., the supersaturation was still high and the flow treatment was changed to MSC or STC.

Subsequent MSC flow treatment led to rapid Alpha formation, which quickly depleted supersaturation. STC flow treatment also nucleated Alpha crystals but much slower. In both cases small amounts of Beta had no significant effect on Alpha nucleation and growth due to secondary flow treatment. Alpha nucleation and growth seemed to be feasible as long as sufficient supersaturation was present, no matter if the small amounts of Beta were already present in the sample.

8.1.5.7.2 Primary PPL & Secondary MSC or STC

Samples exposed to primary PPL flow treatment predominantly yielded the Beta form, with a small amount of large Alpha crystals present. The first Beta crystals were observed after about 3 min., the samples turned turbid and it could be assumed that the supersaturation at this stage was lower than in the primary QC experiments.

However, both secondary units used the remaining supersaturation to nucleate and grow a few Alpha crystals. This result is surprising as with a large number of Beta crystals present, secondary nucleation of Beta should have been favoured over the nucleation of Alpha. This finding gives a strong indication that MSC and STC are in fact Alpha nucleating flow units.

It must however be noted that the MSC was again the more powerful nucleator, which agrees with Figure 8.1-8, where the STC has a much slower overall solid recovery compared to the MSC.

8.1.5.7.3 Primary MSC & Secondary QC or PPL

Samples exposed to primary MSC flow treatment predominantly yielded the Alpha form. The first Alpha crystals were observed after about 35 sec. and samples turned turbid. From Figure 8.1-8 it is obvious that supersaturation after such a short period of primary post-mixing is hardly depleted.

It is striking that both secondary flow units did not manage to nucleate a noticeable amount of Beta and supersaturation was depleted by growth of the Alpha crystals. This

could be due to the rapid growth kinetics of Alpha crystals which very rapidly depleted supersaturation. By the time the PPL could have nucleated the first Beta crystals (after about additional 3 min.) the supersaturation would have halved, which under these conditions made it very hard for Beta to nucleate and grow in the competitive Alpha environment.

Another finding was that there was no indication of solution mediated transformation. This agrees with literature which reports that solution mediated transformation is negligible at room temperature [10.23]. This could be evidence that the PPL is actually a Beta promoter and not just a unit which enhances quick solution mediated transformation of Alpha to Beta crystals.

8.1.5.7.4 Primary STC & Secondary QC or PPL

The final polymorphic composition of samples which were exposed to primary STC flow treatment heavily depended on the secondary flow treatment. The first Alpha crystals could be observed after about 6 min and the samples were exposed to QC or PPL flow treatment. In the case of secondary QC treatment, the final crystal form was predominantly Alpha. However, in the case of secondary PPL treatment the final crystal form was a mixture of Alpha and Beta.

All previous experiments showed that the STC was a less effective in promoting Alpha crystals, which led to smaller numbers of Alpha crystals as well as higher supersaturation at the point when first Alpha crystals were observed.

The QC was such a slow Beta promoter that even the few Alpha crystals, with their quick growth kinetics, provided an environment in which Beta found it hard to nucleate and grow. The PPL on the other hand was a lot more effective in promoting Beta and managed to use the remaining supersaturation to nucleate and grow a considerable amount of Beta crystals. Here again, no indications for solution mediated transformation could be observed, which supports the argument that the PPL is a Beta promoting unit.

8.1.5.8 Temperature effects

The outcome of a crystallisation is very closely connected to the temperature the process is run at. All major steps and properties are temperature dependent (nucleation & growth kinetics, solubility, supersaturation, solution mediated transformation), which can lead to different final results when performed at different temperatures.

In order to investigate these effects the processing temperature range was extended to 5 °C and 45 °C. Pre-mixing and post-mixing were carried out at these temperatures and compared to the results at room temperature 20 °C ± 1 °C.

8.1.5.8.1 Pre-mixing and MSC post-mixing at 5 °C at SS=4

At room temperature, the MSC is considered an Alpha promoter and first crystals in the bulk solution can visually be observed after about 45 sec. Even if the processing temperature is decreased to 5 °C the MSC still exclusively yields the Alpha polymorph. However, the time till first crystals can be observed in the bulk solution is about a factor of 2 longer than at room temperature.

These results could be expected as nucleation and growth kinetics slow down when temperatures are decreased.

8.1.5.8.2 Pre-mixing and PPL post-mixing at 5 °C at SS=4

The results obtained from the PPL unit at room temperature classified it as Beta promoter and first crystals can be observed after about 4.5 min. At a decreased temperature of 5 °C the unit yields a polymorph mix, which consists of substantial amounts of Alpha crystals. At this low temperature it takes 9 min. until first crystals can be observed, which is again twice as long as at room temperature.

From the previous experiences it could be expected that it takes longer until first crystals can be observed. However, the decreased temperatures apparently have a greater impact on the nucleation and growth kinetics of Beta than on Alpha.

8.1.5.8.3 Pre-mixing and MSC post-mixing at 45 °C at SS=4

At elevated temperatures the MSC initially again generates the Alpha polymorph. First crystals can be observed after 2-3 sec., which could be expected and is about 20 times faster than at room temperature. In agreement with most literature, the Alpha crystals go through a solution mediated transformation to Beta, which was not completed after the observation period of 1h. Such behaviour was never observed at room temperature.

8.1.5.8.4 Pre-mixing and STC post-mixing at 45 °C at SS=4

At room temperature a STC generates Alpha crystals, it is much slower than in a MSC and first crystals can be observed after 6 min. In these experiments at 45 °C the first crystals could be observed after 2 min, which is only 3 times quicker than at room temperature and significantly slower than the MSC. However, the expected solution mediated transformation happened very quickly and was complete after 1h.

The MSC is a very harsh Alpha promoter and it might be that it manages to deplete supersaturation before Beta gets a chance to nucleate, despite the elevated temperature. The STC, on the other hand, is a soft Alpha promoter and it might be that at higher temperatures already a mixture of Alpha and Beta nucleates, which then goes through a fairly quick solution mediated transformation process.

8.1.6 Conclusions

Reactive precipitation of H-Glu was achieved by mixing equal streams of Na-Glu and H_2SO_4 in a T-shaped static mixer. The resulting supersaturated solution was homogeneously mixed on a molecular level and was exposed to different post-mixing flow treatments. The objective was to study the influence of different flow conditions on the crystal form present in the final sample.

It was found that quiescent conditions or very gentle stirring as well as soft grinding actions led to the formation of Beta crystals. Without fluid movement or with very gentle stirring/impact the samples behave very similarly and the solid recovery was very slow. Soft grinding actions, on the other hand, increased the solid recovery significantly. Soft impact is not as effective in enhancing secondary Beta nucleation as soft grinding is.

Harsh stirring/impact, a bouncing/shearing stirrer bar as well as a scraping OBC led to the formation of Alpha crystals. The impacting impellor, bouncing stirrer bar and scraping baffle apply stress on Alpha nuclei precursors, which significantly enhances their nucleation. During the step of nucleation crystals get stuck on the surfaces which provide the stress and cause encrustation, which in turn led to secondary nucleation.

In the case of H-Glu, impact and shearing favour the metastable Alpha form, whereas grinding crushes the more brittle appearing Beta form. Once conditions are harsh enough to crush Alpha and Beta, the quicker growth kinetics lead to Alpha being the final product. Softer processing conditions break the more brittle Beta, which despite slower growth kinetics makes Beta the final product.

In this system Alpha is the dominating polymorph. Once Alpha crystals nucleated they will grow, even in the presence of large amounts of Beta, and can be detected in the final sample. Solution mediated transformation under these conditions is negligible and this allows a prediction of which unit promotes which polymorphic form. STC, MSC and OBC are Alpha promoters due to their harsh operating conditions (bouncing, shearing, scraping). QC and PPL (grinding) are Beta promoters due to their softer operating conditions.

Temperature plays an important role in all of these processes and has a significant impact on nucleation and growth kinetics. Lowering the processing temperature slows down crystallisation and shifts the nucleation behaviour towards a higher population of Alpha crystals as Beta gets disadvantaged. Increasing the processing temperature speeds up crystallisation and leads to solution mediated transformation of Alpha to Beta, which cannot be observed at room temperature.

8.2 Continuous operation

Various hydrodynamic conditions in various flow units were investigated with respect to the final polymorph population obtained under batch conditions. For the objective of crystallising the stable Beta polymorph two flow units (Batch-QC & Batch-PPL) were identified yielding the Beta form, where the Batch-PPL outperformed the Batch-QC in terms of solid recovery by an order of magnitude at start times. Based on these findings, a continuous reactive crystallisation process targeting the Beta polymorph was set up.

8.2.1 Experimental setup

The continuous mixing setup consisting of two feed vessels (V1 & V2), two pumps (P1 & P2) and a static mixer (M1/2), the Batch-PPL (V3 & P3) and a sample collection vessel (P4 & V4) were connected in a flow through fashion to a fully continuous crystallisation setup shown in Figure 8.2-1.

Streams 1 & 2 are mixed in M1/2 and transferred into V3 where crystallisation of the Beta polymorph is promoted. A continuous stream of crystal product slurry was withdrawn through P4 into V4.

V: Vessel   P: Pump   M: Mixer
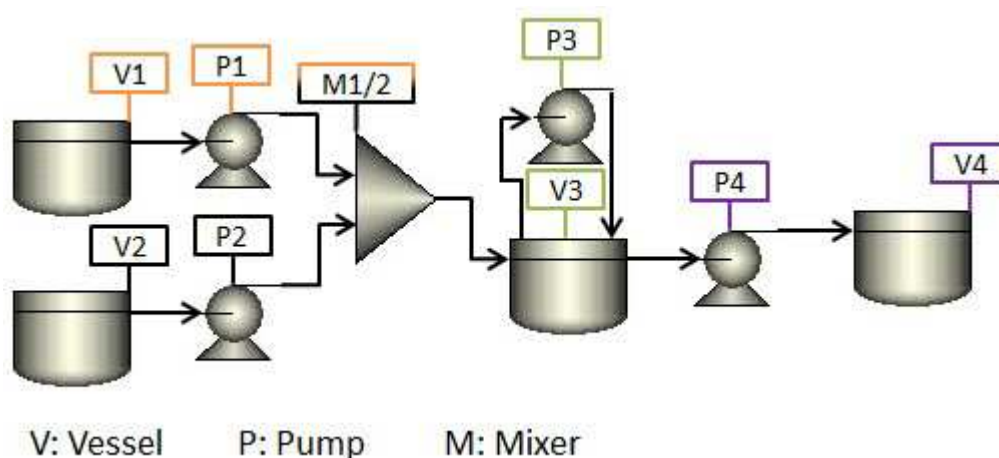
Figure 8.2-1: Continuous reactive crystallisation setup consisting of two separate feed vessels, two pumps, one static mixer, PPL for Beta form promotion, pump for withdrawal and sample collection vessel.

8.2.2 Procedure

The continuous system was operated with the same material and solution concentrations as in the previous batch experiments. Aqueous Na-Glu solution in stream 1 was continuously mixed with diluted H_2SO_4 in stream 2 to generate a supersaturated H-Glu solution. Freshly mixed and supersaturated solution was continuously pumped into V3, which acted as a single stage MSMPR crystalliser with a recirculating PPL. The mean crystalliser residence time in V3 was controlled by maintaining a steady liquid level, which required careful adjustment of the flow rate of P4.

The mean residence time was kept at $\tau \sim 1$ min. to ensure a short crystallisation period and small final product crystals with a narrow particle size distribution. Crystal suspension from V3 was continuously withdrawn by P4 into the sample collection vessel V4.

Experiments were designed with a runtime of 100 min and samples were collected from the outlet of P4 after predetermined time intervals, choice based on Figure 8.1-8, to assess solid recovery and steady-state behaviour of the system.

8.2.3 Results and discussion

8.2.3.1 Change in polymorph population

As expected from Batch-PPL experiments the polymorph population in the first sample of the Continuous-PPL after a process run time of 3 min. (Figure 8.2-2) is of the Beta phase. However, already in the second sample after 10 min. (Figure 8.2-3) the presence of Alpha crystals in coexistence with Beta crystals becomes obvious. Figure 8.2-4, Figure 8.2-5 and Figure 8.2-6 further illustrate the change in polymorph population over time from the stable Beta to the metastable Alpha phase.
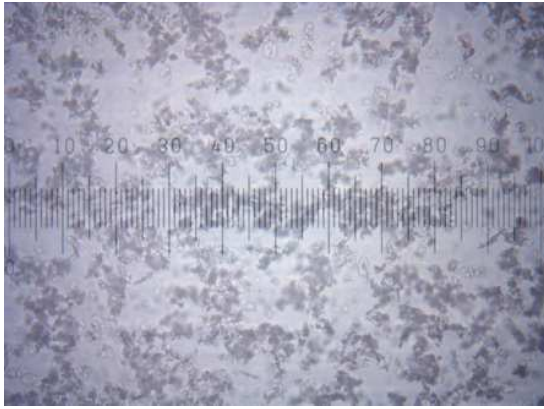
Figure 8.2-2: Beta crystal slurry from V3 after 3 min
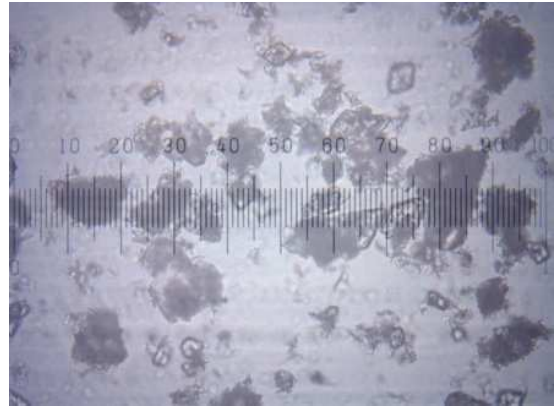
Figure 8.2-3: Beta + Alpha crystal mixture slurry from V3 after 10 min
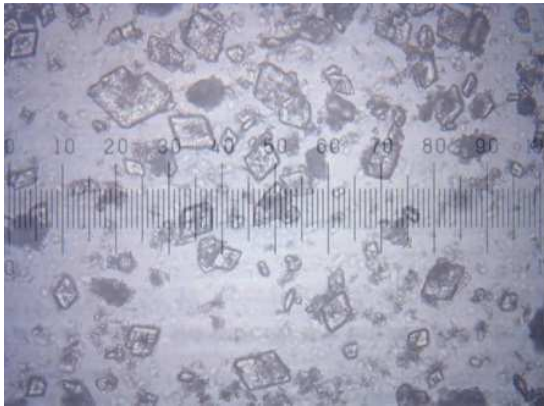
Figure 8.2-4: Alpha + Beta crystal mixture slurry from V3 after 20 min
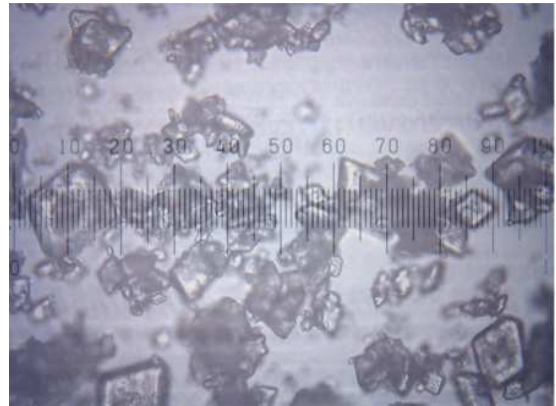
Figure 8.2-5: Alpha crystal slurry from V3 after 30 min
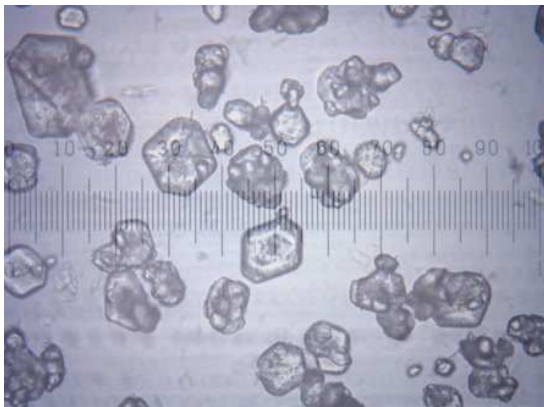
Figure 8.2-6: Alpha crystal slurry from V3 after 100 min

Such results have not been observed in Batch-PPL experiments but a possible explanation can be obtained from considering the operational conditions of continuous processing.

In a Batch-PPL process, proceeding secondary Beta nucleation and subsequent growth deplete the level of supersaturation in the crystallisation vessel making it increasingly difficult for the Alpha polymorph to nucleate and grow.

In the Continuous-PPL setup, on the other hand, the crystallisation vessel (V3) is always fed with freshly mixed, highly supersaturated solution, which keeps bulk supersaturation high despite proceeding crystallisation. High levels of supersaturation allow the Alpha polymorph to nucleate and grow in the presence of Beta crystals and quicker crystal growth kinetics of the Alpha form lead to the change in polymorph population over time.

8.2.3.2   Steady-state operation

Gravimetric solid recovery analysis were carried out after predetermined run time intervals to assess the amount of recoverable crystal product from the crystalliser outlet. Solid recovery over time is a parameter to assess steady-state operation of a process and results are shown in Figure 8.2-7. Over the entire experiment, no steady-state operations could be achieved and the amount of solid recovered from the outlet stream kept increasing until the unit was shut down.
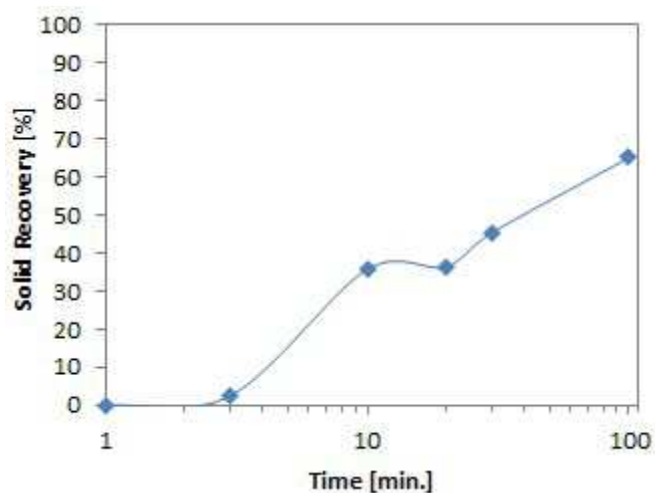
Figure 8.2-7: Solid recovery at outlet of continuous-PPL. Blue line indicates increasing solid recovery over time.

8.2.3.3 Fouling and blockage

Operational challenges started when the first Alpha crystals appeared and sedimented in the crystalliser, leaving a few huge Alpha crystals sitting at the bottom of the vessel V3. Over time, the amount of Alpha crystals increased and fouling on the vessel walls became a significant problem, which eventually lead to blockage of the system.

Another problem in this system originated from the fact that bulk desupersaturation was not complete before crystal slurry was withdrawn from the crystalliser. Pumping supersaturated solution led to crystal agglomeration, fouling and subsequent blockage in downstream transfer lines.

8.2.4 Conclusions

The Continuous-PPL setup did not manage to produce H-Glu of the Beta polymorph in a continuous fashion. In fact a change in the polymorph population from the stable Beta form to the metastable Alpha form was observed, which was not the case in Batch-PPL experiments.

The change in the polymorph population as well as an ongoing increase in crystal solid recovery indicates that the Continuous-PPL process did not reach steady-state operations at any time. On the contrary fouling and blockage in the crystallisation vessel and downstream transfer lines cause operational issues which led to the shutdown of the unit.

The objective to continuously produce crystals of small mean particle size with a narrow particle size distribution was not met. The Beta crystals appeared to have met this objective but did not sustain in this process.

Due to the operational challenges and the fact that this process does not deliver as required, the experiments using reactive precipitation of H-Glu were discontinued. A new and different approach has to be found, which can deal with the challenges encountered during the Continuous-PPL experiments.

9 Continuous crystallisation of L-Glutamic acid in a rapid antisolvent precipitation set up

In the previous chapter, the effect of various different types of post-mixing flow treatment on solid recovery over time and the final polymorph population was investigated. Initially experiments were carried out in batch mode to characterise flow units but later on the continuous mixing unit and a flow unit for secondary Beta nucleation were connected to a fully continuous crystallisation setup.

One of the objectives was to produce Beta crystals with a small mean particle size and a narrow particle size distribution, which could be used as seeding material for a continuous growth process. However, results of the continuous experiments did not show steady-state operation, exhibited severe fouling & blockage problems and the polymorph population changed from the desired stable Beta to the metastable Alpha polymorph.

Based on the results and findings from these experiments, it was decided to discontinue this route of continuous crystallisation development. The focus fell back onto antisolvent crystallisation and a novel continuous crystallisation setup was developed, in order to continuously produce Beta crystals of small mean particle size with a narrow particle size distribution.

9.1 Introduction

Crystallisation processes are widely used for separation and purification in chemical and pharmaceutical industries. Usually stirred tank crystallisers have been employed to perform batch crystallisation, despite the fact that they do not allow straightforward scale-up especially regarding nucleation and polymorphic forms.

The development and adaption of continuous crystallisation processes has several advantages in terms of product quality, cost, scale up, less waste and better sustainability. [2.2] In a continuous modular approach which spatially segregates the

seed crystal generation from subsequent growth, small crystals could rapidly be nucleated at extremely high supersaturation. The seed crystals suspension could be fed into a growth unit, which slowly grows the seeds at very low supersaturation to a desired size without further nucleation.

Antisolvent crystallisation is known for decades and has the ability to rapidly achieve very high supersaturations in a bulk solution. Two miscible fluids, one being a good solvent containing the model compound and the other one being a very poor solvent for the model compound, are mixed together. The poor solvent reduces the solubility in the final mixture, supersaturation is generated and crystallisation starts.

This technique can be used for the generation of very fine particles and has been widely studied in the past. In their review, Thorat et al. (2012) report that this technology has been used for a wide range of compounds like inorganics, polymers, proteins and pharmaceutical ingredients. Through rapid mixing of small amounts of solution with large amounts of antisolvent a very high supersaturation and very small particles can be generated. [9.1]

However, proper micromixing is essential as otherwise crystallisation is carried out under non-uniform processing conditions. Zhao et al. (2007) [9.2] investigated mixing in a Y-shaped static mixer and Zhang et al. (2011) [9.3] in a T-shaped static mixer. Both found that an increased antisolvent ratio yielded smaller particles with a narrower particle size distribution and identified the injection of solution into antisolvent advantageous over the injection of antisolvent into solution. In Chapter 7 mixing times in static mixers were characterised and showed that for fixed solution:antisolvent ratios (1:1), even for low flow rates, the mixing time was shorter than the mixer residence time. Despite full micromixing at low flow rates, increased mixing flow rates reduced particle sizes and generated a higher yield.

A different approach towards rapid mixing is the jet injection of a solution stream into a bulk of antisolvent at a velocity of a few metres per second. Fox et al. (1956) [9.4] compared a jet mixed tank with a conventional stirred tank crystalliser (STC) and found that a jet mixing velocity of 6 m/s corresponds to 500 RPM in their STC set up. Patwardhan (2002) [9.5] modelled and studied how the jet velocity, nozzle angles and

nozzle diameter affect the mixing time in a jet mixed tank. The system showed an exponential decay of mixing time as the injection velocity increased but the nozzle angle or diameter did not affect the system. Brick et al. (2003) [9.6] in a batch process jet injected a variety of crystallisable solutions into a mixed STC filled with antisolvent and generated organic particles of colloidal dimension. Supersaturation was used to control the particle sizes, the particle formation rate increased with increased supersaturation and the process worked best when the solute was particularly insoluble in the final solvent mixture.

A popular area of research is the use of ultrasound in the form of ultrasonic horns, in order to enhance, control or promote nucleation. Guo et al. (2005) [9.7] and Dalvi et al. (2010) [9.8] reported that the use of ultrasound increased mixing within the vessel but Vichare et al. (2001) [9.9] found that the mixing time is a strong function of the horn dimensions, its position, as well as the geometry of the vessel itself. The use of ultrasound during crystallisation reduces the metastable zone width [8.8] and Ruecroft et al. (2005) [9.10] observed a reduction of induction times and enhanced primary and secondary nucleation [9.7, 9.8]. Further analysis showed that using ultrasound lead to smaller particles with a more uniform particle size distribution [9.10] and even the amount of agglomerates was reduced [9.8].

Beck et al. (2010) [9.11] studied the behaviour of a sonicated T-shaped static mixer and obtained contradictory results compared to other research. Higher supersaturation did not necessarily show higher nucleation rates and the compound with the highest supersaturation did not always make the smallest particles. A proposed explanation suggests that molecular interactions between drug, solvent and water molecules greatly influence the precipitation process.

On the other hand, Dalvi et al. (2009) [9.12] set up batch experiments where solution was jet injected into a bulk of antisolvent and surfactant supported by ultrasound. Various nozzle diameters, flow rates and different solution:antisolvent ratios were investigated. Similarly to other research it was found that higher supersaturation lead to

higher nucleation rates and reduced growth. Higher jet velocities increased mixing and yielded smaller particles with narrower particle size distribution. It was concluded that high supersaturation is necessary to generate small particles and larger ultrasonic probes are more beneficial as they process a larger bulk volume.

Fouling and encrustation is a major challenge in crystallisation and especially in continuous crystallisation as it can block the system and lead to undesired shut downs. Narducci et al. (2011) [9.13] carried out sonicated continuous cooling crystallisation and found that crystals nucleated at lower supersaturation, crystal sizes were smaller, their shapes more uniform, the yield was improved and less agglomerates were observed. Interesting from a continuous manufacturing point of view was that the sonicated process reached a steady-state PSD much quicker than the non-sonicated process. Ultrasound also significantly reduced the amount of fouling on baffles, impeller and monitoring probes. However, fouling on the cooling surfaces was still as bad as in the non-sonicated experiments.

Continuous antisolvent crystallisation of H-Glu was carried out by Alvarez et al. (2010) [9.14] in a plug flow kenics type static mixer with single or multiple antisolvent injection points. It took 4 - 10 residence times to achieve steady-state operation and the total run time of experiments lasted 7 residence times. Results show particle size distributions of 10 - 300 μm with a mean particle size as small as 67 μm (FBRM). It was concluded that multiple antisolvent injection points seem to be a good strategy for controlling particle size.

Zhang et al. (2012) [9.15] carried out continuous antisolvent and cooling crystallisation of a pharmaceutical intermediate using a MSMPR crystalliser. The process was operated for four total residence times and yielded particle size distributions of 10 - 300 μm with a mean particle size as small as 80 μm (FBRM). It was found that the antisolvent addition step has significant influence on the final crystal properties.

In this work the different technologies, separately used and described for batch processing, are put together in a novel crystallisation unit for the continuous production of H-Glu seeding suspension. The set-up is investigated with respect to different

solution concentration, solution:antisolvent ratios and jet injection velocities into the bulk solution. Steady-state solid recovery and particle size distribution are assessed for the basic set up, as well as during scale up by a factor of three. The novel hot wall, cold bulk approach as well as ultrasound is investigated with respect to their ability to prevent encrustation and blockage of the system.

9.2 Method

9.2.1 Materials

Beta H-Glu of ≥ 98.5 % purity, containing ≤ 0.1 % of the Alpha form was purchased from Sigma Aldrich, Germany. Isopropanol of ≥ 99.5 % purity, containing ≤ 0.2 % H_2O was purchased from Fisher Scientific, United Kingdom. Deionised water used in all experiments was obtained from a Thermo Scientific (USA) water purification system. Experiments were performed in an air conditioned laboratory at 20 ± 2 °C.

The precipitation of H-Glu was achieved through rapid antisolvent crystallisation at high supersaturation.

9.2.2 Solubility

One of the key parameters in crystallisation is solubility data of the compound in various solvents or solvent mixtures. These were used to calculate supersaturation and formed the basis for solid recovery experiments.

The solubility data for various solvent compositions in dependence of temperature in Figure 9.2-1 was measured in house using a Crystal16 (Avantium) and the trend line is supposed to guide the eye. The data was fitted and extrapolated to predict the temperature and solvent composition space as shown in Figure 9.2-2.
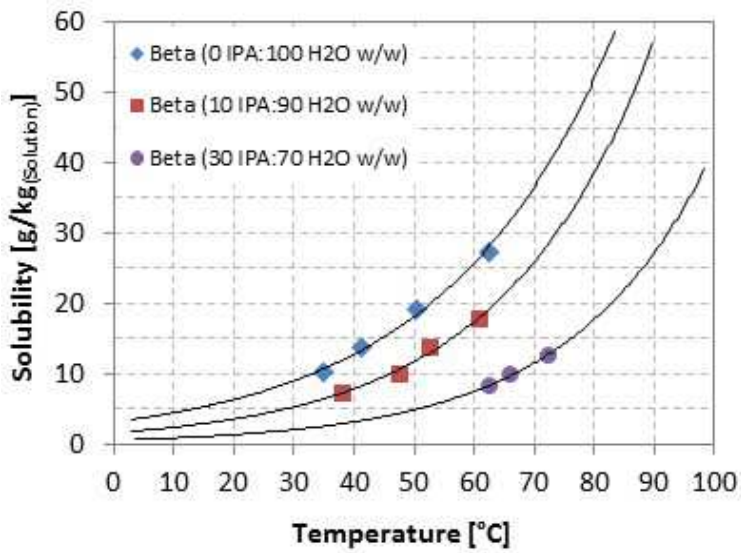
Figure 9.2-1: Solubility of Beta H-Glu at various solvent compositions. Black lines indicate extrapolation to higher and lower temperatures.
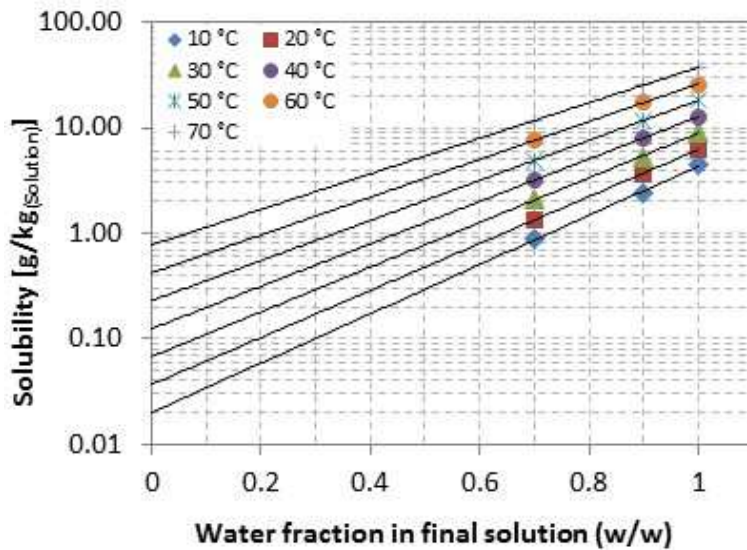
Figure 9.2-2: Solubility of Beta H-Glu at various temperatures. Black lines indicate extrapolation to lower water fractions.

9.3 Experimental set-up

A PFD of the continuous crystallisation equipment developed in our laboratory is shown in Figure 9.3-1 and Figure 9.3-2 shows the real setup in the laboratory. The system combines several technologies, which have individually been investigated and reported for batch or semi-continuous operation in literature before. For example, jet mixing [9.4], hot solution into cold antisolvent [9.12], ultrasound to enhance cleaning of equipment [9.13]. This is the first time we know of that all these technologies have been combined to set up a fully continuous crystalliser in this fashion.
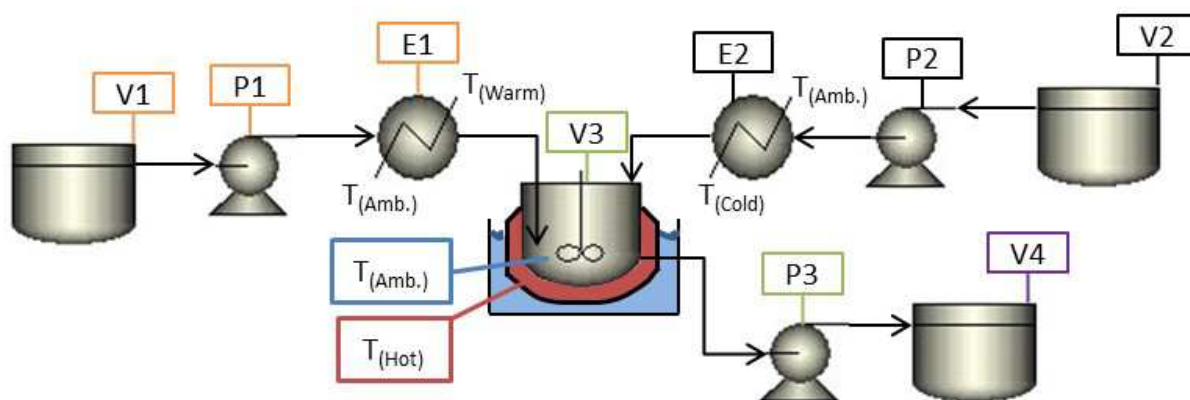
Figure 9.3-1: Rapid continuous antisolvent crystallisation setup (JIM). Stream1 & 2: Vessel, pump and heat exchanger. V3: Jacketed vessel submerged in ultrasonic bath, P3: Withdrawal pump and V4: Sample collection vessel.

During operation, warm H-Glu solution of stream 1 was jet injected through a submerged stainless steel nozzle into the bulk solution of the crystalliser (V3). Various flow rates (5 - 30 g/min) of stream 1 were delivered and controlled by an Ismatec external gear pump (MCP-Z) with magnetically coupled pump head (P1). The heat exchanger (E1) heated up the fluid and undersaturation of 0.4 - 0.5 with respect to the saturation concentration at ambient temperature was achieved. Nozzles with two different internal diameters (0.2 and 0.6 mm), in connection with stream 1 flow rates, generated different jet injection velocities (1.1 – 8.0 m/s) into the bulk solution.
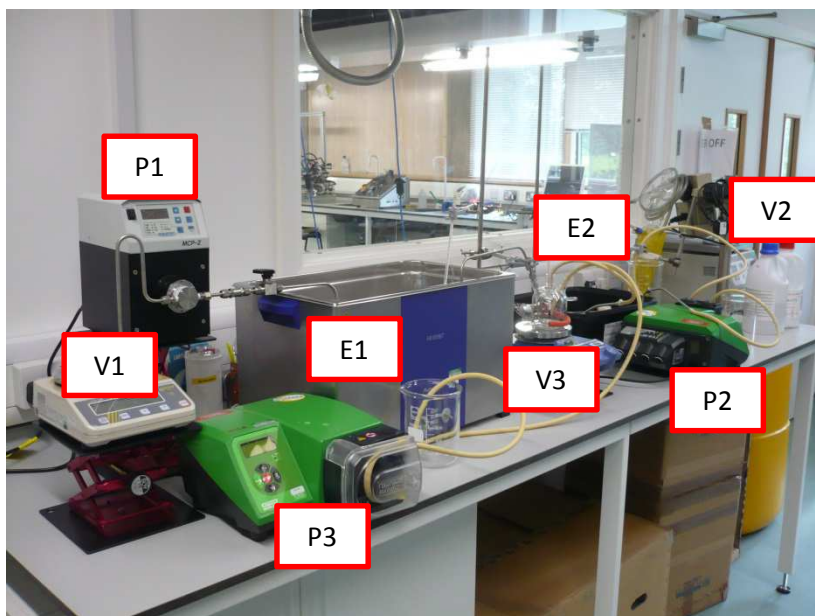
Figure 9.3-2: Real JIM setup in the laboratory

Cold IPA antisolvent of stream 2 entered the crystalliser (V3) through Marprene tubing, "water-falling" from the top of the vessel. The flow rates (70 - 285 g/min.) of stream 2 were delivered and controlled by a Watson-Marlow 520S peristaltic pump (P2) so that a constant mixing ratio of 5-30 % (w/w) stream 1 : 95-70 % (w/w) stream 2 was maintained. The resulting mixing temperature in V3 for any given ratio was always found to be well below the ambient temperature.

Truly rapid crystallisation happens in an instant and keeps nucleation and growth timescales as short as possible but still delivers close to 100 % solid recovery. Experiments showed that for a given mixing ratio (5 % stream 1 and 95 % stream 2) there was no difference in solid recovery behaviour when the residence time was increased from 0.5 min to 1 min or even 2 min A mean residence time of 0.5 min was chosen for all experiments.

Process control required the crystal slurry in V3 to be as close to ambient temperature as possible to avoid crystal dissolution when colder slurry warmed up after V3 withdrawal. Similarly, if the crystal slurry was above ambient temperature and cooled down after V3 withdrawal, blockage of downstream transfer lines occurred due to nucleation and growth. To achieve desired ambient temperature in the crystal slurry,

during the mean residence time of 0.5 min, the jacket of V3 needed to be heated substantially (55 °C). With the vessel jacket being significantly warmer than the bulk slurry, fouling of the crystalliser walls was reduced significantly. The hot jacket increased the temperature and solubility in the wall-liquid boundary layer sufficiently so that it stayed very close to the saturation concentration. The short crystalliser mean residence time of 0.5 min, the constant flow of stream 1, stream 2 and withdrawal established a temperature gradient from the vessel wall to the vessel centre. This gradient made the bulk temperature only increase very little compared to the jacket and kept its high supersaturation, which was required for rapid crystallisation. This mode of operation was named "hot wall, cold bulk" approach.

Fouling and system blockage is a major challenge in continuous crystallisation and often leads to unwanted unit shut down. Preventing fouling is essential and for that reason V3 was inserted into an ultrasonic bath (40 kHz, 50W), which was continuously operated during the run time of the experiment.

Table 9.3-1 summarises all operating parameters and their respective range of settings.

Table 9.3-1: Rapid continuous antisolvent crystallization operating parameters

Operating parameters	Range of settings
$\dot{m}_1$ [g/min]	5 – 30
$\dot{m}_2$ [g/min]	70 - 285
$\dot{m}_{Total}$ [g/min]	100 - 300
$v_{Injection-Nozzle}$ [m/s]	1.1 – 8.0
Ratio (Solution:Antisolvent)	5:95 – 30:70
$t_{(residence)}$ [sec]	30
Ultrasound	Yes & No
T_1 [°C]	30 – 45
T_2 [°C]	3.4 – 4.5
T_{Bulk} [°C]	16 - 24
$c_{Aq.-Solution}$ [$mg_{(LGA)}/g_{(Solution)}$]	6.2 – 8.4

9.4 Procedure

Preparing the continuous crystallisation set up for operation started with a warm water cleaning programme of stream 1 and the withdrawal line. The duration of about 10 crystalliser residence times (5 min) ensured that no crystal contamination from previous runs was present in the system.

In the next step, the flow rate of stream 1 was calibrated using deionised water and stream 2 was calibrated using the appropriate antisolvent. Calibration of mass flow rates was considered successful when $\Delta \dot{m} \leq 1\%$ was achieved for each individual stream.

After the calibration, the water in the solution storage tank (V1) was changed to the working solution and both pumps (P1, P2) were started simultaneously. The ultrasonic bath was turned on and as the crystalliser filled up, the overhead stirrer was switched on. Once the liquid level in the crystalliser corresponded to the 0.5 min. mean residence time liquid level, the continuous withdrawal through pump 3 began. A constant crystalliser liquid level and mean residence time was achieved by slight adjustments of the P3 flow rate, when required. Once turbid crystal slurry exited the withdrawal line, samples were collected for analysis or further downstream processing.

9.5 Results and discussion

For a neat jet-injecting, without splashing, of solution into antisolvent it is required to submerge the injection nozzle into the bulk solution. This however means that the nozzle is always surrounded by antisolvent and a very high supersaturation which makes encrustation and blockage of the nozzle very likely.

The aqueous H-Glu solutions were prepared at room temperature with the solution concentration very close to the saturation concentration at 20 °C. As the solution was pumped towards the injection nozzle it passed through a heat exchanger (E1) where it was heated up to 30 - 45 °C and the supersaturation was reduced to 0.4 - 0.5. This procedure ensured that the nozzle outlet was always flushed with warm, sufficiently undersaturated solution to dissolve any encrustation which might have deposited and the nozzle never blocked.

The antisolvent was introduced into the crystalliser in a way that it freely ran down the shaft of the overhead stirrer which agitated the vessel. Heating stream 1 for undersaturation required stream 2 to be cooled in order to maintain ambient temperature in the crystallisation vessel. The antisolvent was pumped through a heat exchanger (E2 – ice bath) and was cooled down to about 3 °C, which however resulted in a crystalliser temperature well below the ambient temperature.

The hot wall cold bulk approach increased the temperature in the crystallisation vessel closely back to the desired ambient temperature (16 - 24° C). With the walls being significantly warmer than the bulk, fouling on the vessel walls was significantly reduced.

9.5.1 Solid recovery

A truly rapid crystallisation process recovers large quantities of the crystallisable material present in the sample in a very short timescale. In this work these values are expressed as solid recovery, considering the theoretically recoverable material and disregarding the material which stays dissolved in the mother liquor at operating temperature. Complete solid recovery can reach a value of 100 %, which is the benchmark for all subsequent experiments. Initial experiments were conducted

without the use of ultrasound and the results can be seen in Figure 9.5-1. At a solution:antisolvent ratio (50:50 w/w) the solid recovery is only about 20 % and reached steady-state operation after 3 min. (6 residence times). A low solid recovery means that a lot of material is still available for crystallisation and generates supersaturation in the outlet stream. Conveying supersaturated solution caused problems and led to encrustation and blockage of the system after 50 min.
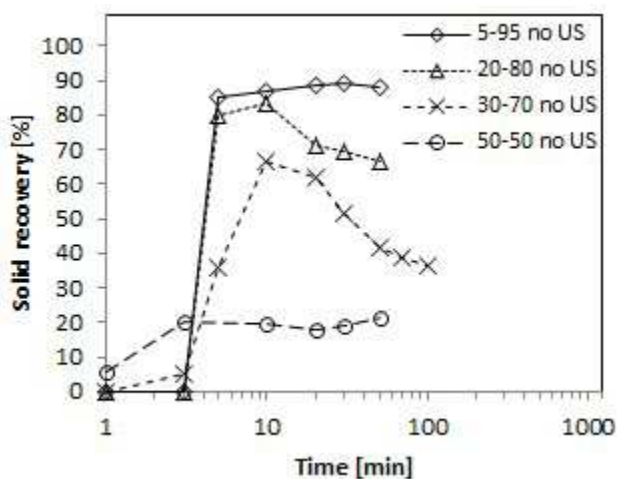
Figure 9.5-1: Solid recovery over time at various antisolvent mass fractions without ultrasound (US)

Changing the solution:antisolvent ratio to 30:70 (w/w) initially shows a slow solid recovery before increasing significantly to a maximum after 10 min (20 residence times) and dropping again later. Encrustation in the crystallisation vessel was visible and initial signs of blockage were observed after a run time of 100 min (200 residence times). The crystal form obtained under these conditions was a mixture of the metastable Alpha and the stable Beta polymorph, which was confirmed by XRPD (Figure 9.5-2) measurements. Due to peak heights, it can be suspected that there is more Alpha than Beta present in the sample.
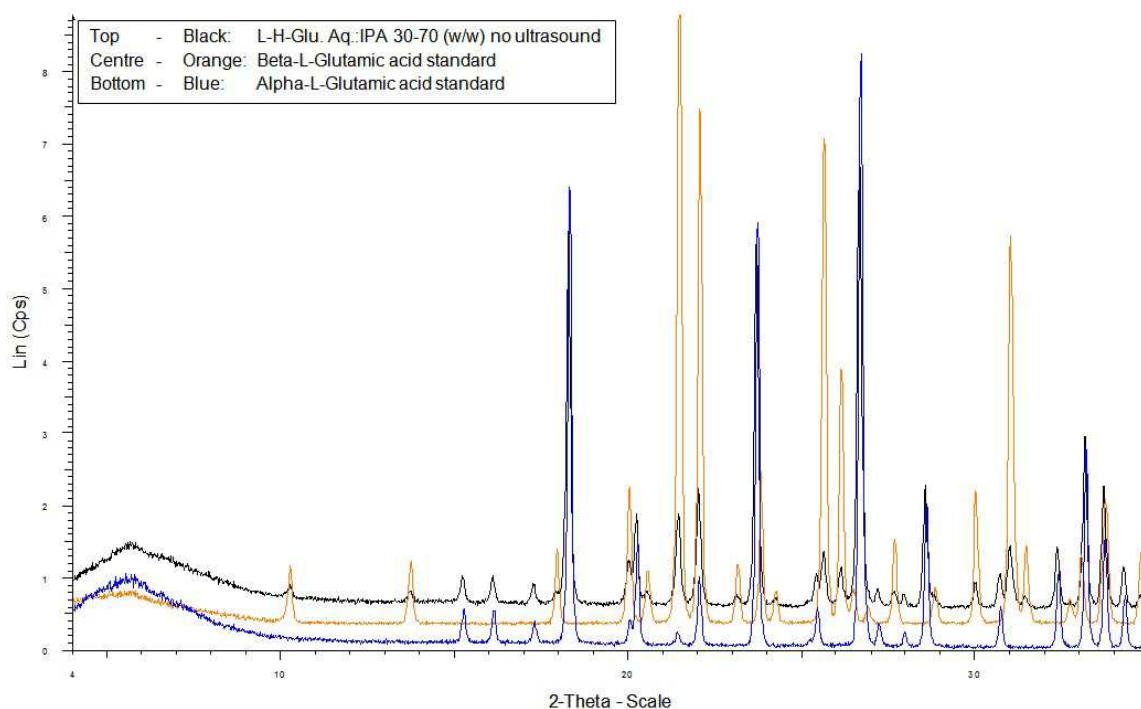
Figure 9.5-2: XRPD pattern of H-Glu in Water:IPA 30-70 (w/w) without ultrasound

Operations at solution:antisolvent ratios of 20:80 (w/w) or 5:95 (w/w) show a solid recovery jump after 3 min (6 residence times) to about 80-90 % but thereafter behave differently. The 20:80 (w/w) experiments show a drop in solid recovery, whereas the 5:95 (w/w) experiments remain at a steady high just below 90 % solid recovery.

However, as the outlet streams of both ratios were still supersaturated the crystallisation vessel encrusted and both systems blocked after 50 min (100 residence times) of operations.

The crystal form obtained under both conditions was a mixture of the metastable Alpha and the stable Beta polymorph, which was confirmed by XRPD (Figure 9.5-3, Figure 9.5-4) measurements. Due to peak heights, it can be suspected that the sample contains similar quantities of Alpha and Beta.
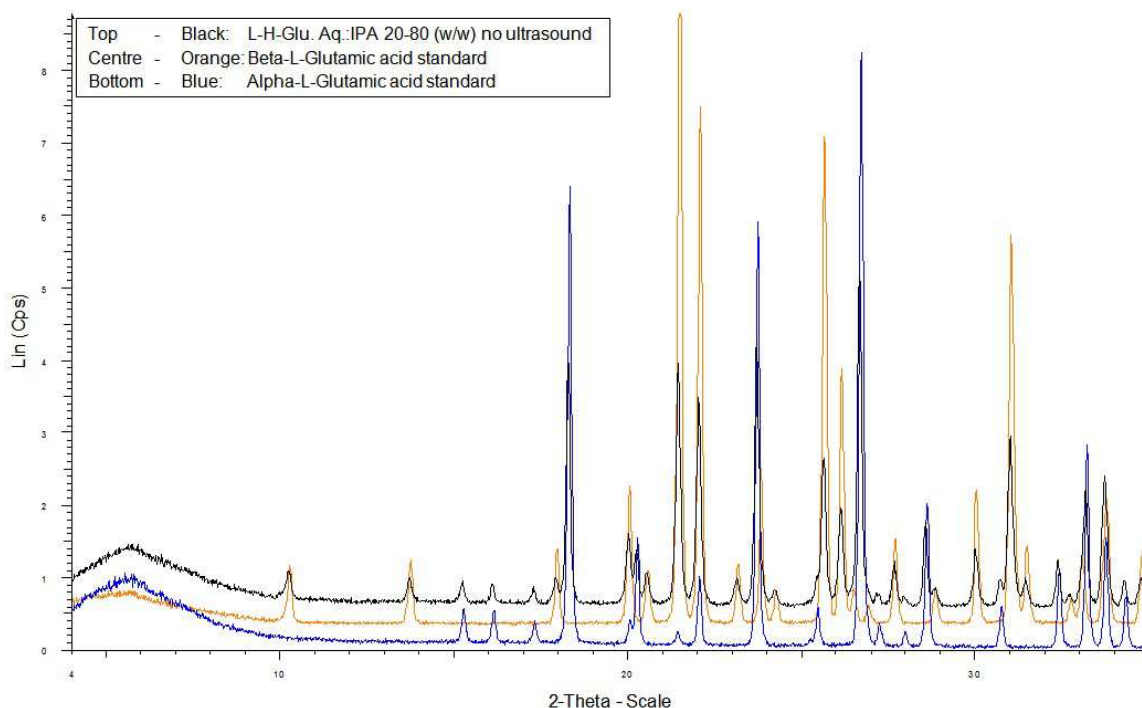
Figure 9.5-3: XRPD pattern of H-Glu in Water:IPA 20-80 (w/w) without ultrasound
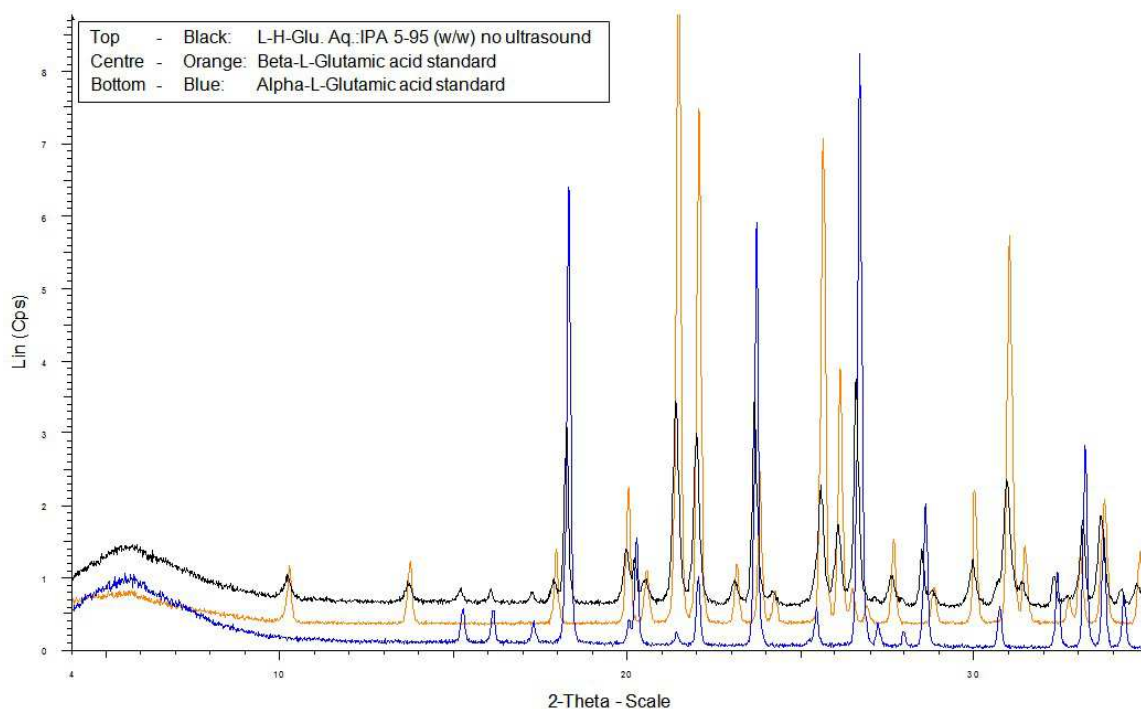
Figure 9.5-4: XRPD pattern of H-Glu in Water:IPA 5-95 (w/w) without ultrasound

The very low solid recovery of the 50:50 (w/w) and the extremely volatile behaviour of the 30:70 (w/w) run made these ratios appear unfavourable for further experiments. The other ratios showed more promising results and were investigated in more detail. Implementation of ultrasound into the system was supposed to help nucleation and to continuously clean the crystallisation vessel as well as all submerged equipment of encrusting crystals during the run.

The continuous cleaning objective was met and no obvious encrustation or blockage could be observed after a runtime of 100 min. (200 residence times) However, the effect of ultrasound through a jacketed vessel on nucleation was less obvious.
For all solution:antisolvent ratios, as shown in Figure 9.5-5, the solid recovery slowed down slightly compared to the experiments without ultrasound, which was not expected. However, the general solid recovery trends from the previous experiments

were confirmed. At a solution:antisolvent ratio of 20:80 (w/w) the solid recovery increases to its maximum after 10 min. (20 residence times), before it dropped again to a steady-state level around 60 %. The crystal form obtained under these conditions was a mixture of the metastable Alpha and the stable Beta polymorph, which was confirmed by XRPD (Figure 9.5-6) measurements. Peak heights indicate that the sample contains more Alpha than Beta.
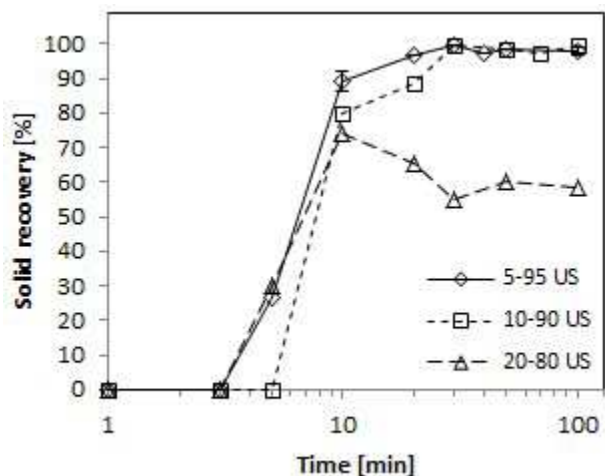
Figure 9.5-5: Solid recovery over time at various antisolvent mass fractions with ultrasound (US)
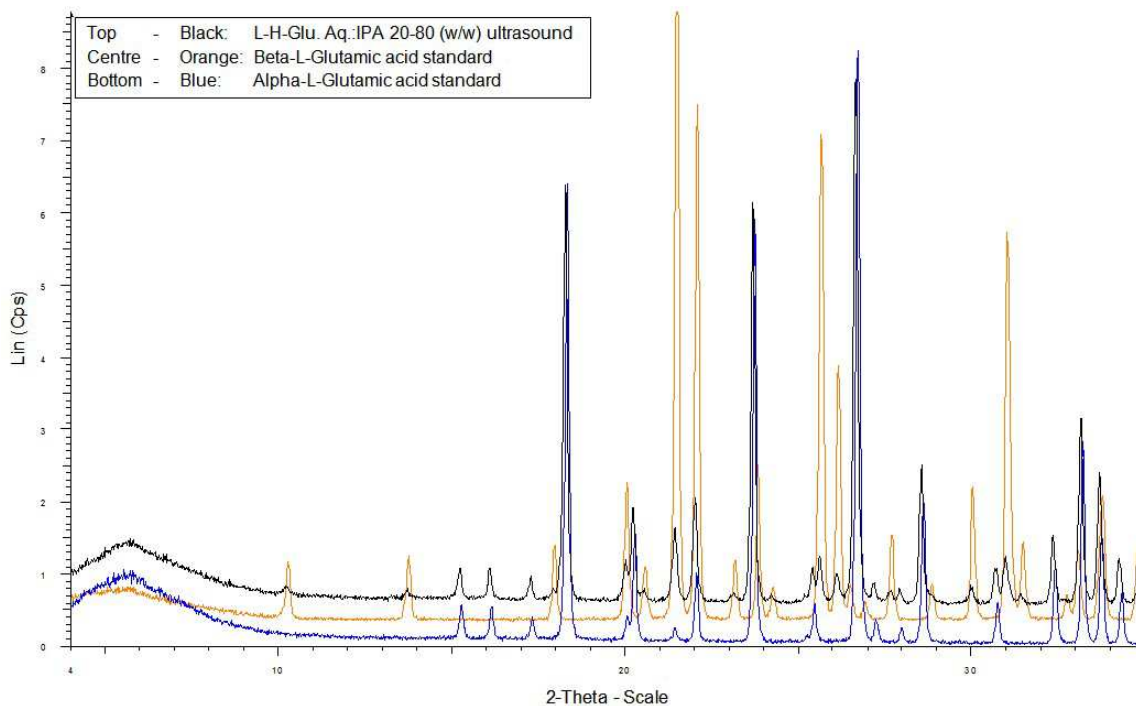
Figure 9.5-6: XRPD pattern of H-Glu in Water:IPA 20-80 (w/w) with ultrasound

The experiments at ratios of 10:90 (w/w) and 5:95 (w/w) behave very similarly, as both solid recoveries increase and reach a steady-state just below 100 % solid recovery after about 20 min. (40 residence times). The crystal form obtained for the 5:95 (w/w) ratio is Beta only (Figure 9.5-7), with possible Alpha trace amounts below the detection limit.
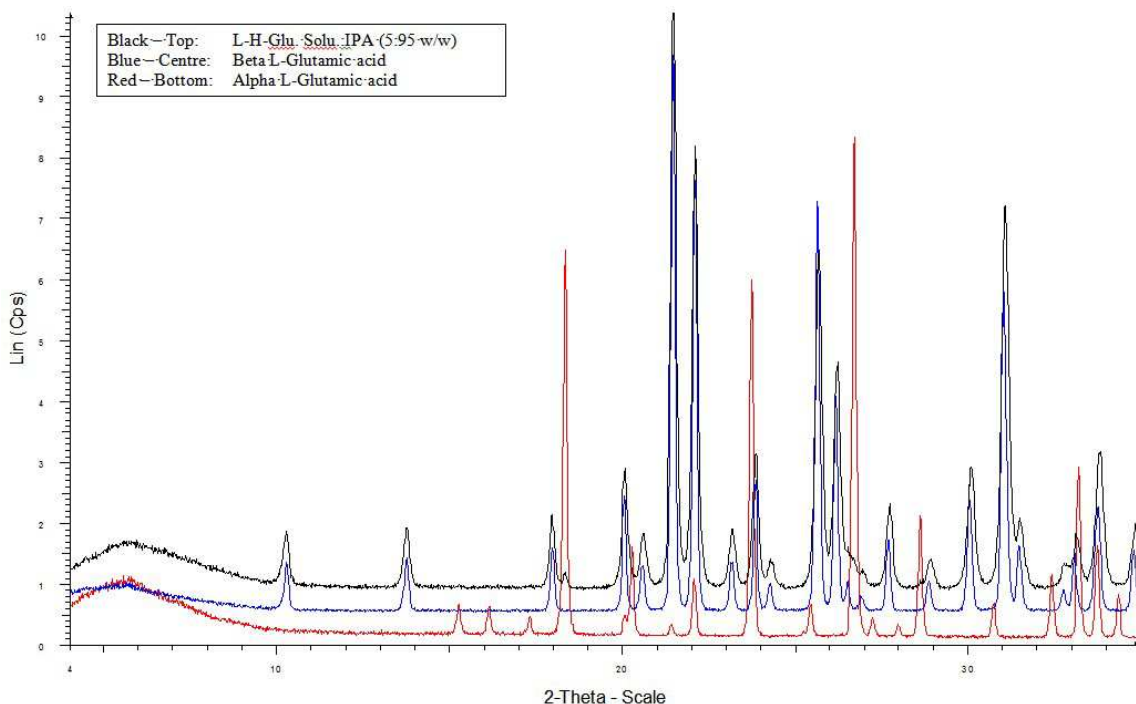
Figure 9.5-7: XRPD pattern of H-Glu in Water:IPA 5-95 (w/w) with ultrasound

The set up was operated with a solution:antisolvent ratio of 5:95 (w/w) for continuous production of seed suspension to be used in a different process for continuous growth. During a total run time of 2.5 hours (300 residence times), no obvious fouling could be observed and the system showed no symptoms of a possible blockage.

9.5.2 Particle size distribution (PSD)

Seed suspensions are generally used to grow larger product crystals. Sufficient growth and a satisfactory yield can only be achieved when the initial seed crystals are very small and can be grown at least 10 – 15 times in size.

Seed suspensions, generated for various solution:antisolvent ratios 30:70 (w/w) to 5:95 (w/w), were analysed by an offline laser diffraction technique and are shown in Figure 9.5-8. By reducing the solution fraction from 30 wt% down to 5 wt% it is possible to change the PSD from a broad bi-modal to a narrow mono-modal distribution.

The PSD obtained at a solution:antisolvent ratio 5:95 (w/w) is mono-modal, narrow and the product slurry is suitable for acting as a seed suspension. With a mean particle size of around 10 µm the particles are small enough to act as seeds and can be grown in a separate process to any desirable larger size.

By increasing both, the mass flow rates of stream 1 and stream 2 (keeping the ratio 5:95 (w/w) constant), as shown in Figure 9.5-9, and changing to a bigger crystallisation vessel it was possible to scale the process up by three times.

Figure 9.5-8: Particle size distribution (laser diffraction) of seed suspension at various antisolvent mass fraction and injection velocities

Scale up did not have a significant effect on the PSD apart from 10:190 (w/w) where a noticeable amount of agglomerates could be found in the seed suspension.

The only disadvantage of working with the 5:95 (w/w) ratio is the low solid loading in the seed slurry. A solution fraction of 5 wt% and a low saturation concentration of H-Glu at ambient temperatures required a seed concentration step. Concentration was achieved by batch centrifuging off major amounts of the antisolvent and re-suspending the seed material in saturated H-Glu solution. Particle size distributions of the concentrated seed suspension are shown in Figure 9.5-10.
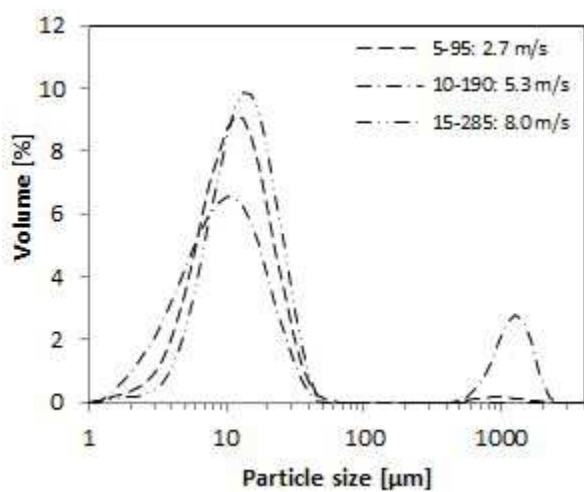
Figure 9.5-9: Particle size distribution (laser diffraction) at various process scales (Scale up)

The mean particle size of the major seed fraction is not significantly affected by the concentration step and only shows a small shift toward larger sizes. However, it must be noted that the amount of larger agglomerates increased considerably.
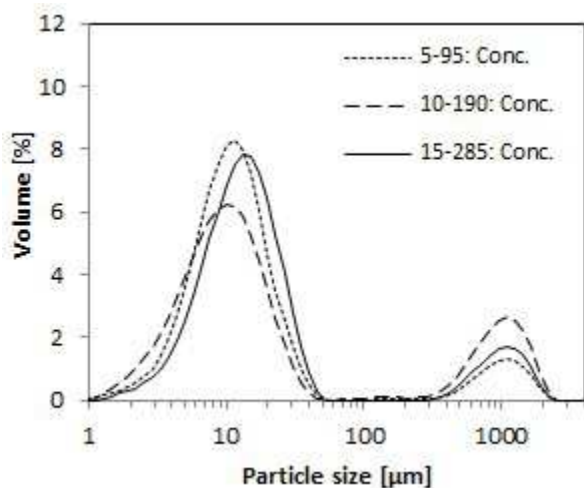
Figure 9.5-10: Particle size distribution (laser diffraction) of concentrated seed suspension at various process scales

9.5.3　Mean particle size

Mixing is a fundamental unit operation in the chemical industry and plays a crucial role especially in crystallisation, as it determines how effective and homogeneous supersaturation is generated. Previously we have shown how mixing in static mixers, using various mixer types and different mixing velocities, can have an influence on nucleation and subsequent growth processes. The general conclusion was that higher mixing flow rates lead to more nuclei and smaller final crystal sizes [9.4].
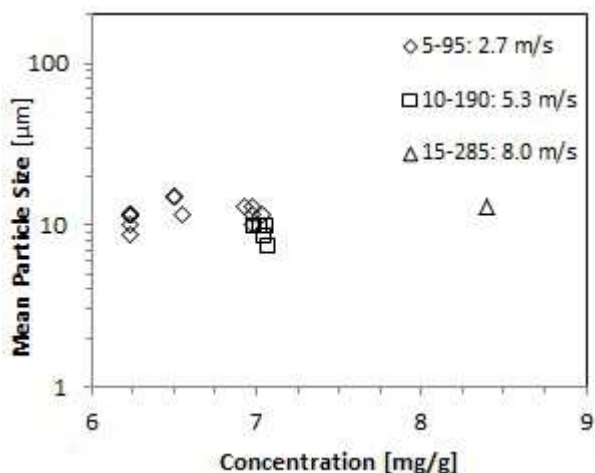
Figure 9.5-11: Mean particle sizes (laser diffraction) at various injection velocities

Jet injecting an aqueous solution through a nozzle with small internal diameter into antisolvent can generate injection velocities of several meters per second. It can be assumed that such high velocities also have an effect on nucleation and the final particle size.

However, results in Figure 9.5-11 indicate that the injection velocity in these experiments did not show the effects described by Brown et al. [5.5]. Increasing the injection velocity from 2.7 m/s to 8.0 m/s did not result in a significant decrease in mean particle size. It is also shown that small changes in solution concentration, within the narrow window between 6.2 – 8.4 mg/g$_{(Solution)}$, did not show significant influence.

Solubility and supersaturation are important parameters in crystallisation especially when rapid nucleation is supposed to instantly consume all crystallisable material, in order to avoid growth. In antisolvent crystallisation, high supersaturation is achieved by mixing small amounts of solution with large amounts of antisolvent and the actual ratio determines the solubility and supersaturation in the bulk suspension.

Starting at solution:antisolvent ratio of 5:95 (w/w) and increasing it to 30:70 (w/w) changes both parameters so that the bulk solubility increases and the supersaturation decreases. In Figure 9.5-12 a clear trend can be observed that the mean particle size increased with increased solution fraction, increased bulk solubility and decreased supersaturation. Figure 9.5-13 shows the mean particle size against the solution fraction for better illustration of the results. These experiments also highlight that different injection velocities do not influence the mean particle size.
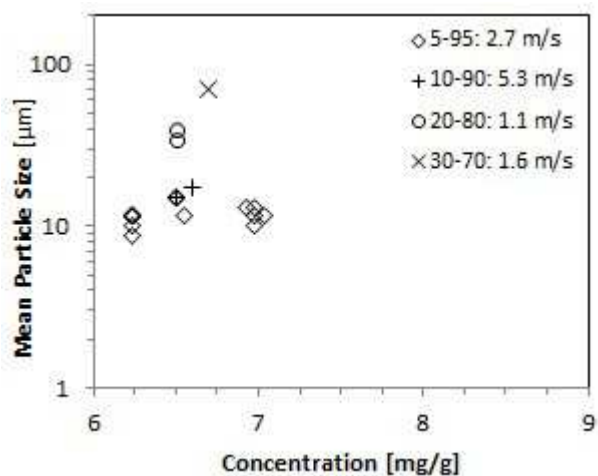
Figure 9.5-12: Mean particle size (laser diffraction) at various injection velocities and concentrations
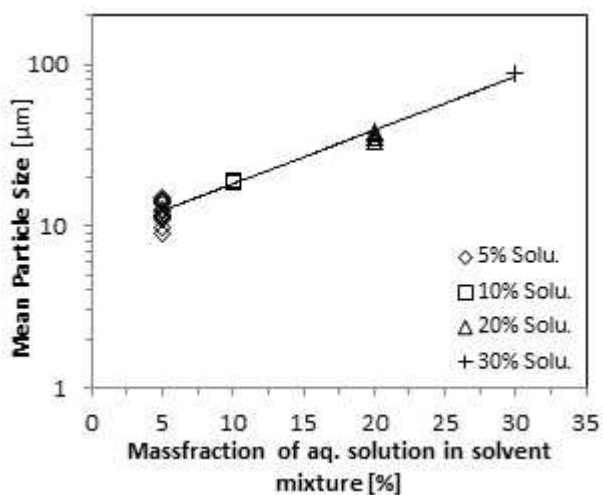
Figure 9.5-13: Mean particle size D[4,3] (laser diffraction) vs. water solution fraction

9.5.4 Fouling

Surfaces of all kinds, some better than others, as well as already present product crystals provide sources for heterogeneous nucleation. Crystal growth on thermocouples, tubing or vessel walls cause impairments resulting in blockage of the system.

The traditional crystallisation set-up (without wall heating or ultrasound) suffered from fouling and blockages and was not suitable for continuous crystallisation over longer periods. Figure 9.5-14, Figure 9.5-15, Figure 9.5-16 and Figure 9.5-17 show how bad fouling typically was in this system after a run of about 100 min.

Figure 9.5-14: Bottom view into crystallisation vessel without hot wall or ultrasound indicates fouling on vessel walls

Figure 9.5-15: Fouling on injection nozzle

Figure 9.5-16: Fouling on outlet tube

Figure 9.5-17: Fouling on thermocouple

The hot wall cold bulk approach was implemented to reduce fouling on the walls of the crystallisation vessel. By keeping the walls significantly warmer than the bulk solution, the solubility in the wall-liquid boundary layer was increased and supersaturation on the wall was kept at a minimum.

Figure 9.5-18 shows the crystallisation vessel after a 100 min. run utilising the hot wall cold bulk approach. The degree of fouling on the walls is significantly reduced, appears to be a thin layer rather than grown crystals and looks uneven and patchy. The injection nozzle in Figure 9.5-19, on the other hand, shows the usual degree of fouling and exhibits large crystals on its surfaces.

Figure 9.5-18: Bottom view into crystallisation vessel with heated walls. Significantly reduced, uneven fouling in hot wall cold bulk set up

Figure 9.5-19: Fouling on injection nozzle

An additional approach to deal with the fouling problem was to submerge the entire set up into an ultrasonic bath. Laboratories commonly use ultrasonic baths for cleaning of equipment and this approach was investigated for the crystallisation run as well.

Figure 9.5-20 and Figure 9.5-21 clearly illustrate the effect of the ultrasound cleaning action after a run of 100 min. The only fouling which can be observed is a thin layer of crystalline material at the previous liquid level inside the crystalliser. Due to the hot wall, it happened that solvent from the surface evaporates and product crystals in that area stuck to the wall. All other submerged parts or walls do not show any obvious indication of fouling of any kind.

Figure 9.5-20: Top view into crystallisation vessel hot wall + ultrasound after run time of 100 min.

Figure 9.5-21: Bottom view into crystallisation vessel hot wall + ultrasound after run time of 100 min.

9.5.5 Optical microscopy and Scanning Electron Microscopy (SEM)

For an optical impression of the concentrated seed suspension, micrographs were taken of a run with a solution:antisolvent ratio of 5:95 (w/w). A representative image is shown in Figure 9.5-22 which illustrates the needle or thin platelet shape of the Beta seed crystals. The fact that no prismatic Alpha crystals can be found, supports the XRPD (Figure 9.5-7) analysis, which indicated pure Beta phase.
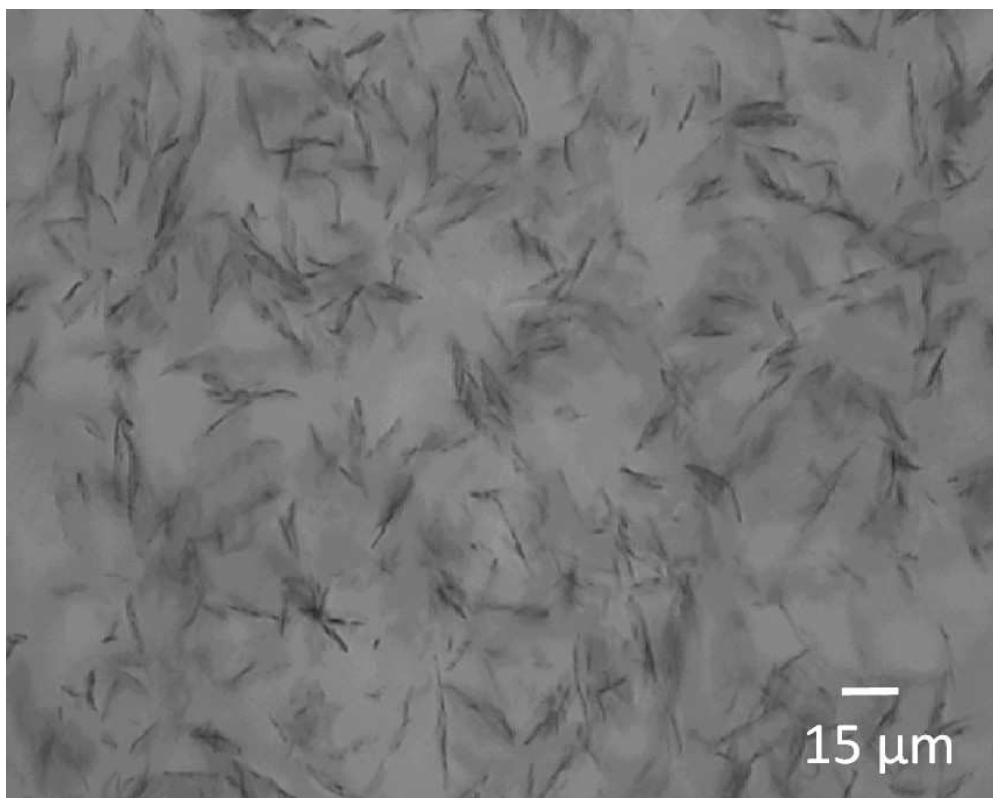
Figure 9.5-22: Micrograph of concentrated seed suspension. Dark grey lines indicate platelet like crystals pointing into various directions.

For more detailed pictures and the illustration of individual particles and shapes, SEM images of the seed crystals were taken. Figure 9.5-23 shows the pores of the filter membrane used and Figure 9.5-24 as well as Figure 9.5-25 illustrate the shape and size of the actual seed crystals on the filter membrane. The images clearly show the flake or platelet like structure of the Beta seed crystals and again no Alpha prisms can be observed as indicated by XRPD (Figure 9.5-7) analysis.
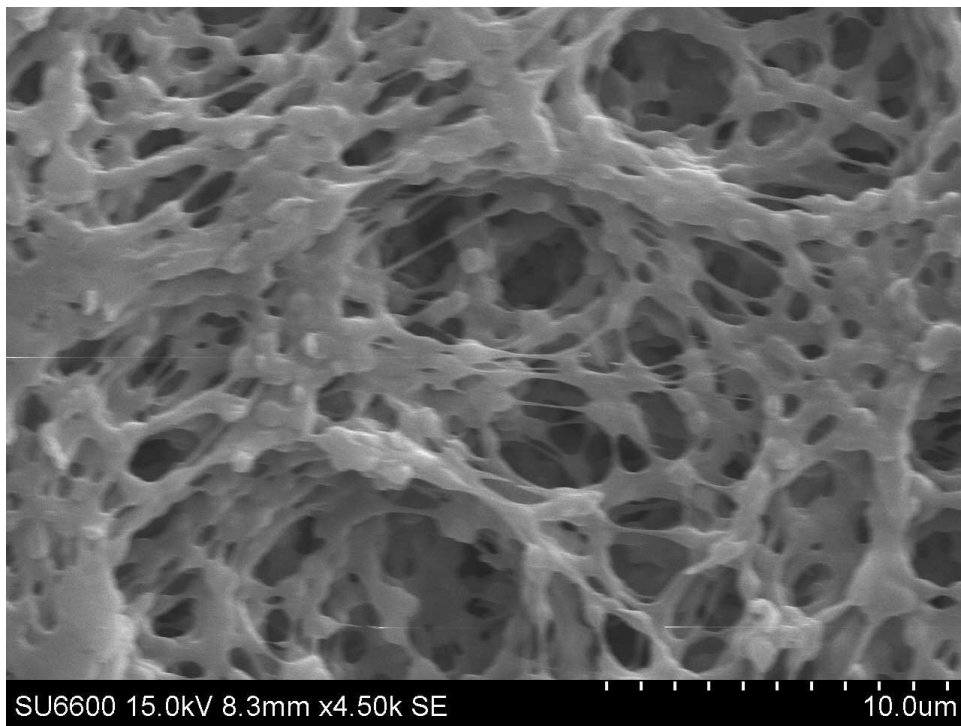
Figure 9.5-23: Image of PTFE filter membrane pore structure
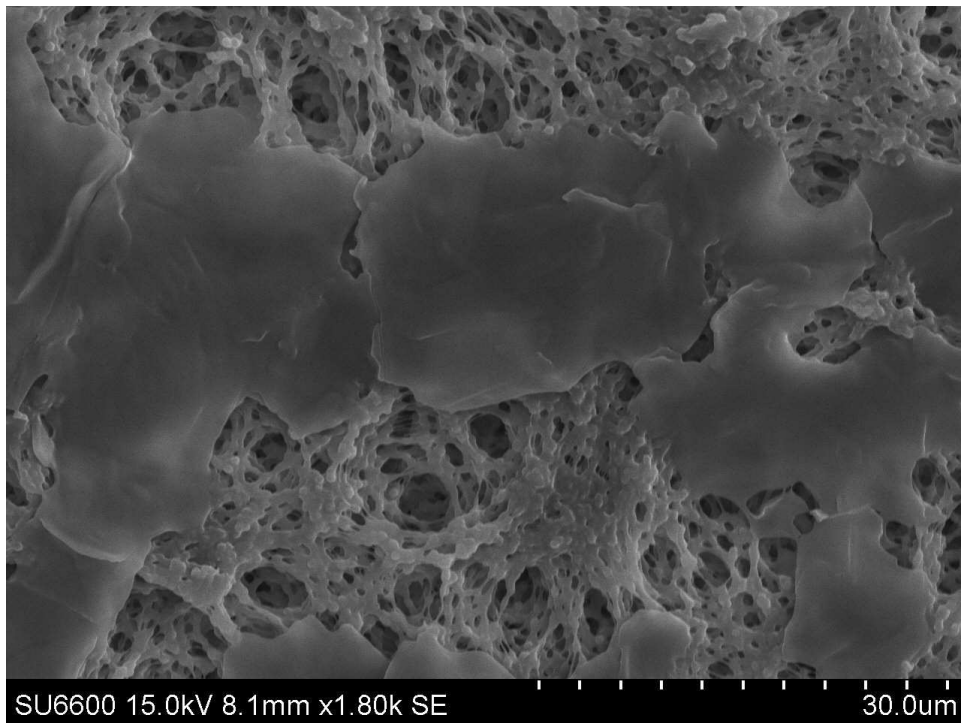
Figure 9.5-24: Platelet like Beta H-Glu seed crystals on PTFE filter membrane
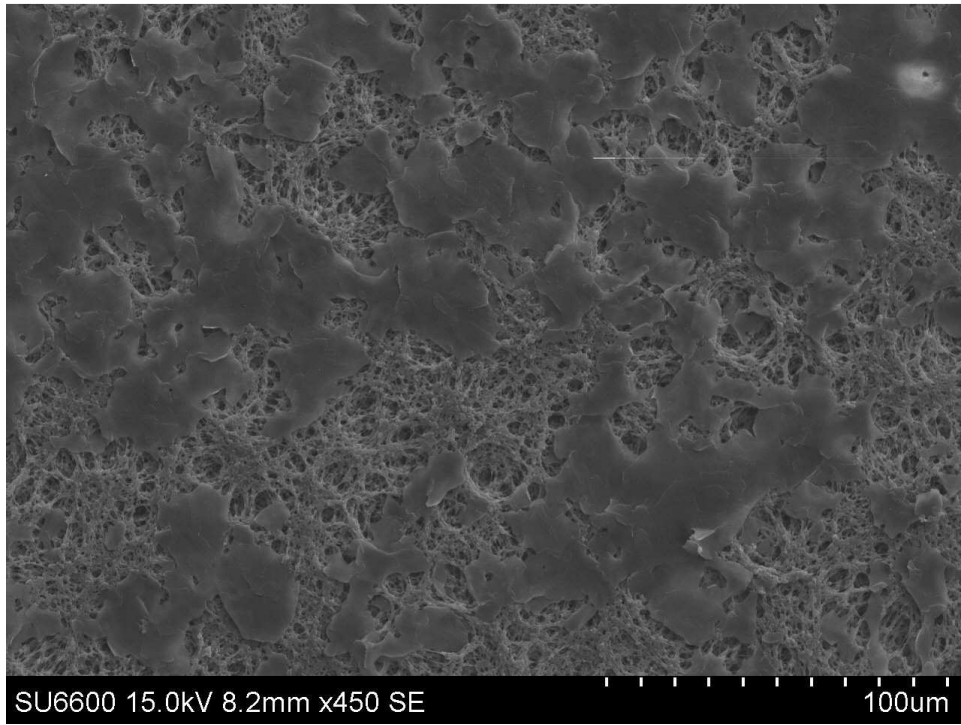
Figure 9.5-25: Platelet like Beta H-Glu seed crystals on PTFE filter membrane (lower magnification)

9.6   Conclusions

In this work, we presented a set up for the continuous production of seeding suspension through continuous rapid antisolvent crystallisation as part of a modular Plug & Play crystalliser technology. The system reproducibly generated crystals with a narrow particle size distribution, a consistent mean particle size was obtained and steady-state operation was achieved. Scale up by a factor of three was successfully carried out and it was shown that product parameters like mean particle size and particle size distribution could be kept steady. A centrifuge concentration step was carried out, due to low solid loading, and did not show significant effects on product quality.

Heating the aqueous solution stream prevented blockages of the submerged jet-injection nozzle but different injection velocities did not influence the mean particle size. An increase in mean particle size could only be observed by increasing the aqueous fraction in the bulk solution. The hot wall cold bulk approach reduces fouling on the vessel walls and submerging the whole crystallisation vessel into an ultrasonic bath cleaned all exposed surfaces off encrusting crystals. The ultrasound furthermore increased solid recovery, helped obtaining pure crystal phases and prevented blockage of the system. The only disadvantage was a slower approach towards steady-state operation.

SEM images of the product seed suspension revealed the platelet like shape of the seed crystals, which are of ideal size to be used for further growth processes.

10 Steady-state near plug-flow crystal growth of L-Glutamic acid seeds in a continuously seeded continuous oscillatory baffled crystalliser (COBC)

In the previous chapter a novel continuous antisolvent crystallisation setup for the continuous production of crystal suspension was developed and characterised. It was shown that crystals of small mean particle size and narrow particle size distribution could be produced at a high yield under steady-state operations. The results obtained are very promising so that these crystals could make a good seeding suspension for a continuous crystal growth process.

10.1 Introduction

Crystallisation is an important separation and purification process in the pharmaceutical and fine chemical industry. Most API are small organic molecules synthesised in solution, which need to be crystallised to transform them into usable solid material. However, the science behind solution crystallisation is still very complex and requires a high degree of operational flexibility.

Traditionally, the industry operates in batch mode, which provides the required flexibility but batch-to-batch variations cause undesired deviations in crystal quality, for example, purity, polymorph, particle size distribution, shape and yield. Inconsistent crystal quality also impacts downstream operations and leads to problems during filtration, drying or milling. The necessary product scale-up is difficult as it causes less uniform mixing in larger equipment and the loss of heat transfer area compared to the bulk volume. Both parameters negatively impact the control over the process and increase the need for recrystallisation of out-of-specification product. Apart from the technical challenges, there is also a growing demand from regulatory bodies for consistent product quality and better understanding of controlling parameters in solution crystallisation.

A possible alternative to the challenges in batch operation could be offered by continuous manufacturing and crystallisation in flow without interruptions. An automated and efficient continuous set up could save solvent, energy and space, deliver better product quality, minimise maintenance as well as cleaning and downtimes. [2.2, 10.1-10.3]

Various research groups investigate different continuous crystallisation methods and equipment from conventional large-scale sugar crystallisers to small scale systems with very high mixing intensities. [10.3] In continuous processes where narrow particle size distributions are a priority, the system should exhibit hydrodynamics in the near plug flow regime in order to assure that every fluid element in a similar area experiences the same treatment.

Static mixer systems with optional tubular crystallisers as described and studied by Schwarzer et al. (2002) [10.5], Kawase et al. (2007) [10.6], Eder et al. (2010-2012) [10.3, 10.7, 10.8] and Ferguson et al. (2013) [10.9] rely on a high net flow rate to ensure sufficient mixing and near plug flow hydrodynamics. A tubular crystalliser with Kenics static mixing inserts, investigated by Alvarez et al. (2010) [10.10], is reported to converge towards plug flow behaviour the more Kenics elements are connected. However, due to the required high flow rates even long crystalliser lengths exhibit a relatively short residence time, which makes these systems more suitable for fast growing compounds. [10.1, 10.2]

A different approach towards continuous crystallisation is a conventional STC, fitted with a continuous sample inlet/outlet stream and turned into a flow through unit, which is then called continuous MSMPR. A single stage MSMPR, as described by Takiyama et al. (2001) [10.11], Narducci et al. (2011) [10.12] and Ferguson et al. (2013) [10.9], operates far from plug flow conditions and generates undesirable very broad particle size distributions. Multistage MSMPR, studied by Alvarez et al. (2011) [10.13], Quon et al. (2012) [10.2] and Zhang et al. (2012) [10.14], where a larger number of STC (usually 5-10) are connected in series, show a residence time distribution closer to plug flow. [10.15] In practice, however, even these set ups can only achieve near plug flow conditions. [10.1, 10.3]

The necessary hydrodynamics for particle suspension are generated in each individual STC and are hence decoupled from the net flow rate through the system. This feature allows very small flow rates through the system and makes a multistage MSMPR suitable for slow growing compounds, which require long residence times. [10.2]

A hybrid technology between the net flow driven tubular crystalliser and the individually stirred MSMPR cascades is the Continuous Oscillatory Baffled Crystalliser (COBC). This technology consists of a periodically spaced, baffled tubular crystalliser which generates vortexes and eddies when the oscillating fluid interacts with the baffles. These vortexes and eddies provide the required hydrodynamics to keep particles suspended and decouple mixing from the net flow through the unit. [10.1] The COBC technology combines the near plug flow residence time distribution with the long residence times of the continuous MSMPR. However, the length and thus the residence time of a single COBC is limited and depends on the power of the oscillating motor connected to the system. This is a major disadvantage compared to a continuous MSMPR and restricts the COBC to average or fast growing compounds, which require a medium or short residence time.

Solution crystallisation is a two-step process consisting of nucleation of new crystals and subsequent growth to final product. Process control over spontaneous nucleation is limited but, as the initial step of crystallisation, it is responsible for the physical and chemical properties of the final product crystals. Lack of control over nucleation can lead to undesirable off-specification product, which is unsuitable for the market and might need reprocessing. A common way to obtain better control over crystallisation is through seeding. A known quantity of crystal suspension with desired mean particle size, particle size distribution and polymorphic form is added to the crystallisation vessel in order to avoid spontaneous nucleation and only allowing crystal growth. Seeding has the potential to turn the two-step crystallisation process into a one-step crystal growth process, which achieves better control over the final crystal product. [2.2, 10.1]

A widely adapted procedure for the generation of seeding suspension is milling larger product crystals down to a size at which they can be used as seeds. However, milling crystals to smaller sizes leads to broad particle size distributions and undesirable physical stress within the crystal lattice. On top of that, crystals tend to break along the facet with the weakest attachment energy and with reducing particle size exposes more of those surfaces to the outside. Different surfaces can have different physical properties so that a seed which is, for example, exposing hydrophobic surfaces, would be less effective for crystal growth in an aqueous system. [2.2, 10.4]

The right timing for seed addition to the crystallisation vessel plays a crucial role as seeding of undersaturated solution leads to seed dissolution, which makes seeding ineffective. Late seeding, after the system reached the unstable zone and uncontrolled nucleation already happened, defeats the purpose of the seeding as the desired process control is lost. [2.2]

The Continuous Oscillatory Baffled Reactor (COBR) technology was first described by Mackley (1991) [10.16] and was optimised by Harvey et al. (2001) [10.17] due to industrial demands for continuous processes. Over the last decade, the COBR equipment received significant research attention. A large number of different chemical processes were performed, ranging from hydrolysis of esters by Harvey et al. (2001) [10.17] over biodiesel production by Harvey et al. (2003) [10.18] to the synthesis of Vanisal Sodium and Aspirin by Ricardo et al. (2009) [10.19].

The first continuous crystallisation study was published by Lawton et al. (2009) [10.1] and compared the performance of a Batch Oscillatory Baffled Crystalliser (BOBC) to the COBC both seeded and unseeded. It was reported that the COBC shows good mass and heat transfer capabilities especially during scale up and that good mixing can be achieved at low fluid shear rates.

In more recent time further COBC studies on the precipitation of hydoxyapatite by Castro et al. (2013) [10.20], heterogeneous catalysis by Eze et al. (2013) [10.21] and various biological processes reviewed by Abbott et al. (2013) [10.22] were published.

In this work, as part of the Plug & Play crystalliser set-up development, we are presenting a modular continuous crystallisation set up. Seeding suspension was continuously produced through rapid antisolvent crystallisation (described in Chapter 9) at high supersaturation with a narrow particle size distribution, small mean particle size and of desired polymorph. The seeding suspension was centrifuge concentrated, resuspended in saturated H-Glu solution and continuously injected into a cooling crystallisation COBC to ensure crystal growth at low supersaturation to various different product mean particle sizes.

It is also shown how to use thermodynamic and kinetic information to select cooling profiles which ensure low bulk supersaturation levels and desired desupersaturation behaviour as crystallisation progresses.

At various positions along the rig, offline gravimetric solid recovery measurements were carried out and the final crystal product was analysed by laser diffraction, XRPD as well as by optical microscopy and SEM analysis.

10.2 Methods

10.2.1 Materials

Beta H-Glu (purity ≥ 98.5 %) containing ≤ 0.1 % of the Alpha form was purchased from Sigma Aldrich, Germany. Deionised water used in all experiments was obtained from a Thermo Scientific (USA) water purification system.

Experiments were performed in an air conditioned laboratory at 20 ± 2 °C. H-Glu seeds in saturated H-Glu solution were provided from a precursor process.

10.3 Experimental setup

10.3.1 Continuously seeded cooling crystallisation

A schematic drawing of the COBC equipment used in these experiments is shown in Figure 5.3-7: Continuous Oscillatory Baffled Crystalliser (COBC) consisting of control box, motor and bellow to generate oscillation. Growth solution and seeding suspension are provided in two jacketed and stirred holding tanks. Different colours along the rig represent different temperature zones from warm (red) to cold (violette). The system consists of a control box used to set oscillation amplitude and frequency of the linear motor which drives a bellow to generate turbulent oscillating hydrodynamics in the rig. Two individually heated STCs provide H-Glu solution as well as seeding suspension and the tubular crystalliser contains seven bend ports (P2 - P8) as well as P1, which serves as the crystalliser product outlet.

The COBC is manufactured from glass to allow easy observation of proceeding crystallisation. 32 straights and 8 bends achieve 24.8 m in length with a total volume of 4.22 l. However, the seeding port is located behind straight 31 and hence only 30 straights and 8 bends can be used for crystal growth, which reduces the volume to 3.98 l.

The unit dimensions are as follows: $d_{(Cell)}$: 16.3 mm, $l_{(Cell)}$: 25.2 mm and a $d_{(Orifice)}$: 7.8 mm. At an oscillation amplitude of 30 mm and a frequency of 1 Hz it achieves an oscillatory Reynolds number $Re_O = \frac{x_o \omega D \rho}{\mu} = 1536$ and Strouhal number $St = \frac{D}{4\pi x_o} = 0.09$.

x_o: Amplitude of oscillation (centre to peak) $[m]$

ω: Angular frequency of oscillation $\left[\frac{1}{s}\right]$

D: Tube internal diameter $[m]$

ρ: Fluid density $\left[\frac{kg}{m^3}\right]$

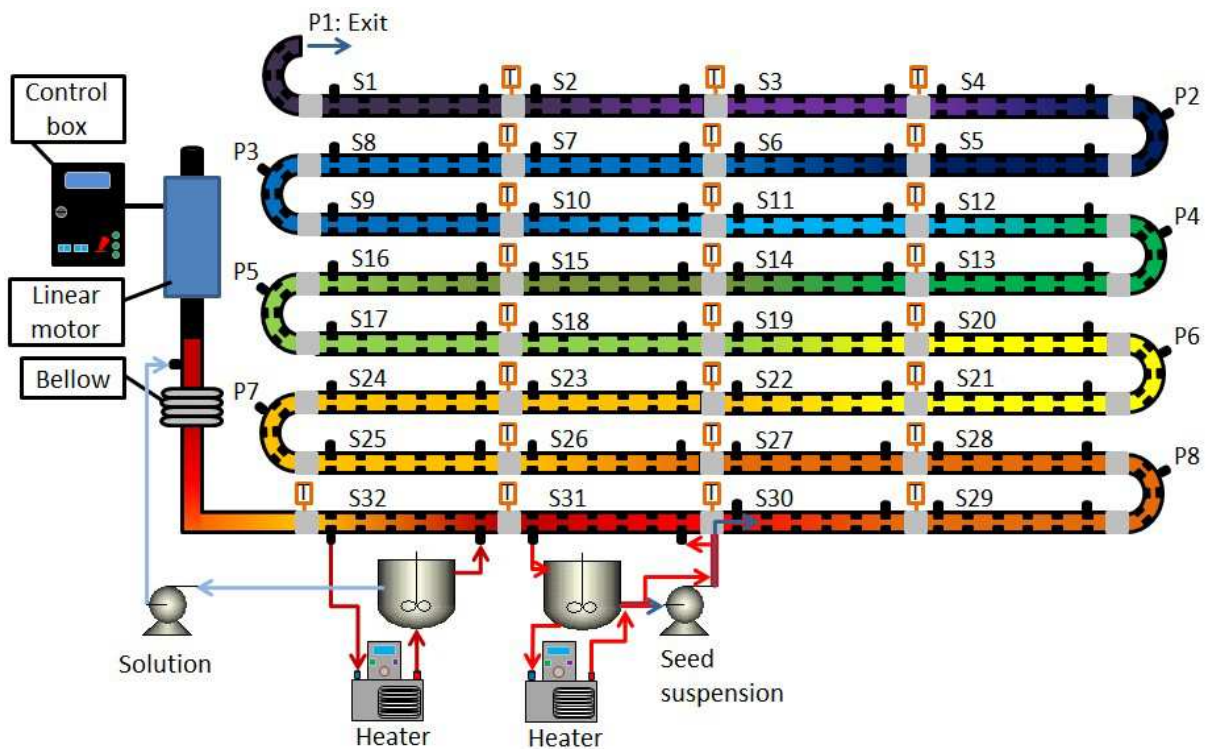μ: Dynamic fluid viscosity $\left[\frac{kg}{s \cdot m}\right]$

Figure 5.3-7: Continuous Oscillatory Baffled Crystalliser (COBC) consisting of control box, motor and bellow to generate oscillation. Growth solution and seeding suspension are provided in two jacketed and stirred holding tanks. Different colours along the rig represent different temperature zones from warm (red) to cold (violette).

In order to prepare the COBC for operation it was filled with water. Air bubbles which would dampen oscillation were flushed out of the system. After that, the oscillation amplitude was calibrated to 30 mm at a frequency of 1 Hz, the solution flow rate to 30 g/min and the seeding suspension flow rate to 20 g/min The total net flow rate of 50 g/min and the total crystalliser solution content of 3.98 kg created a mean residence time of 79.7 min available for crystal growth.

With a constant flow of water through the rig, 13 heater/chiller units were calibrated to their respective temperatures to deliver the cooling profile required for the experiments. The ideal cooling profile matches the proceeding crystal growth process and ensures that an optimal level of supersaturation for crystal growth is constantly maintained at every point along the rig.

H-Glu solution was prepared at two different concentrations (18 & 40 $g/kg_{(Solution)}$) and kept 25 °C above its solubility temperature in order to ensure complete dissolution. H-Glu seeding suspension in warm saturated H-Glu solution was provided at two different seed loadings (0.2 & 0.9 $g/kg_{(Solution)}$) ready for use.

Hot undersaturated H-Glu solution is pumped through the bellow and an unjacketed elbow so that slightly colder but still undersaturated growth solution reaches straight 32 (S32). The jacket of S32 is connected to the jacket of the growth solution STC and heats the liquid in S32 back up to the required temperature. This procedure ensures dissolution of any possible encrustation within the bellow and down to S32.

The jacket of S31 is connected to the jacket of the seed suspension STC and cools the liquid in S31 down to the temperature, corresponding to SS = 1.05, at which seeds are introduced into the system.

The straight connector between S31 and S30 simultaneously serves as a seeding port (SP) through which seeding suspension is injected into the H-Glu solution. Mixing

solution with seeding suspension creates four different scenarios of operation, namely low & high solution concentration and low & high seed loading.

After the first crystalliser volume was replaced by seeded solution, samples were taken at the crystalliser outlet P1. Analysis of product crystals covered gravimetric solid recovery, particle size distribution (Malvern Mastersizer), chord length distribution (FBRM), XRPD analysis and micrographs as well as SEM images. At the same time ~ 2 g samples were taken from the bends P2 – P8, which were only analysed for gravimetric solid recovery. After each completed crystalliser residence time, this procedure was repeated to assess steady-state operation of the system.

In order to shut the unit down, the H-Glu solution and seed suspension pumps were stopped, all heater/chiller units heated up to about 70 °C and the rig was flushed with pure water for at least five crystalliser residence times.

10.3.2 Calculation of temperature and concentration profiles

In a continuous process the mean residence time is finite, fixed and determined by the equipment as well as operating conditions, unlike in batch processes. Product material continuously exits the crystalliser even when crystallisation is not completed and the bulk solution is still supersaturated. Under these conditions it is essential to design a continuous crystallisation process which ensures proper bulk desupersaturation within the given residence time. Influencing factors for desupersaturation are for example solution concentrations, seed loading, morphology and surface area, crystal growth kinetics, temperature and crystalliser mean residence time.

Massbalance & solubility data

- Determine solution concentration of seed stock solution at operating temperature so that seeds do not dissolve
- Match growth solution concentration at operating temperature so that upon mixing no seeds dissolve
- Define seed loading in the rig and calculate back to determine seed mass loading in seed stock suspension

153

Particle size & volume

- Assumption: All seeds are monodisperse particles with a diameter of the mean particle size determined by Malvern Mastersizer
- Laser diffraction assumes spherical crystal shape and hence the diameter can be used to calculate the crystal volume

Crystal density & mass of single crystal

- With crystal volume and density available the mass of a single crystal can be calculated
- The seed mass loading from step 1 can then be coverted into a seed number loading

Crystal morphology

- The crystal volume from step two is converted to two different pre-selected crystal morphologies
- Cube (L x W x H): 6,45 x 6,45 x 6,45 µm
- Platelet (L x W x H): 16,2 x 8,2 x 2 µm
- Aspect ratios of the platelet were obtained from literature [10.23] as well as from in house SEM images

Growth data

- Supersaturation dependent crystal growth data at constant temperature [8.9] was used to determine overall crystal growth (volume & mass increase) per every second.

Residence time & desupersaturation

- The residence time in each temperature zone is determined based on crystal growth and supersaturation depletion rates
- Seed and growth solution flow rates determine the number of COBC straights required for each temperature zone
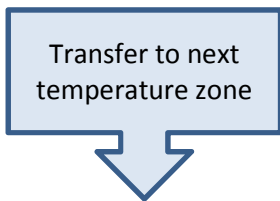
| Transfer to next temperature zone | - To keep crystal growth rates high the crystal slurry is transferred into the next colder temperature section. Supersaturation and growth rates are ramped up again [10.24] |

The number of COBC straights (in this case a maximum of 32) determines the volume of the crystalliser and the net flow rate determines the crystalliser mean residence time. The maximum supersaturation and crystal growth rates are capped by the metastable zone width of the system. The available solution concentration sets the required total ΔT over the COBC and the seed number loading as well the length of each temperature section determine whether bulk desupersaturation can be achieved or not.

This process defines the temperature zones in the COBC and how many straights at constant temperature are required in order not to penetrate the MSZ with supersaturation spikes. The validity of this process and the actual desupersaturation behaviour in the COBC were checked with offline solid recovery analysis.

10.4 Results and discussion

10.4.1 Seed crystals

Continuously produced H-Glu seeding suspension for the crystal growth experiments was provided by a precursor process (described in Chapter 9). The mean seed size was about 10 μm with a narrow particle size distribution (Figure 10.4-1) and XRPD analysis (Figure 9.5-7) confirmed the polymorphic pure form of Beta H-Glu.
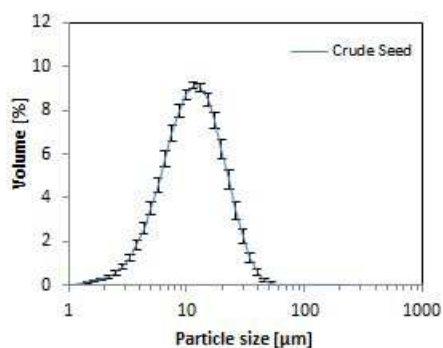
Figure 10.4-1: Crude seed particle size distribution (laser diffraction) with error bars of 35 different batches
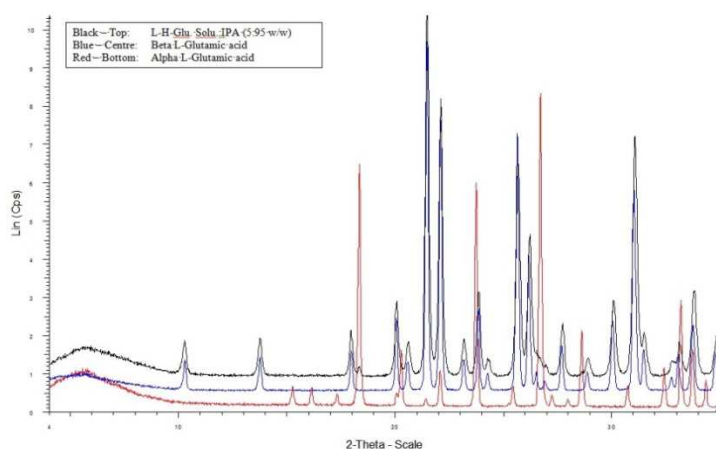
Figure 9.5-7: XRPD pattern of H-Glu in Water:IPA 5-95 (w/w) with ultrasound

10.4.2 Solution concentration, seed loading and COBC temperature sections

The solution of pure H-Glu was prepared in two different concentrations $c \sim 18$ g/kg$_{(Solution)}$ and $c \sim 40$ g/kg$_{(Solution)}$ in order to study the effect of solution concentration on final crystal size. In a similar way the concentrated seeding suspension was diluted to achieve two different seed loadings s-load ~ 0.1 g/kg$_{(Solution)}$ and s-load ~ 0.4 g/kg$_{(Solution)}$ in order to study the effect of seed loading on final crystal size. The four different experimental combinations of growth solution and seeding suspension are summarised in Table 10.4-1.

Table 10.4-1: Selection of operating conditions in operational space in seeded COBC experiments

c(Solution) / Seed loading	Low	High
Low	LL (1) conc.: 18.7 g/kg$_{(Solution)}$ s-load: 0.1 g/kg$_{(Solution)}$	HL (2) conc.: 40.2 g/kg$_{(Solution)}$ s-load: 0.1 g/kg$_{(Solution)}$
High	LH (3) conc.: 18.3 g/kg$_{(Solution)}$	HH (4) conc.: 39.8 g/kg$_{(Solution)}$

	s-load: 0.4 g/kg$_{(Solution)}$	s-load: 0.3 g/kg$_{(Solution)}$

These concentrations and seed loadings, mass balance calculations, crystal growth data, bulk supersaturation and residence time in a constant temperature section were considered when the cooling and desupersaturation profiles were calculated. The level of bulk supersaturation was kept as low as possible to avoid secondary nucleation and fouling but as high as necessary to achieve crystal growth. Table 10.4-2 outlines the different temperatures and temperature section lengths for the individual experiments.

Table 10.4-2: Selection of temperature sections in COBC cooling crystallisation

	LL (1) T [°C]	HL (2) T [°C]	LH (3) T [°C]	HH(4) T [°C]
S31	42.1	68.0	43.3	63.2
S30				
S29 & Bend	39.4	57.5	40.2	
S28				
S27				60.6
S26				
S25 & Bend	39.0	56.7	38.6	
S24				
S23				
S22				
S21 & Bend	37.8	55.8	37.4	55.0
S20				
S19	36.2	51.9	34.7	

S18				
S17 & Bend				49.6
S16	34.2	50.4	32.6	
S15				
S14	32.6	47.1	30.6	43.4
S13 & Bend				
S12	30.3	40.5	28.1	36.9
S11				
S10				
S9 & Bend	27.7	37.0	25.5	31.4
S8				
S7				
S6	23.9	28.5	22.5	26.2
S5 & Bend				
S4	20.0	20.6	20.0	20.4
S3				
S2	17.0	17.1	17.1	14.0
S1 & Bend				

The geometry of the COBC requires very high cooling liquid jacket flow rates ($\dot{m} > 2.5$ kg/min) to ensure turbulent hydrodynamics for good mixing and heat transfer on the shell side of the straights. When the jacket flow rate fell below this value, the liquid split into two sections. The first one being a cold stream of liquid, travelling along the bottom of the COBC straight and the second one being a stagnant, hot body of liquid, resting in the upper section of the straight. Under these conditions no consistent heat exchange could be obtained.

In contrast, the oscillating crystal suspension on the tube side of the straight was only pumped with a net flow of $\dot{m} \sim 0.05$ kg/min. in order to maximise the crystalliser residence time.

The mismatch between the shell and the tube flow rate as well as the very quick heat exchange in the COBC did not permit the establishment of linear cooling profiles across the COBC straights. Figure 10.4-2 shows the typically obtained cooling profiles, where all ΔT between the shell and tube stream was exchanged over the first straight of a new temperature zone. The straight section after the temperature drop indicates a constant temperature zone for crystal growth.
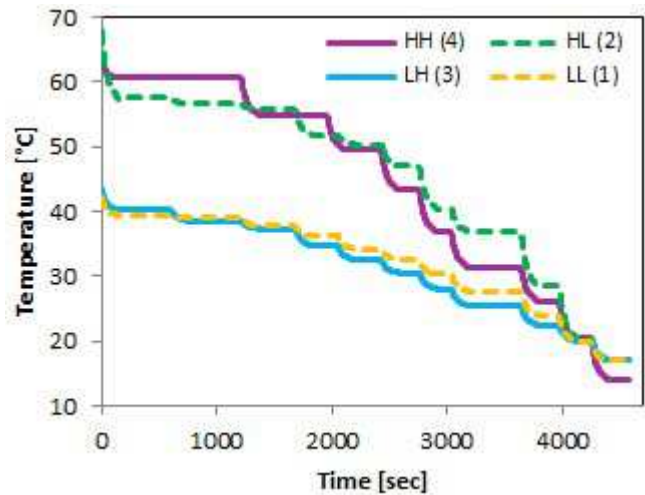
Figure 10.4-2: Cooling profiles along the COBC. Coloured lines indicate different temperature profiles over times suitable for various solution concentrations and seed loadings.

10.4.3 Predicted and measured desupersaturation

Straightforward initial desupersaturation experiments suggested that the assumption of a cube-like crystal shape would best describe the overall bulk desupersaturation profile in the COBC. In the same fashion, crystal growth experiments 1, 3 & 4 were designed according to the cooling profiles shown in Figure 10.4-2.
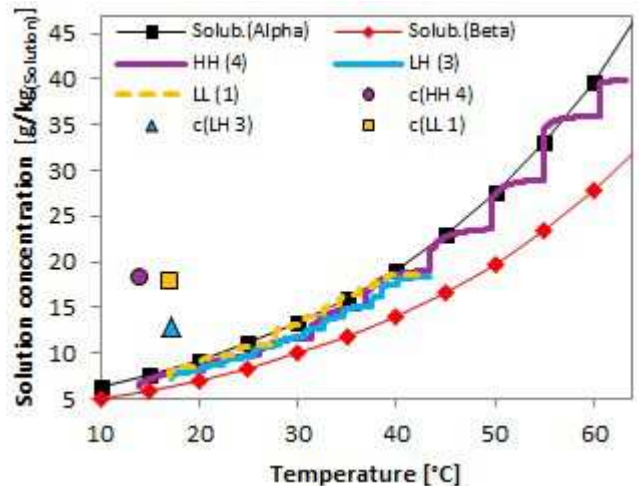
The concentration profile in Figure 10.4-3 shows crystal growth between the solubility lines of the Alpha and Beta polymorph and almost reaches bulk

Figure 10.4-3: Coloured lines show predicted concentration profile along COBC (cube-like crystal shape model), Δ, ■, ● = measured concentrations at COBC outlet.

desupersaturation at the end of the crystalliser.

The bulk supersaturation profile in Figure 10.4-4 indicates that at any time during the process low levels of supersaturation (SS < 1.6) are maintained, which should suppress nucleation of the Alpha polymorph. In unseeded H-Glu cooling crystallisation experiments the bulk supersaturation had to reach high levels (SS ≥ 3.7) before primary nucleation of the Alpha form was observed.
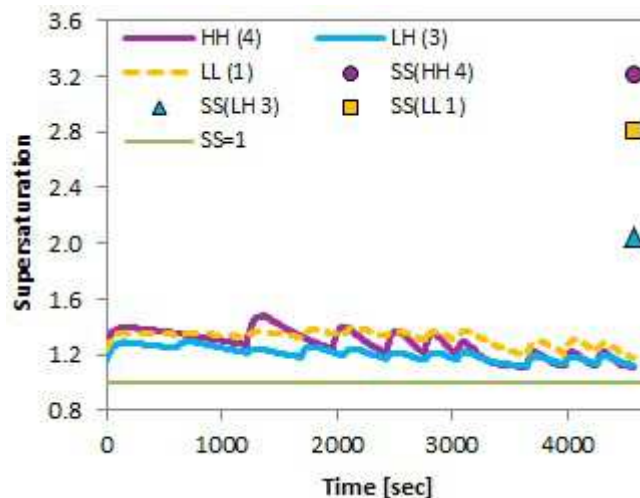
Figure 10.4-4: Coloured lines show predicted bulk supersaturation profile along COBC (cube-like crystal shape model), Δ, ■, ● = measured supersaturation at COBC outlet.

However, contrary to the predicted desupersaturation behaviour, offline solid recovery measurements at the end of the crystalliser showed a substantial degree of remaining bulk supersaturation. This fact indicates that the available H-Glu in solution is not fully consumed by the seed crystals and that the crystallisation process was not completed within the crystalliser residence time.

The final level of bulk supersaturation SS ≤ 3.7 should however not be high enough for nucleation of the Alpha polymorph to occur.

Possible reasons for the mismatch of predicted and actual results
- Fewer seed crystals present than anticipated
- Inaccurate crystal growth data in literature
- Wrong assumptions about morphology and available crystal growth surfaces
- Excessive agglomeration masks crystal growth surfaces

In the next step the assumed crystal morphology and available surface area was changed from the cube-like shape to the platelet/needle-like crystal shape as reported

in literature. All other parameters like the number of seeds available and the growth kinetics of the individual crystal facets were kept constant.

Figure 10.4-5 shows the predicted solution concentration profile (dashed line), which was confirmed by offline solid recovery analysis and mass balance calculations (diamonds). Both concentrations are in good agreement, which indicates that the assumption of needle-like crystals delivers a better fit for the real experiment.

Figure 10.4-5: The dashed green line predicts the concentration profile along COBC (needle-like crystal shape model), ◊ = measured concentrations in the rig

The predicted bulk supersaturation profile in Figure 10.4-6 (dashed line) indicates a continuous increase of supersaturation throughout the entire experiment, which was confirmed by offline solid recovery analysis and mass balance calculations (diamond). Under the most unfavourable operating conditions for a seeded process (high solution concentration & low seed loading) the bulk supersaturation ramps up
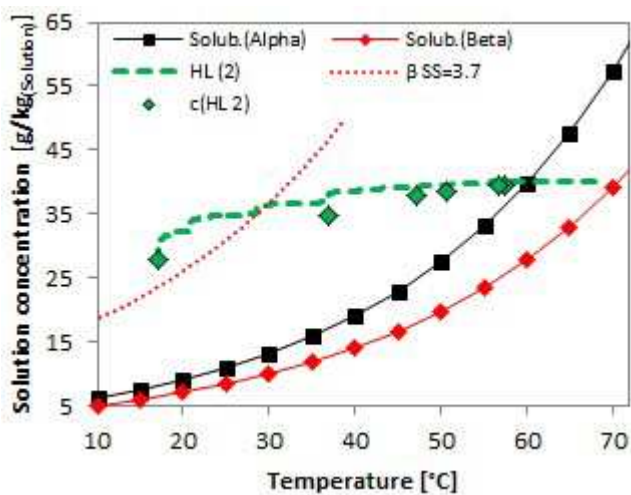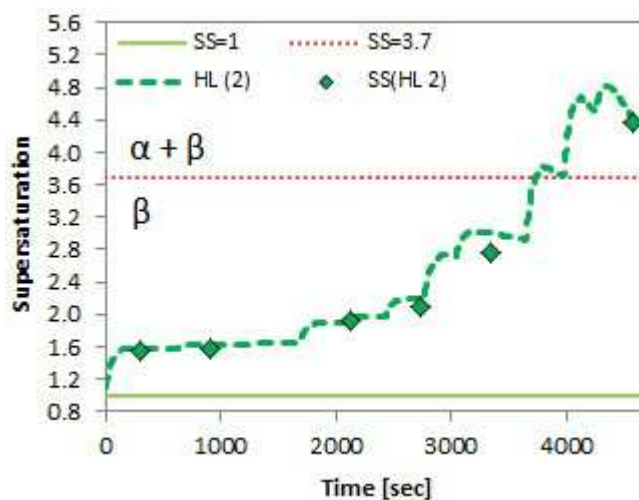

Figure 10.4-6: The dashed green line is the predicted bulk supersaturation profile along COBC (needle-like crystal shape model), ◊ = measured concentrations in the rig

to a level SS ≥ 3.7, fouling occurred in the system and the Alpha polymorph was observed in the presence of the Beta form.

After the successful prediction of solution concentration and bulk supersaturation for experiment 2, the same refitting procedure (cube shape changed to platelet/needle shape) was carried out for experiments 1, 3 & 4. Results in Figure 10.4-7 show that assuming needle-like crystal morphology very accurately predicts the final remaining bulk supersaturation in all four experiments.
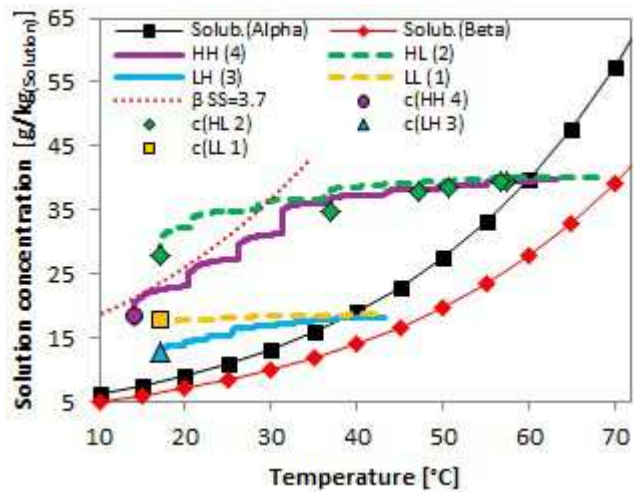
Figure 10.4-7: Green, purple, yellow and blue lines predict concentration profiles along COBC (needle-like crystal shape model), ◊, ○, □, ∆ = measured supersaturation along and at outlet of COBC

The results obtained for the bulk supersaturation profile in Figure 10.4-8 illustrate probable trajectories along the COBC before the final bulk supersaturation is reached at the end of the crystalliser.

Changing the crystal morphology and available crystal growth surfaces from cube-like to needle-like allowed a successful prediction of solution concentration and bulk supersaturation behaviour along
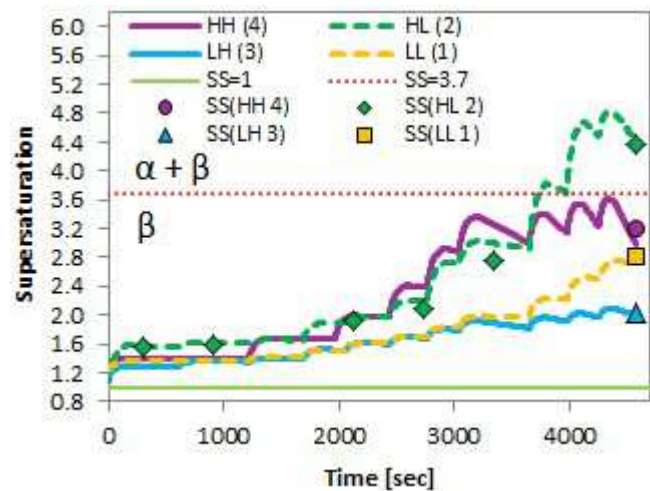
Figure 10.4-8: Green, purple, yellow and blue lines indicate bulk supersaturation profiles along COBC (needle-like crystal shape model), ◊, ○, □, ∆ = measured supersaturation along and at outlet of COBC

the COBC. Other influencing factors such as number of available seed crystals and crystal growth data from literature were kept constant in both approaches.

Results show that the procedure of relating Malvern Mastersizer data to volume, mass, dimension and aspect ratio of needle-like crystals can generate valuable information for the design of a crystal growth process. Careful control over residence times in constant temperature sections and supersaturation enable detailed prediction of the full crystal growth process.

10.4.4 From seed to product crystals

In a continuous cooling crystallisation process small seed crystals were grown to large final product crystals. Figure 10.4-9 shows a micrograph of the seeding suspension and Figure 10.4-10 illustrates the final product crystals. The pictures convey a qualitative impression of crystal growth happening during the process.
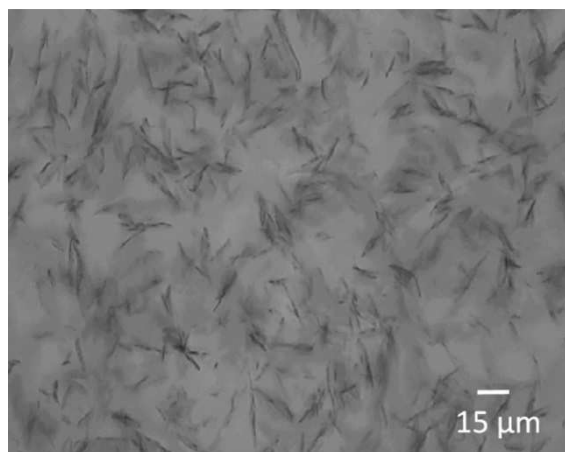
Figure 10.4-9: Optical microscopy image of seeding suspension before injected into COBC
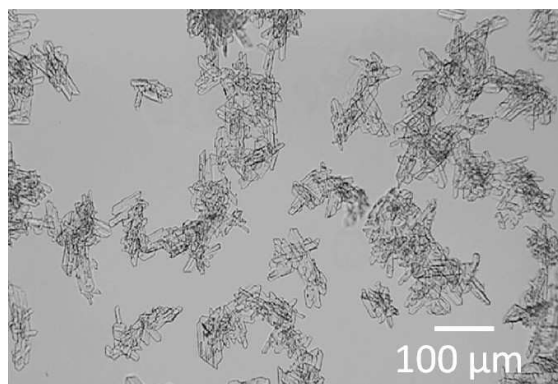
Figure 10.4-10: Optical microscopy image of product suspension after grown in COBC to final product size

SEM images of seed and product crystals were taken. Figure 10.4-11 shows the irregularly shaped seed crystals of plate-like morphology on a filter membrane structure,

as they were provided from the seed generation process. Agglomerated final product crystals from experiment 2 are shown in Figure 10.4-12, which illustrates the elongated platelet crystal morphology. This picture is representative for all product crystals obtained from the COBC runs carried out in this study, including experiments 1, 3 & 4.
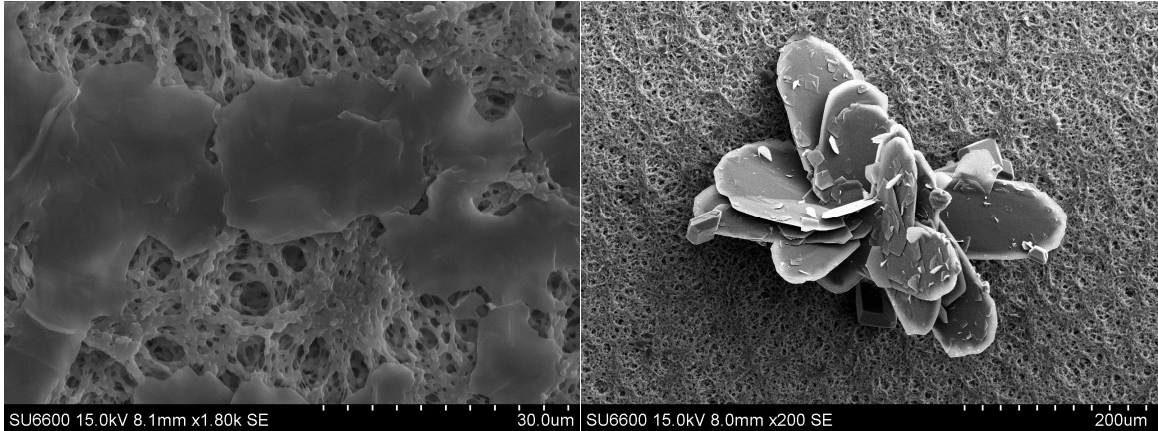
Figure 10.4-11: Glutamic acid seed crystals on PTFE filter membrane

Figure 10.4-12: Agglomerated Glutamic acid product crystal on PTFE filter membrane from COBC outlet

Crystal growth was also monitored by online FBRM measurements of seeding suspension and product crystals in the last bend (P2) before the crystalliser outlet. Figure 10.4-13 shows the unweighted, normalised chord length distribution (CLD) of the seeding suspension (orange) and the product crystals (blue). As the crystals move through the COBC the CLD
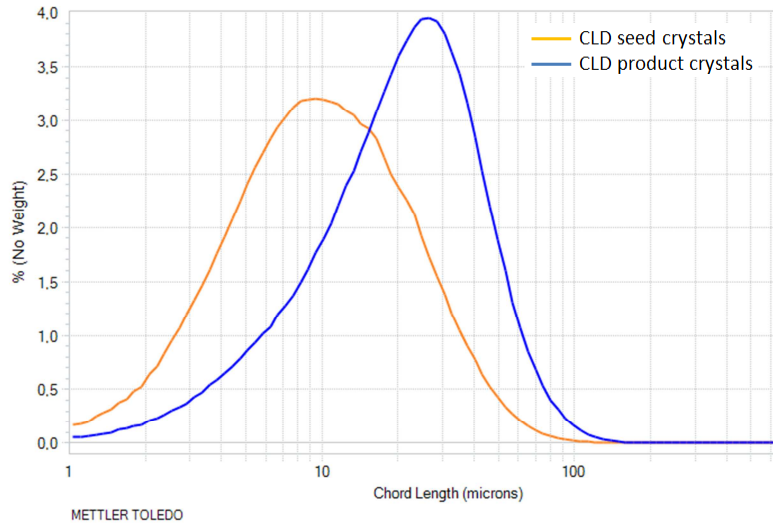
Figure 10.4-13: Chord length distribution (CLD) of seed crystals (orange) and product crystals (blue) indicating an increase in size along the rig

shifts to the right, the number of small counts decreases and the number of large counts increases. This behaviour indicates that crystals at the end of the COBC are larger than at the beginning.

10.4.5 Effect of solution concentration and seed loading on mean particle size

In a proceeding crystallisation process the available product crystals consume supersaturation made accessible during the cooling process due to a reduction in temperature and bulk solubility. Mass balance calculations use thermodynamic data to assess the yield of the crystal product at the final crystallisation temperature. Considering the total number of seed crystals as well as the amount of H-Glu made available during cooling, this approach allows predictions about final product crystal sizes.

Figure 10.4-14 shows the final product particle size distributions (Malvern Mastersizer) of the four different conditions investigated in this study. In the experiments with low seed loading (run 1 & 2) as well as the experiments with high seed loading (run 3 & 4) a clear trend can be observed. A low solution concentration leads to a small final mean crystal size (~70 µm & ~90 µm) and a high solution concentration leads to a large final mean crystal size (~240 µm & ~320 µm).
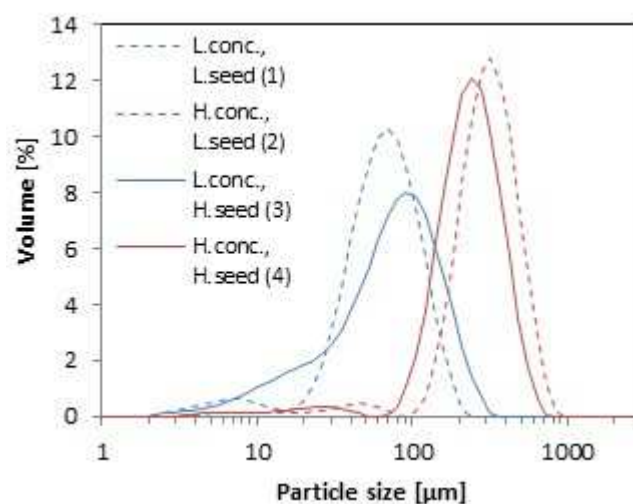
Figure 10.4-14: Particle size distribution (laser diffraction) of agglomerated product crystals at COBC outlet.

In the experiments with low solution concentration (run 1 & 3) as well as the experiments with high solution concentration (run 2 & 4) the results are less obvious

and even contradictory. Counter intuitively at low solution concentration the low seed loading achieves a smaller mean particle size (~70 µm) than the high seed loading (~90 µm), which according to mass balance should be the other way round. On the other hand, at high solution concentration the low seed loading does achieve a larger mean particle size (~320 µm) than the high seed loading (~240 µm).

It must however be noted that the obtained particle size distributions are those of agglomerated crystals, which do not follow the predicted crystal growth behaviour of individual crystals. It is hence difficult to draw conclusions about the relationship between seed loading and solution concentration from these experiments.

10.4.6 Steady-state operation

While batch processes provide a large degree of process flexibility they also deal with the challenges of batch-to-batch variations, inconsistent output product quality and large quantities of waste. Continuous processes, on the other hand, are known to be less flexible but potentially deliver the benefit of operating at steady-state, where numerous parameters remain unchanged/constant over time. After an ideally short unsteady start-up period a continuous system should reach steady-state in which recent observations from the system predict future behaviour and constantly high product quality is produced.

Initially the COBC was filled with pure water and during start-up the water was replaced with crystal slurry so that the first crystalliser volume exiting did not contain any crystal product. The first sample was taken when the first crystal appeared at the crystalliser exit.

Steady-state operation in continuous crystallisation is demonstrated by looking at the final particle size distribution and desupersaturation behaviour during the experiments 1 – 4. Figure 10.4-15 and Figure 10.4-16, representative for all four experiments, after the first residence time (RT) show a PSD which deviates from the measurements after

two and more RT. The first crystals to exit the crystalliser were exposed to unsteady operation but all subsequent product crystals, collected after integer crystalliser RT, showed steady-state PSD.
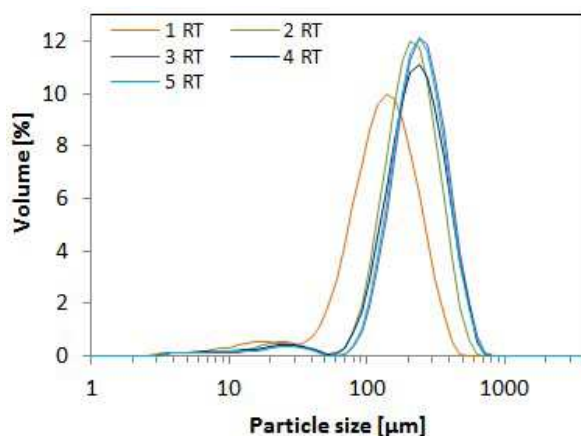
Figure 10.4-15: Steady-state particle size distributions after 1 – 5 residence times (HH4)
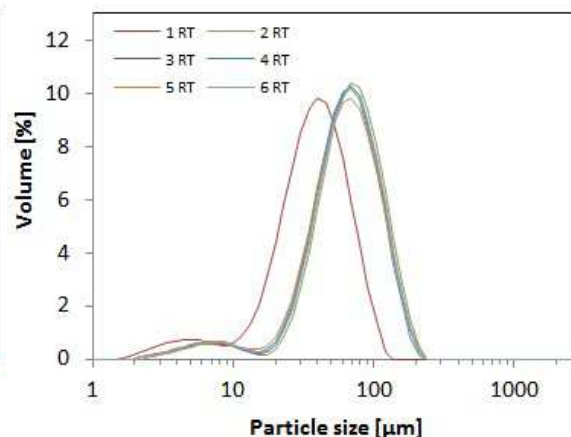
Figure 10.4-16: Steady-state particle size distributions after 1 – 6 residence times (LL1)

A similar trend can be observed when looking at Figure 10.4-17 and the remaining bulk supersaturation at the exit of the COBC. The first sample was taken when crystals started leaving the crystalliser and for experiments 2, 3 & 4 these samples exhibit a significantly higher supersaturation compared to samples taken after subsequent RT.

Results show similar initial supersaturation values for run 2 & 4 with a high solution concentration as well as 1 & 3 with the low solution concentration. Samples from experiments 1 & 2 with a low seed loading contain a higher level of final bulk supersaturation compared to experiments 3 & 4 with a high seed loading. So even if different seed loadings did not show strong effects on agglomerated final mean crystal sizes, in terms of final bulk supersaturation they do.

However, all samples have in common that after the start-up period (first residence time) the final bulk supersaturation remains at a steady-state level.
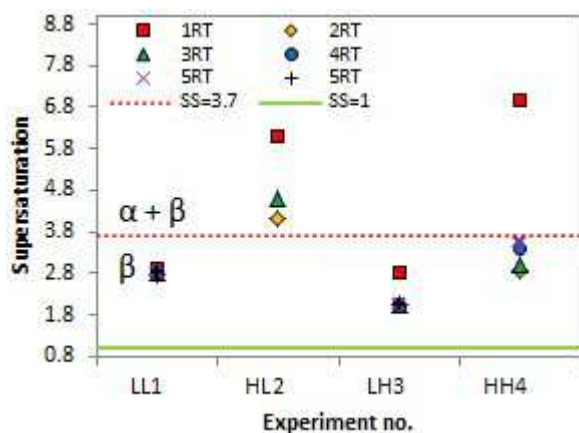
Figure 10.4-17: Remaining bulk super-saturation at the end of the crystalliser of all four crystallisation experiments
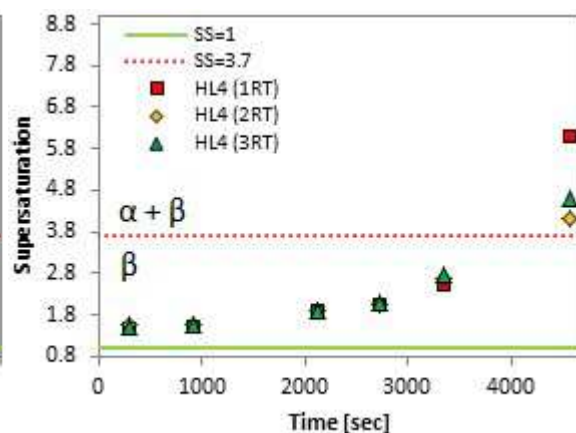
Figure 10.4-18: Remaining bulk super-saturation along the COBC during all four crystallisation experiments

Solid recovery analysis of slurry samples being taken from the bends of the crystalliser were used to determine bulk supersaturation data at multiple points along the rig. When the first crystals arrived at the outlet, as well as after 2 & 3 RT, six samples were extracted from the COBC at various positions. Figure 10.4-18 shows that only the first sample at the crystalliser outlet showed unsteady behaviour and at all other locations along the rig steady-state operation was already achieved.

These results suggest that a short section of unsteady conditions travels through the rig and that only a small unsteady volume needs to be disposed of during start-up. It is not necessary to discard a full crystalliser volume of product slurry.

The section of unsteady operation was located between the crystalliser outlet and sampling port P3, which covers eight straights and one bend. The volume of this section is about 1 L, which would require disposal before steady-state operation is achieved. This means that a consistent stream of product crystals can be collected from the COBC about 20 min. after the first crystals appeared at the outlet.

These laboratory scale experiments produced about 1 g/min of H-Glu product crystals, which multiplies to about 1.5 kg/24h.

10.4.7 Fouling, blockage and polymorphic purity

Processing equipment used for batch operation has to be cleaned after every run to be ready for the next batch. Fouling crystals growing on heat exchange surfaces or submerged equipment are hence frequently cleaned away and usually do not cause major disruptions during operation.

A continuous process on the other hand is operated for extended periods of time without going through a cleaning procedure, which makes fouling a potential problem. Crystals growing on surfaces inside a tubular crystalliser can lead to blockages in the equipment and the process needs to be shut down.

In unseeded continuous H-Glu cooling crystallisation experiments the bulk supersaturation had to reach a level of SS ≥ 3.7 before first crystals could visually be observed. XRPD analysis showed that product crystals were of pure Alpha polymorph. In all unseeded experiments heavy fouling occurred at about one crystalliser residence time and to prevent subsequent blockages operations were stopped after about two residence times.

In the continuously seeded cooling crystallisation experiments 1, 3 & 4 the steady-state bulk supersaturation remained at SS ≤ 3.7 and XRPD analysis in Figure 10.4-19 indicates that product crystals are of pure Beta polymorph.

Thorough inspections of the shutdown COBC unit after ≥ 5 crystalliser residence times did not show any indications of fouling or possible blockage.
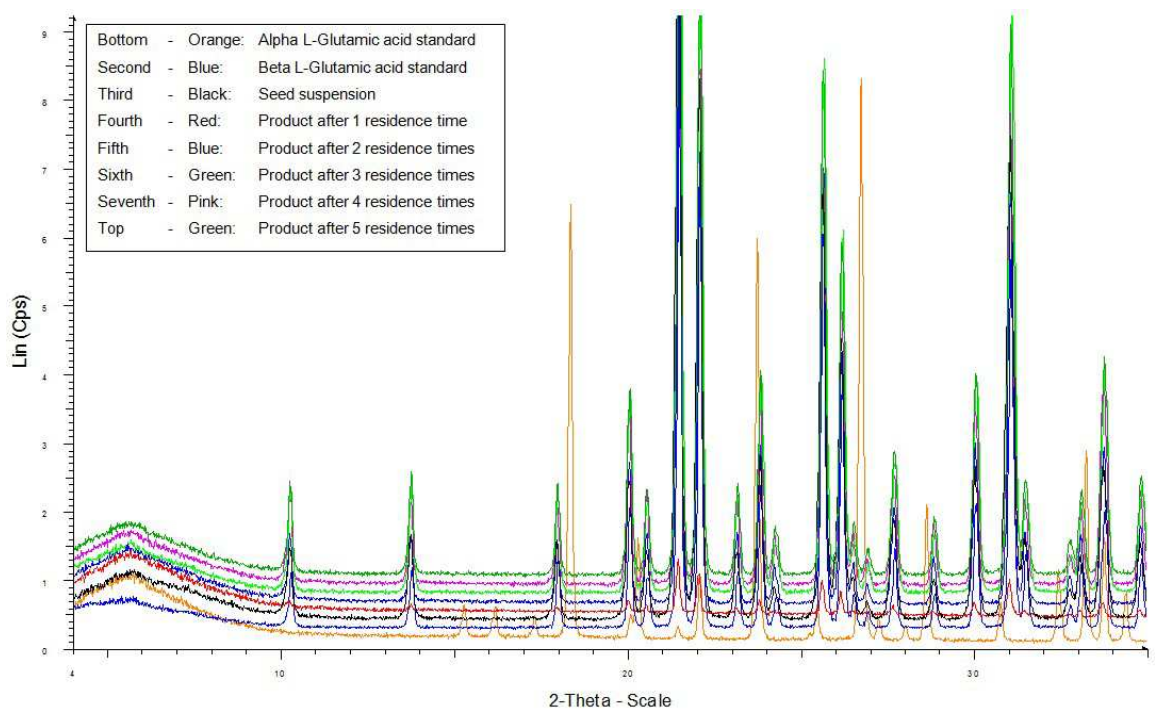
Figure 10.4-19: XRPD analysis of Glutamic acid product crystals SS ≤ 3.7. No Alpha form can be detected.

In experiment 2, on the other hand, the steady-state bulk supersaturation reached a level of SS ≥ 3.7 and XRPD analysis in Figure 10.4-20 indicate that the product crystals after three crystalliser residence times are of mixed polymorphic phase.
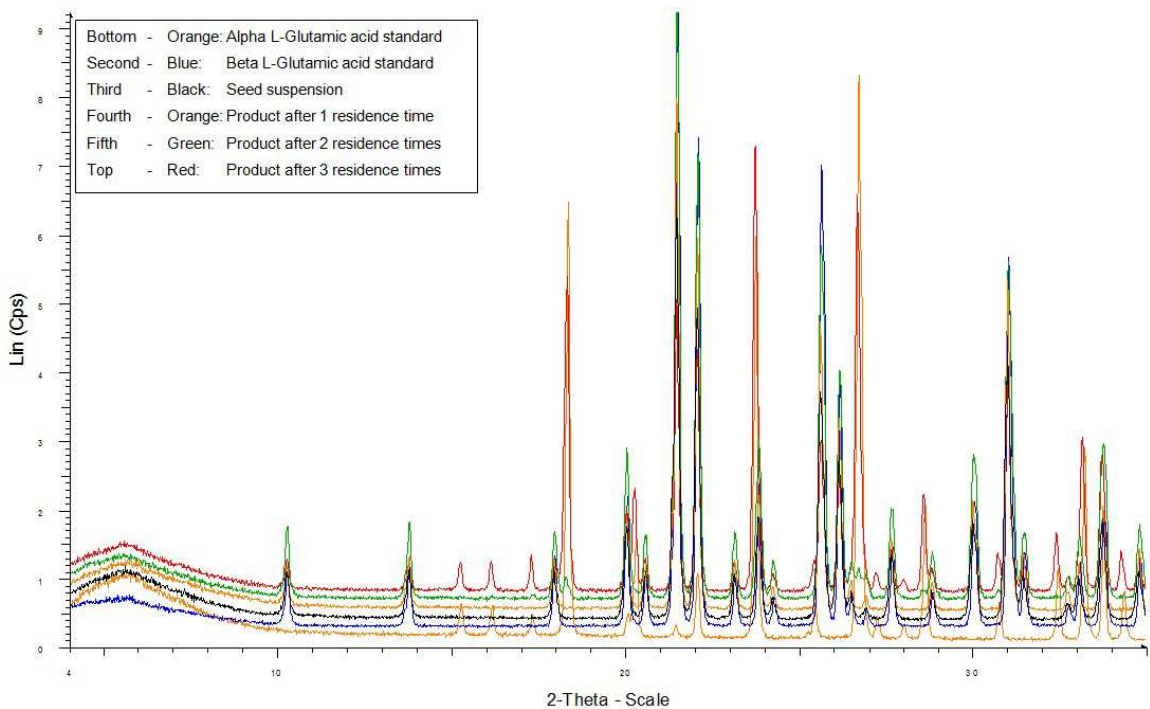
Figure 10.4-20: XRPD analysis of Glutamic acid product crystals SS ≥ 3.7. The presence of the Alpha form can be detected after only three crystalliser residence times.

Unlike the other three runs, experiment 2 had to be shut down after only three crystalliser residence times due to substantial fouling and blockage. Figure 10.4-21 shows fouling in a front section of a COBC straight, which reduces the crystalliser cross-section and leads to unfavourable hydrodynamics in the rig.

If crystals are no longer suspended properly they sediment and tend to form large crystal agglomerates at the bottom of the straight, as shown in Figure 10.4-22. This in turn affects crystal growth and desupersaturation behaviour, which makes supersaturation ramp up even further and the problem of fouling increases.

Figure 10.4-21: Fouling in COBC under conditions where the Alpha form nucleates in the presence of Beta seeds

Figure 10.4-22: Sedimentation in COBC indicating poor mixing hydrodynamics or agglomerated heavy crystals

Once fouling gets so bad that the COBC is blocked completely, the weakest link in the system is the oscillating bellow. If the blockage is not picked up immediately, the pumps continue to feed growth solution and seeding suspension into the COBC, which builds up pressure in the bellow. At the point when the pressure becomes too high the bellow buckles and becomes corrupted for future experiments. An example of a buckled bellow is shown in Figure 10.4-23.

Figure 10.4-23: Buckled bellow after the COBC was blocked due to excessive fouling along the rig

10.5 Design of continuous crystallisation experiments

The current approach, assuming plate/needle like crystals, successfully predicted concentration and desupersaturation profiles as well as remaining bulk supersaturation at the crystalliser outlet. However, full bulk desupersaturation at ambient conditions within the crystalliser mean residence time is desirable in order to avoid operational problems in downstream transfer lines. The current approach is used to design four different, fully desupersaturating experiments at two different H-Glu concentrations (conc.) and two different seed loadings (s-load), which are outlined in Table 10.5-1.

Table 10.5-1: Selection of operating conditions in operational space in seeded, fully desupersaturated COBC experiments

c(Solution) / Seed loading	Low	High
Low	LL (5) conc.: 20.0 g/kg$_{(Solution)}$ s-load: 0.5 g/kg$_{(Solution)}$	HL (6) conc.: 40.0 g/kg$_{(Solution)}$ s-load: 0.5 g/kg$_{(Solution)}$
High	LH (7) conc.: 20.0 g/kg$_{(Solution)}$ s-load: 5.0 g/kg$_{(Solution)}$	HH (8) conc.: 40.0 g/kg$_{(Solution)}$ s-load: 5.0 g/kg$_{(Solution)}$

Solution concentrations and seed loadings, mass balance calculations, crystal growth data, bulk supersaturation and residence time information were used to select appropriate cooling profiles. All experiments were designed to keep the bulk supersaturation below a level of SS ≤ 3.7 in order to avoid unwanted nucleation of the Alpha polymorph, which previously caused mixed phase product crystals, fouling and system blockage.

Bulk supersaturation was kept as low as possible but as high as necessary for sufficient crystal growth to reach full desupersaturation within the crystalliser mean residence time.

Depleting supersaturation slows down crystal growth rates, which significantly extends the time required for full bulk desupersaturation and can exceed the available crystalliser mean residence time. To avoid this problem, the bulk solution is cooled well below ambient conditions to keep supersaturation and crystal growth rates high and to reach a solution concentration which corresponds to saturation concentration at ambient conditions. Once the right solution concentration is reached, the cold bulk solution is heated up to ambient conditions, which achieves full desupersaturation of the bulk solution at ambient conditions. Table 10.5-2 outlines the different temperatures and temperature section lengths for the individual experiments.

Table 10.5-2: Selection of temperature sections in COBC cooling crystallisation

	LL (5) T [°C]	HL (6) T [°C]	LH (7) T [°C]	HH (8) T [°C]
S31	49.0	69.0	49.0	69.0
S30	29.0	42.0	40.0	56.0
S29 & Bend				
S28				
S27				
S26	28.0	41.0	37.0	53.0
S25 & Bend				
S24				
S23				
S22	25.0	38.0	37.5	48.5
S21 & Bend				
S20				
S19				
S18	22.0	34.0	28.5	42.5
S17 & Bend				
S16				
S15				
S14	18.0	28.0	23.5	34.0
S13 & Bend				

S12				
S11				
S10	11.0	19.0	17.0	22.5
S9 & Bend				
S8				
S7				
S6	7.0	8.0	16.0	15.0
S5 & Bend				
S4				
S3				
S2	20.0	20.0	20.0	20.0
S1 & Bend				

Figure 10.5-1 shows the typically obtained parabolic cooling profiles along the COBC and the temperature increase towards the end to ensure full bulk desupersaturation. Figure 10.5-2 illustrates the corresponding concentration profiles and Figure 10.5-3 demonstrates predicted bulk desupersaturation trajectories.
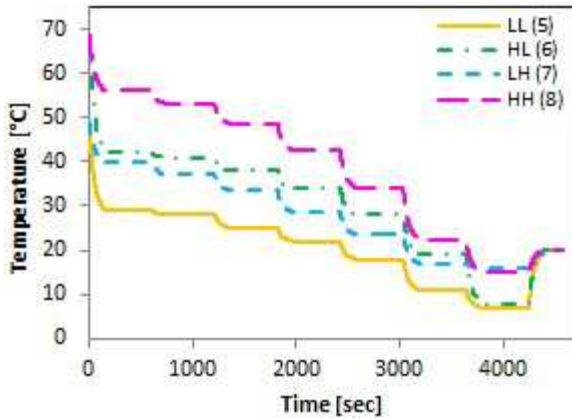

Figure 10.5-1: Cooling profiles along the COBC. Coloured lines describe predicted temperature trajectory.
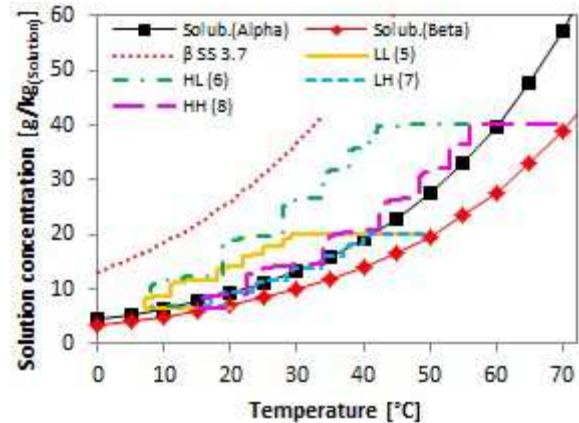

Figure 10.5-2: Concentration profiles along COBC. Green, purple, yellow and blue line describe predicted concentration trajectory.
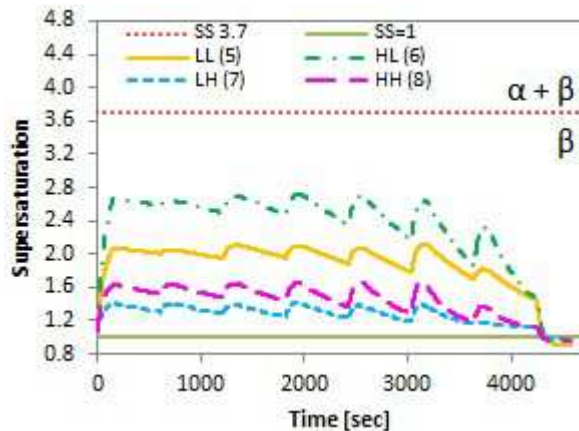

Figure 10.5-3: Bulk supersaturation profiles along COBC. Green, yellow, purple and blue line describe predicted supersaturation trajectory.

10.6 Conclusions

Continuously produced H-Glu seeds were continuously grown to various final crystal product sizes using a COBC. An approach was suggested how mass balance calculations, particle size distributions, crystal morphology and growth data can be used to predict cooling profiles for continuous bulk desupersaturation within a fixed mean residence time.

Online FBRM data suggested that seeds grew to larger product crystals. However, as FBRM cannot distinguish between crystal growth and agglomeration, this data should only be used to complement other analysis.

Micrographs and SEM images provided a visual confirmation of actual seed crystal growth but also of agglomeration happening during the process. The effect of solution concentration on the agglomerated final mean particle size was demonstrated with higher solution concentrations leading to larger mean particle sizes. However, different seed loadings used in these experiments counter intuitively did not show a clear trend in terms of mean particle size but did with respect to final bulk supersaturation.

Steady-state operation, which is very important for continuous processes, was demonstrated using parameters like final mean particle size, particle size distribution and bulk supersaturation along the COBC. Steady-state operation was reached ~20 min after the first crystals left the crystalliser outlet and the volume of unsteady crystal slurry to be disposed of was ~1 L.

Fouling and blockage in the system was successfully prevented by keeping the supersaturation at a level of SS ≤ 3.7, which yielded product crystals of pure Beta polymorph. When the supersaturation level exceeded SS ≥ 3.7 extensive fouling was observed, which quickly led to blockage in the system and yielded product crystals of Alpha & Beta mixed polymorphs.

These laboratory scale experiments produced about 1 g/min of H-Glu product crystals, which makes it possible to produce about 1.5 kg/24h.

11 Overall conclusions

The experiments carried out as part of this work have clearly shown that crystallisation processes are complex and system-specific unit operations with many relevant process parameters. In antisolvent crystallisation the valine system showed mixing sensitive behaviour at all levels of supersaturation, whereas glycine only showed mixing sensitivity at high supersaturations. The systems of L-Asparagine and L-Glutamic acid were not sensitive to mixing at all, which was also true for the reactive precipitation of L-Glutamic acid in aqueous solution.

Polymorphism, nucleation and growth kinetics as well as different levels of supersaturation play a key role in crystallisation, which has been clearly shown during the reactive precipitation experiments of L-Glutamic acid. Harsh hydrodynamic conditions led to excessive secondary nucleation of the metastable Alpha polymorph, whereas mild hydrodynamics favoured the stable Beta polymorph. This behaviour is the result of significantly different nucleation and crystal growth kinetics of the two polymorphs and might be applicable to other crystallisation processes.

The assumption of straightforward transfer from a batch into a continuous process cannot be made readily. Batch processes can be operated with limited understanding of the compound and the system. However, for continuous operation, a much deeper understanding about polymorphism, kinetics, thermodynamics, impurities, supersaturation and the process in particular is required. But once this information and process understanding is available, continuous crystallisation processes can be designed successfully.

The concept of thorough process understanding for continuous crystallisation design was demonstrated by developing the rapid continuous antisolvent crystallisation set up. Thermodynamic, kinetic and supersaturation information about the model compound were taken into account for the design of a unit, which continuously produced crystal seeding suspension of pure Beta phase with a small mean particle size and a narrow particle size distribution. Continuous steady-state operation for about 150 crystalliser residence times without visible fouling or blockage ensured a highly reproducible crystal product material.

A continuously seeded continuous crystal growth cooling crystallisation process was designed utilising all available information about the compound and the process itself. Solution concentration, desupersaturation behaviour and the temperature profile along the COBC were predicted by combining mass balance calculations, supersaturation data, seed loading & starting solution concentration, crystal morphology & growth rates as well as mean residence times in each temperature zone. With this approach, a continuously seeded continuous cooling crystallisation process was designed, which was operated under steady-state conditions for up to six crystalliser residence times without visible fouling or blockage.

A complete understanding about the compound and process is key for the successful design of continuous crystallisation processes.

12 References

[2.1]   W. Beckmann, Crystallization – Basic concepts and industrial applications Wiley-VCH Verlag GmbH & Co. KGaA, Weinheim 2013

[2.2]   H. Tung, E.L. Paul, M. Midler and J.A. McCauley, Crystallization of organic compounds, John Wiley & Sons, INC., New Jersey 2009

[2.3]   Allan S. Myerson, Handbook of industrial crystallisation, Butterworth-Heinemann, Boston 2002

[3.1]   P. Atkins, J. de Paula, Atkins' Physical Chemistry (seventh edition), Oxford University Press, Oxford 2002

[3.2]   E. Ignatowitz, Chemietechnik (8. Auflage), Verlag Europa-Lehrmittel, Haan-Gruiten 2007

[3.3]   Vekilov P.G., The two-step mechanism of nucleation of crystals in solution, Nanoscale, 2010, 2, 2346–2357.

[4.1]   Globalsino (2013) Practical Electron Microscopy and Database, [Online], Available: http://www.globalsino.com/EM/ [01.03.2013]

[4.2]   J. P. Glusker and K. N. Trueblood, Crystal Structure Analysis (Second Edition), Oxford University Press, Oxford 1985

[4.3]   Malvern (2013) Laser Diffraction, [Online], Available: http://www.malvern.com/labeng/technology/laser_diffraction/laser_diffraction.htm [13.04.2013]

[4.4]   W. Hergert and T. Wriedt, The Mie Theory – Basics and Applications, Springer-Verlag, Berlin Heidelberg 2012

[4.5]   Malvern (2013) Laser Diffraction Particle Sizing, [Online], Available: http://www.malvern.com/labeng/technology/laser_diffraction/particle_sizing.htm [13.04.2013]

[4.6]   A. Chianese and H.J.M. Kramer, Industrial crystallisation process monitoring and control, Wiley-VCH Verlag, Weinheim, Germany 2012

[4.7]   Fang Y., Selomulya C., Chen X.D., Characterization of milk protein concentrate solubility using focused beam reflectance measurement, Dairy Sci. Technol 2010, 90, 253-270

[4.8]   iScope Corp (2013) 40X-1000X LED Lab Binocular Compound Microscope w 3D Two-Layer Mechanical Stage, [Online], Available: http://www.iscopecorp.com/40x-1000x-led-lab-siedentopf-binocular-compound-microscope-with-3-d-double-layer-mechanical-stage.html [29.04.13]

[4.9]   T. G. Rochow and P. A. Tucker, Introduction to microscopy by means of light, electrons, X-rays or acoustics (Second Edition), Plenum Press, New York 1994

[4.10]   C. Cashell, D. Corcoran, B. K. Hodnett, Secondary nucleation of the β–polymorph of L-Glutamic acid on the surface of α–form crystals, Chem. Commun., 2003, 374-375

[4.11]   L. Reimer, Scanning Electron Microscopy – Physics of image formation and microanalysis (Second edition), Springer-Verlag, Heidelberg 1998

[5.1]   W. E. Wilson, Positive-displacement pumps and fluid motors, Pitman Publishing Corporation, New York 1950

[5.2]   Elsevier, Plant and process engineering 360°, Butterworth-Heinemann, Oxford 2010

[5.3]   Powermechanic (2013) Mechanical hydraulic pumps, [Online], Available: http://powermechanic.blogspot.co.uk/ [10.05.13]

[5.4]   G. Fastert, E. Ignatowitz, Chemietechnik - 10. Auflage, Europa Lehrmittel, Haan-Gruiten 2011

[5.5]   Brown, A., PhD thesis, University of Strathclyde (2012) Characterisation of turbulent mixing and its influence on antisolvent crystallisation, Glasgow: Department of Chemical and Process Engineering

[5.6]   Branson Ultrasonics, Ultrasonic cleaners – operator's manual, Bransonic, Soest 2013

[7.1]   Myerson A., Handbook of Industrial Crystallisation; 2nd ed.; Butterworth-Heinemann, 2002.

[7.2]   Bałdyga J., Makowski Ł., Orciuch W., Industrial & Engineering Chemistry Research 2005, 44, 5342-5352.

[7.3]   Lince F., Marchisio D.L., Barresi A.A., Journal of Colloid and Interface Science 2008, 322, 505-515.

[7.4]   Chattopadhyay S., Erdemir D., Evans J.M.B., Ilavsky J., Amenitsch H., Segre C.U., Myerson A. S., Crystal Growth & Design 2005, 5, 523-527.

[7.5]   Baldyga J., Podgorska W., Pohorecki R., Chemical Engineering Science 1995, 50, 1281-1300.

[7.6]   Mullin J.W., Crystallization; 4th ed.; Elsevier Butterworth-Heinemann, 2001.

[7.7]   Jones A., Crystallization Process Systems; Butterworth-Heinemann, 2002.

[7.8]   Paul E., Atiemo-Obeng V., Kresta S., Handbook of Industrial Mixing: Science and Practice; Wiley, 2003.

[7.9]   Nienow A., Edwards M., Harnby N., Mixing in the Process Industries; 2nd ed.; Butterworth-Heinemann, 1997.

[7.10]   Shekunov B.Y., York P., Journal of Crystal Growth 2000, 211, 122-136.

[7.11]   Marchisio D.L., Rivautella L., Barresi A.A., AIChE J. 2006, 52, 1877-1887.

[7.12]   Alvarez A.J., Myerson A.S., Crystal Growth & Design 2010, 10, 2219-2228.

[7.13]   Dove P., De Yoreo J., Weiner S., Biomineralization; Mineralogical Society of America, 2004.

[7.14]   Horn D., Rieger J., Angewandte Chemie International Edition 2001, 40, 4330-4361.

[7.15]   Baldyga J., Bourne J.R., Turbulent Mixing and Chemical Reactions; Wiley, 1999.

[7.16]   Roelands C., Derksen J., Horst J.T., Kramer H., Jansens P., Chemical Engineering & Technology 2003, 26, 296-303.

[7.17]   Bourne J.R., Organic Process Research & Development 2003, 7, 471-508.

[7.18]   Johnson B.K., Prud'homme R.K., Australian Journal of Chemistry 2003, 56, 1021-1024.

[7.19]   Gavi E., Rivautella L., Marchisio D.L., Vanni M., Barresi A.A., Baldi G., Chemical Engineering Research & Design 2007, 85, 735-744.

[7.20]   Gavi E., Marchisio D.L., Barresi A.A., Chemical Engineering Science 2007, 62, 2228-2241.

[7.21]   Siddiqui S.W., Zhao Y., Kukukova A., Kresta S.M., Industrial & Engineering Chemistry Research 2009, 48, 7945-7958.

[7.22]   Johnson B.K., Prud'homme R.K., AIChE Journal 2003, 49, 2264-2282.

[7.23]   Baldyga J., Bourne J.R., Walker B., The Canadian Journal of Chemical Engineering 1998, 76, 641-649.

[7.24]   Gillian J. M., Kirwan D.J., Chemical Engineering Communications 2008, 195, 1552-1574.

[7.25]   Matteucci M.E., Hotze M.A., Johnston K.P., Williams R.O., Drug nanoparticles by antisolvent precipitation: Mixing energy versus surfactant stabilization, Langmuir, 2006, 22, 8951-8959.

[7.26]   Lince F., Marchisio D.L., Barresi A.A., A comparative study for nanoparticle production with passive mixers via solvent-displacement: Use of CFD models for optimization and design, Chemical Engineering and Processing, 2011, 50, 356–368.

[7.27]   Variny M., Alvarez S., Moore B.D., Sefcik J., et al., Journal of Dispersion Science and Technology, 2008, 29, 617-620.

[7.28]   Jawor-Baczynska A., Moore B. D., Sefcik J. "Effect of mixing, concentration and temperature on formation of mesostructured solutions and their role in nucleation of DL-valine crystals" Faraday Discussions (2015). doi: 10.1039/C4FD00262H

[8.1]   Alatalo H., American Institute of Chemical Engineers AIChE J, 2010, 56, 8: 2063–2076

[8.2]   Bernal J. D., The crystal structure of the natural amino acids and related compounds, Z. Kristallogr. Kristallgeom., 1931, 78, 363

[8.3]   Hirokawa F., A new modification of L-Glutamic acid and its crystal structure, Acta Cryst. 1955, 8, 637

[8.4]   Cashell C., Corcoranac D., Hodnettab B.K., Secondary nucleation of the β–polymorph of L-Glutamic acid on the surface of α–form crystals, CHEM. COMMUN. , 2003, 374–375

[8.5]   Sakata Y., Horikawa T., Takenouchi K., Studies on the behaviors of impurities on the crystallization of L-Glutamic acid, Agric. Biol. Chem., 1961, 25, 921-925

[8.6]   Garti N., Zour H., The effect of surfactants on the crystallization and polymorphic transformation of glutamic acid, Journal of Crystal Growth, 1997, 172, 486-498

[8.7]   Cashell C., Corcoran D., Hodnett B.K., Control of polymorphism and crystal size of L-glutamic acid in the absence of additives, 2004, 273, 258-265

[8.8]   Schöll J., Vicum L., Müller M., Mazzotti M., Precipitation of L-Glutamic Acid: Determination of Nucleation Kinetics, 2006, 29, 257-264

[8.9]   Schöll J., Lindenberg C., Vicum L., Brozio J., Mazzotti M., Precipitation of α L-glutamic acid: Determination of growth kinetics, 2007, 136, 247-264

[8.10]   Cornel J., Lindenberg C., Mazzotti M., Experimental characterization and population balance modeling of the polymorph transformation of L-Glutamic acid, 2009, 9, 243-252

[8.11]   Roelands C.P.M., Ter Horst J.H., Kramer H.J.M., Jansens P.J., The unexpected formation of the stable beta phase of L-glutamic acid during pH-shift precipitation, 2005, 275, 1389-1395

[8.12]   Roelands C.P.M., Ter Horst J.H., Kramer H.J.M., Jansens P.J., Precipitation mechanism of stable and metastable polymorphs of L-glutamic acid, 2007, 53, 354-362

[8.13]   Schöll J., Bonalumi D., Vicum L., Mazzotti M., In Situ monitoring and modeling of the solvent-mediated polymorphic transformation of L-Glutamic acid, 2006, 6, 881-891

[8.14]   Ono T., Kramer H.J.M., Ter Horst J.H., Jansens P.J., Process modeling of the polymorphic transformation of L-Glutamic acid, 2004, 4, 1161-1167

[8.15]   Ostwald W., Studien über die Bildung und Umwandlung fester Körper, Z. Phys. Chem., 1897, 22, 289

[9.1]   Thorat A. A., Dalvi S. V., Liquid antisolvent precipitation and stabilisation of nanoparticles of poorly water soluble drugs in aqueous suspensions: Recent developments and future perspective, Chemical Engineering Journal 2012, 1-34, 181-182

[9.2]   Zhao H., Wang J., Wang Q., Chen J., Yun J., Controlled liquid antisolvent precipitation of hydrophobic pharmaceutical nanoparticles in a microchannel reactor, Ind. Eng. Chem. Res. 2007, 46, 8229-8235

[9.3]   Zhang Q., Xu L., Zhou Y., Wang J., Chen J., Preparation of drug nanoparticles using a T-junction microchannel system, Ind. Eng. Chem. Res. 2011, 50, 13805-13812

[9.4]   Fox E. A, Gex V. E., Single-phase blending of liquids, A.I.Ch.E.J. 1956, 2 (4), 539-544

[9.5]   A.W. Patwardhan, Chemical Engineering Science 2002, 57, 1307-1318

[9.6]   M.C. Brick, H.J. Palmer, T.H. Whitesides, Formation of colloidal dispersions of organic materials in aqueous media by solvent shifting, Langmuir 19 (2003) 6367–6380.

[9.7]   S.V. Dalvi, R.N. Dave, Analysis of nucleation kinetics of poorly water-soluble drugs in presence of ultrasound and hydroxypropyl methyl cellulose during antisolvent precipitation, International Journal of Pharmaceutics 387 (2010) 172–179.

[9.8]   Z. Guo, M. Zhang, H. Li, J. Wang, E. Kougoulos, Effect of ultrasound on anti-solvent crystallization process, Journal of Crystal Growth 273 (2005) 555–563.

[9.9]   Vichare N. P., Gogate P. R., Dindore V. Y., Pandit A. B., Ultrasonics Sonochemistry 2001, 8, 23-33

[9.10]   G. Ruecroft, D. Hipkiss, T. Ly, N. Maxted, P.W. Cains, Sonocrystallization: the use of ultrasound for improved industrial crystallization, Organic Process Research & Development 9 (2005) 923–932.

[9.11]   Beck C., Dalvi S.V., Dave R.N., Controlled liquid antisolvent precipitation using a rapid mixing device, Chemical Engineering Science 2010, 65, 5669-5675

[9.12]   S.V. Dalvi, R.N. Dave, Controlling particle size of a poorly water-soluble drug using ultrasound and stabilizers in antisolvent precipitation, Industrial & Engineering Chemistry Research 48 (2009) 7581–7593.

[9.13]   Narducci O., Jones A.G., Kougoulos E., Chemical Engineering Science 2011, 66, 1069-1076

[9.14]   Alvarez A.J., Myerson A.S., Continuous plug flow crystallization of pharmaceutical compounds, Crystal Growth & Design 2010, 10, 2219-2228

[9.15]   Zhang H., Quon J., Alvarez A.J., Evans J., Myerson A.S., Development of continuous anti-solvent/cooling crystallization process using cascaded mixed suspension, mixed product removal crystallizer, Org. Process Res. Dev. 2012, 16, 915-924

[10.1]   Lawton S., Steele G., Shering P., Continuous crystallization of pharmaceuticals using a continuous oscillatory baffled crystalliser, Organic Process Research & Development 2009, 13, 1357-1363

[10.2]   Quon J. L., Zhang H., Alvarez A., Evans J., Myerson A. S., Trout B. L., Continuous crystallization of aliskiren hemifumarate, Cryst. Growth Des. 2012, 12, 3036-3044

[10.3]   Eder R. J. P., Schrank S., Besenhard M. O., Roblegg E., Gruber-Woelfler H., Khinast J. G., Continuous sonocrystallization of acetylsalicylic acid (ASA): Control of crystal size, Cryst. Growth Des. 2012, 12, 4733-4738

[10.4]   Heng J. Y. Y., Thielmann F., Williams D. R., The effects of milling on the surface properties of form I paracetamol crystals, Pharmaceutical Research 2006, 23, 1918-1927

[10.5]   Schwarzer H. C., Peukert W., Experimental investigation into the influence of mixing on nanoparticle precipitation, Chem. Eng. Technol. 2002, 25, 657-661

[10.6]   Kawase M., Muira K., Fine particle synthesis by continuous precipitation using a tubular reactor, Advanced Powder Technol. 2007, 18, 725-738

[10.7]   Eder R. J. P., Radl S., Schmitt E., Innerhofer S., Maier M., Gruber-Woelfler H., Khinast J. G., Continuously seeded, continuously operated tubular crystallizer for the production of active pharmaceutical ingredients, Crystal Growth & Design 2010, 10, 2247-2257

[10.8]   Eder R. J. P., Schmitt E. K., Grill J., Radl S., Gruber-Woelfler H., Khinast J. G., Seed loading effects on the mean crystal size of acetylsalicylic acid in a continuous-flow crystallization device, Cryst. Res. Technol. 2011, 46, 227-237

[10.9]   Ferguson S., Morris G., Hao H., Barrett M., Glennon B., Characterization of the anti-solvent batch, plug flow and MSMPR crystallization of benzoic acid, Chemical Engineering Science 2013, 104, 44-54

[10.10] Alvarez A. J., Myerson A. S., Continuous plug flow crystallization of pharmaceutical compounds, Crystal Growth & Design 2010, 10, 2219-2228

[10.11] Takiyama H., Matsuoka M., Design of seed crystal specifications for start-up operation of a continuous MSMPR crystallizer, Powder Technology 2011, 121, 99-105

[10.12] Narducci O., Jones A. G., Kougoulos E., Continuous crystallization of adipic acid with ultrasound, Chemical Engineering Science 2011, 66, 1069-1076

[10.13] Alvarez A. J., Singh A., Myerson A. S., Crystallization of cyclosporine in a multistage continuous MSMPR crystallizer, Cryst. Growth & Des. 2011, 11, 4392-4400

[10.14] Zhang H., Quon J., Alvarez A. J., Evans J., Myerson A. S., Development of continuous anti-solvent/cooling crystallization process using cascaded mixed suspension, mixed product removal crystallizers, Org. Process Res. Dev. 2012, 16, 915-924

[10.15] Octave Levenspiel
         Chemical Reaction Engineering
         John Wiley & Sons, INC., New Jersey 1999

[10.16] Mackley M. R., Process innovation using oscillatory flow within baffled tubes, Trans IChemE 1991, 69197-199

[10.17] Harvey A. P., Mackley M. R., Stonestreet P., Operation and optimization of an oscillatory flow continuous reactor, Ind. Eng. Chem. Res. 2001, 40, 5371-5377

[10.18] Harvey A. P., Mackley M. R., Seliger T., Process intensification of biodiesel production using a continuous oscillatory flow reactor, Chem. Technol. Biotechnol. 2003, 78, 338-341

[10.19] Ricardo C., Ni X., Evaluation and establishment of a cleaning protocol for the production of vanisal sodium and aspirin using a continuous oscillatory baffled reactor, Organic Process & Development 2009, 13, 1080-1087

[10.20] Castro F., Ferreira A., Rocha F., Vicente A., Teixeira J. A., Continuous-Flow precipitation of hydroxyapatite at 37 °C in a Meso Oscillatory Flow Reactor, Ind. Eng. Chem. Res. 2013, 52, 9816-9821

[10.21] Eze V.C., Phan A.N., Pirez C., Harvey A.P., Lee A.F., Wilson K., Heterogeneous catalysis in an oscillatory baffled flow reactor, Catal. Sci. Technol. 2013, 3, 2373-2379

[10.22] Abbott M.S.R., Harvey A.P., Valente Perez G., Theodorou M.K., Biological processing in oscillatory baffled reactors: Operation, advantages and potential, Interface Focus 2013, 3, 1-13

[10.23] Kitamura M., Ishizu T., Growth kinetics and morphological change of polymorphs of L-Glutamic acid, Journal of Crystal Growth 2000, 209, 138-145

[10.24] Kim K.J., Mersmann A., Estimation of metastable zone width in different nucleation processes, Chemical Engineering Science 2001, 56, 2315-2324